THE DIELECTROPHORESIS OF CELLS

By

JOE STANLEY CRANE

Bachelor of Science
Oklahoma State University
Stillwater, Oklahoma
1964

Master of Science
Oklahoma State University
Stillwater, Oklahoma
1966

Submitted to the Faculty of the Graduate College
of the Oklahoma State University
in partial fulfillment of the requirements
for the Degree of
DOCTOR OF PHILOSOPHY
May, 1970

THE DIELECTROPHORESIS OF CELLS

Thesis Approved:

Herbert A Pohl
Thesis Adviser

James Lange

Thomas Winter

Eric C. Miller

J. Durham
Dean of the Graduate College

ACKNOWLEDGMENTS

The author is indebted to many persons in connection with this work. Special thanks go to Professor H. A. Pohl, Thesis Committee Chairman, for his invaluable patience, understanding, and overall guidance. The author also wishes to express his gratitude to the Thesis Committee members, Professor T. Winter, Professor J. Lange, and Professor E. Noller, for their interest and assistance.

Further appreciation goes to his associates: Dr. R. D. Hartman, Mr. J. Wyhof, Mr. I. Hawk, Mr. C. Feeley, and Mr. D. Fowler, for their helpful discussions; Mr. W. Chen for his assistance in taking data; and Mr. W. Melton, Mr. J. Cantril, and Mr. D. Mickish for their assistance with the development of the computer program. The author is also grateful to Mr. H. Hall and Mr. W. Adkins for their assistance in the design and construction of apparatus, and to Mrs. Janet Sallee for her typing of the manuscript.

Financial support has been received from the National Institutes of Health in the form of a three year research grant, for which the author is sincerely grateful.

Finally, to his wife, Charlene, goes his deepest appreciation for her untiring support, patience and understanding, her typing, and her drawing of the figures.

TABLE OF CONTENTS

Chapter		Page
I.	INTRODUCTION.	1
II.	EXPERIMENTAL PROCEDURES AND EQUIPMENT	11
III.	EXPERIMENTAL RESULTS FOR YEAST.	34
IV.	POSSIBLE MECHANISMS	65
V.	GENERAL EXPRESSION FOR DIELECTROPHORETIC FORCE.	75
VI.	FORCE ON A YEAST CELL MODEL	93
VII.	DERIVATION OF YIELD FOR A RADIAL FIELD.	111
VIII.	CALCULATED FREQUENCY AND CONDUCTIVITY DEPENDENCE OF YIELD	116
IX.	SUMMARY AND DISCUSSION.	130
BIBLIOGRAPHY.		136
APPENDIX A.	CONDUCTIVITY CONSDIERATIONS.	140
APPENDIX B.	COMPUTER PROGRAM FOR CALCULATING FORCE AND YIELD FOR A TWO SHELL SPHERE.	148
APPENDIX C.	LIST OF SYMBOLS.	152
APPENDIX D.	ERROR ANALYSIS	157

LIST OF TABLES

Table | Page

I. Values of Parameters Used in Calculations for Living Yeast Cells. 122

LIST OF FIGURES

Figure		Page
1.	Electrophoresis and Dielectrophoresis.	3
2.	Dielectrophoretic Separation for Different Particles with $\varepsilon_3 > \varepsilon_2 > \varepsilon_1$	5
3.	Diagram of Pin-Pin Dielectrophoresis Cell.	16
4.	Photograph of Pin-Pin Cell	17
5.	Schematic for 2.55 MHz Oscillator.	20
6.	Cross-Section of Optical Density Apparatus	25
7.	Schematic of Optical Density Apparatus Circuitry	26
8.	Conversion Curve Relating Cell Concentration to Detector Current.	28
9.	Photographs of Yeast Collecting.	32
10.	Voltage Dependence of Yield at Frequencies of 10^5 Hz and $2.55 \cdot 10^6$ Hz.	36
11.	Dependence of Yield on Concentration	37
12.	Variation of Collection with the Square Root of the Length of Time the Field is Applied	39
13.	Frequency Dependence of Yield.	40
14.	Variation of Yield with Frequency and Suspension Conductivity	42
15.	Low Conductivity Collection for Cells from Cultures of Different Ages	44
16.	High Conductivity Collection for Cells from Cultures of Different Ages	45
17.	Collection of Dead Cells	47
18.	Collection of Dead Cells; Repeat	48

LIST OF FIGURES (Continued)

Figure		Page
19.	Effect of Ion Valence on Yield.	52
20.	Ion Effect as a Function of Ion Concentration as Expressed Through Resulting Conductivities.	53
21.	Ion Effect; Repeat.	54
22.	Occurrence of Cell Rotation as a Function of Frequency and Conductivity for Cells of Different Ages.	59
23.	Phasor Diagram of Complex Permittivity in Terms of its Real and Imaginary Components	78
24.	Phasor Representation When the Conduction Current and Displacement Lag Behind the Impressed Field.	78
25.	Total Current for the Ideal Case of No Phase Differences. .	82
26.	Total Current for the Case of Phase Differences	82
27.	Illustration of Complex Conduction Factor	85
28.	Two Shell Model of Yeast Cell	99
29.	Polar Coordinate System	101
30.	Relation of Volume Occupied by Cells to Volume Swept Out. .	101
31.	Theoretical Variation of $\chi^{\frac{1}{2}}$ with Frequency at Various Experimental Conductivities for Two Shell Model	122
32.	Comparison of Experimental and Theoretical Frequency Dependences	124
33.	Theoretical Calculations of $\chi^{\frac{1}{2}}$ Assuming All Permittivities and Conductivities to be Real and Frequency Independent .	125
34.	Theoretical Calculation of $\chi^{\frac{1}{2}}$ Using Two Shell Model to Represent Autoclaved Cells.	128
35.	Electrical Model for Conductivity Measuring Device Including Electrode Polarization.	143
36.	Equivalent Circuit as Measured on an Impedance Bridge . . .	143
37.	Resistance at Different Frequencies of a Standard 10^{-2} N KCl Solution as Measured with Stainless Steel Electrodes.	146

LIST OF FIGURES (Continued)

Figure Page

38. FORTRAN IV Program for Computing χ and $\chi^{\frac{1}{2}}$ for Dead Cells at Different Frequencies. 150

CHAPTER I

INTRODUCTION

In recent years living organisms, especially microorganisms, have become the objects of study of a large and diverse segment of the scientific community. They are no longer the private domain of the life scientist but are now being investigated by chemists, physicists, and engineers. This influx of physical scientists has resulted in the development of many new approaches to biological problems. Many of the new methods, for example, electrophoresis, have subsequently become routine procedures for the microbiologist. It is one purpose of this work to add still another technique, dielectrophoresis, to this rapidly expanding arsenal. It is based on the fact that cells with different electrical characteristics will behave differently in a nonuniform electric field.

The effect a nonuniform electric field on an ideal particle (a perfect insulator) free to move depends on the charge and the dielectric constant of the particle considered. If the particle possesses a net charge then there is an electrostatic interaction between the charge and the field, resulting in particle motion. This motion is known as electrophoresis. If the material contains permanent dipoles, they will tend to become aligned with the field and will then experience a force in the direction of strongest field. The material will also contain

dipoles induced by the field, and these too will be forced in the direction of increasing field strength. The translational motion of a particle due to the interaction of a nonuniform electric field with all of its dipoles, either permanent or induced and expressed through the dielectric constant, has been defined by Pohl (1) as dielectrophoresis. The force associated with this motion is termed the dielectrophoretic force. Dielectrophoresis is normally a much smaller effect than electrophoresis.

An illustration of the contrast between electrophoresis and dielectrophoresis is given in Figure 1. Here positive, negative, and neutral particles are in a nonuniform field produced by two concentric spheres. The charged particles obey the laws of electrostatics and move toward the oppositely charged electrodes, the positive charge toward the outer wall and the negative charge toward the central sphere. The neutral particle is polarized by the field and its individual charges also experience forces toward the oppositely charged electrodes. Since the negative charges lie in a stronger field then the positive charges, they experience a stronger force. The result is a net force on the particle in the direction of the central electrode. A change in polarity of the electrodes causes the charged particles to reverse their directions of motion. The neutral particle, however, continues to be pulled inward. An alternating voltage will cause the electrophoresis to average to zero, leaving only the dielectrophoretic effects. It is important, then, in dielectrophoretic studies to use alternating fields.

If the particle is not in a vacuum but rather in some suspending fluid then the field also attracts the fluid. The resultant force on the particle in this case is the difference between the forces on each constituent separately and is proportional to the difference in their

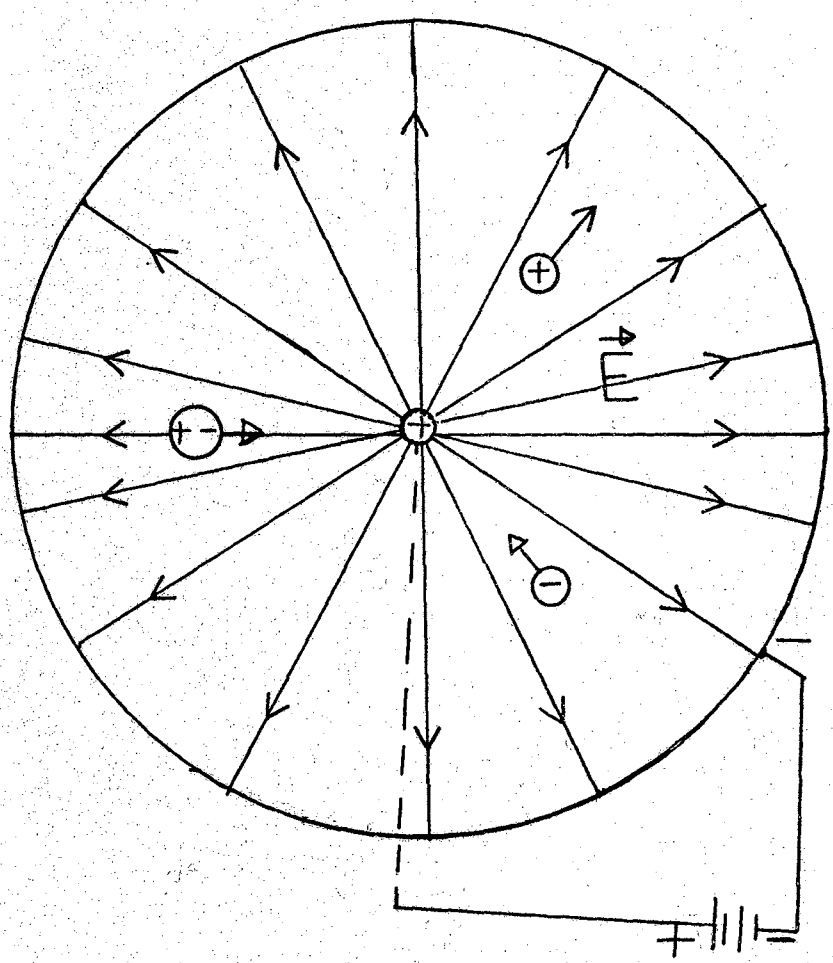

Figure 1. Electrophoresis and Dielectrophoresis

dielectric constants. This results in the following general statement for ideal cases. "The material with the higher dielectric constant will be forced to the region of highest field strength."

Thus if the neutral particle in Figure 1 has a dielectric constant greater than that of the suspending fluid, then it will move to the central electrode. If the dielectric constant of the particle is less than that of the fluid, the particle will be attracted less than the surrounding fluid, resulting in a net force outward, away from the center. If there were two types of particles suspended in a fluid of dielectric constant intermediate between those of the particles, such as is Figure 2, then the particles with the higher dielectric constant would be attracted to the central electrode, while those with the lower one would be repelled. This is the basis of separation using dielectrophoresis.

Adequate theories exist which explain the dielectrophoresis of ideal particles in ideal fluids. However, there is no accepted theory to explain the behavior of nonideal particles in real environments with alternating fields. The second purpose of this work is to put forth such a theory, based on an appropriate model, which will explain the dielectrophoresis of an aqueous suspension of a specific organism, namely yeast cells. This theory allows not only for dispersions with frequency of the dielectric constants but for dispersions in the conductivities as well. As a result, the high "apparent" dielectric constants of organic materials at low frequencies are seen to be due to Maxwell-Wagner type surface effects.

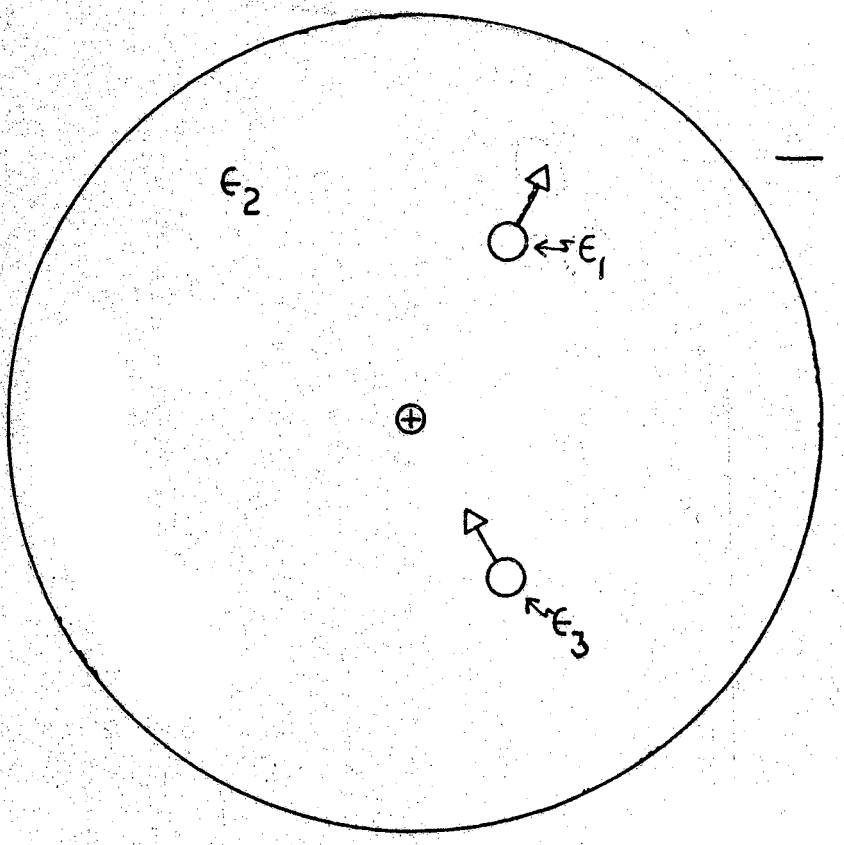

Figure 2. Dielectrophoretic Separation for Different Particles with $\varepsilon_3 > \varepsilon_2 > \varepsilon_1$.

Choice of a Model

As has already been pointed out, the dielectrophoretic force on an ideal suspended particle depends on the dielectric constant of both the particle and the suspending fluid. For nonideal particles the force is not so simple in that it is also a function of frequency and conductivity. There are two approaches that can be taken for the nonideal case. One is to continue to use the ideal particle equations and use the experimental results to define corresponding apparent dielectric constants which would be frequency and conductivity sensitive for the materials. A similar approach is often used for the case of A.C. capacitance measurements, wherein the variation of capacitance with frequency is attributed solely to a changing dielectric constant. This leads to enormously high dielectric constants for some materials and suspensions in the low frequency range.

The alternative approach is to develop a more complex force expression which also takes into account the other relevant factors and explains the results in terms of plausible physical processes. The latter course allows the results of a dielectrophoresis experiment to be predicted using parameters that are obtained by other unrelated techniques. For example, suppose the only determining factors are the dielectric constants of the materials, their conductivities, and the frequency of the applied field. If these parameters are each determined ahead of time, and if the theory is correct, then the dielectrophoresis of the mixture can be foretold. This approach then provides a check for the correctness of the theory. In the first appraoch the theory is correct by definition of the parameters and so cannot provide any new information about the underlying physical processes.

The second method is the preferred one and will be the one used. It requires the derivation of an expression for the dielectrophoretic force on an arbitrary configuration of materials. So that the expression may be general, each material is not only assigned a conductivity and a permitivity but these are allowed to be complex in time.

As a check of the correctness of the theory, the force equation is applied to a sample system consisting of an aqueous suspension of yeast cells which for calculation purposes is represented by an appropriate model. The comparison of these calculations with the experimental results for the same system tests the validity of the theory and the correctness of the model.

History of Dielectrophoresis

The effects of nonuniform fields were first noted, although probably not appreciated, by Gilbert (2) when he observed the deformation of a water droplet when rubbed amber was brought near it. The first useful dielectrophoretic technique was not developed until much later when Quincke (3) determined the permitivities of insulating liquids by measuring the height of the liquid between parallel plate electrodes as a function of the applied voltage. Similar measurements, differing only in minor details, have since been made by several investigators (4-9).

The use of nonuniform electric fields to produce particle motion was introduced by Soyenoff (10) when he observed the coalescence of coal dust suspended in toluene. He was the first to note that a body of dielectric constant higher than the medium would move into the region of strongest field. Similar results were obtained by Winslow (11) for silica gel in kerosene. Pohl (1) removed carbon black from a polyvinyl

chloride-di-isopropyl ketone solution and defined the motion as dielectrophoresis. Later he studied the quantitative effects of the variation of several important parameters, including field strength, electrode size, and particle size (12), and developed the basic theory (13, 14). Pohl and Plymale (15) were able to separate mixtures of minerals according to dielectric constant using dielectrophoresis and introduced a field shape which provides a constant dielectrophoretic force. Using a different apparatus, Verschure (16) was also able to separate mineral mixtures into their component parts according to dielectric constant. All of the work to this time involved the ideal case of insulating particles in insulating liquids. The study of particles in conducting liquids was initiated by Hawk (17) and continued by Feeley (18) and Chen (19), with the results that the dielectrophoresis was not only a function of the dielectric constants, but also depended on conductivities and frequency of the applied field.

The reaction of biological materials to electric fields was probably first studied by Muth (20), who subjected fat particle emulsions to high frequencies and noticed pearl-chain formation (the end-to-end attachment of the particles producing a formation similar in appearance to a chain of pearls). Liebesny (21) also observed these formations for erythrocytes in high frequency fields. In a penetrating analysis Heller and his coworkers (22) studied the responses of various organisms to high field strengths in the frequency range 10^5-10^8 Hz. He observed pearl-chain formation, orientation, preferential movement, rapid rotation, and frequency optima for alignment. Schwan and his co-workers (23, 24) have presented theoretical treatments for pearl-chain formation and orientation of biological particles. Schwan (25) has also given a

comprehensive review of the electrical properties of tissue and cell suspensions. His reports of extraordinarily high dielectric constants (10^2-10^4) for cell and tissue suspensions, prompted Pohl and Hawk (26) to apply dielectrophoresis to such a suspension. Their results were that under the proper conditions of high frequency and low suspension conductivity, live yeast cells could be separated from dead ones.

It is convenient to delay further literature references to the various chapters dealing with the particular topics of interest. For example, in the chapter concerned with the different possible mechanisms for polarization dispersion, a review of the various polarization models, beginning with Debye's rotating dipole model (27), will be given.

Scope of This Study and its Implications

The present study extends the work of Pohl and Hawk in that it investigates in detail the response of yeast cells to a nonuniform electric field and attempts to explain the results. The problem can be broken into seven major parts. They are:

1. Development of the necessary equipment and procedures to ensure meaningful results.

2. Investigation of the response of yeast and its dependence on various controllable parameters.

3. Derivation of a general expression for the dielectrophoretic force of an arbitrary system of materials.

4. Selection of an appropriate model to represent the special case of a yeast cell in aqueous suspension.

5. Application of the general force expression to this model and calculation of the theoretical force.

6. Calculation of the expected response to this force as a function of the same experimentally controllable parameters.

7. Comparison of the calculated behavior to that which is experimentally observed.

The possibilities for the future uses of the dielectrophoresis of biological systems seems almost limitless in extent and variation. The only organism to be studied in detail to date has been yeast, although preliminary studies have been made on canine erythrocytes and thrombocytes, and on flavobacteria. Detailed investigations of these organisms are under way in this laboratory (28). The number of organisms remaining to be studied is vast indeed. At present, the techniques and theory are still comparatively crude and yet it has been possible to separate live cells form dead ones and give a plausible explanation. In the future, with refined equipment, methods, and theory, it may be quite possible to distinguish cells which have more subtle differences, such as differing cell constituents or growth rates, and explain these differences. This would give us a powerful tool for rapidly investigating the effects of some external agent and locating the site of its action.

CHAPTER II

EXPERIMENTAL PROCEDURES AND EQUIPMENT

Experiments in General

Before dielectrophoresis can be applied to a particular test system, there are several decisions concerning experimental approach which must be made. The important considerations are the configuration of the electrodes which will produce the nonuniform field, the selection of a critical parameter which reflects changes in the dielectrophoresis and thus measures the effect of the field, and the determination of the variable quantities upon which the chosen critical parameter depends.

A nonuniform field will be produced by any electrode design other than parallel plates. The number of possible configurations can be greatly reduced by requiring that the electric field be easily calculable. This desire for mathematical simplicity leads to the standard geometries of concentric spheres and concentric cylinders. Other configurations have been devised which can be approximated as cylinders or spheres but are easier to construct and offer experimental advantages. These include a wire perpendicular to a flat plate (pin-plate), a wire parallel to a flat plate (wire-plate), two coaxial wires end-to-end, (pin-pin) and two parallel wires side-by-side (wire-wire). The choice between these four designs for a particular experiment depends upon the experimental characteristics desired. Once a field shape has been chosen, the

next problem is to select a dependent variable which will give an indication of the effect of the field. Several such critical parameters exist including the dielectrophoretic force, the velocity of a test particle, and the rate at which material is built up at one of the electrodes. The force has been used as the critical parameter on several occasions (17, 18, 19) and is convenient when dealing with a single, large particle. The velocity of a particle has not been used, but there are no obvious reasons why it would not be useful in certain systems. The most widely used critical parameter is the rate of collection at an electrode (12, 13, 15, 29, 30). It is most often expressed as a "yield", which is the amount collected within a specified time, and is best suited to systems which are suspensions of large numbers of particles.

After the dependent variable has been selected, the various independent variables need to be ascertained so that the necessary equipment and procedures can be provided which will allow these quantities to be varied. For the case of a suspension of particles with the yield as the critical parameter, these independent variables are: the size and shape of the particles, the conductivities and permittivities of both the particles and the suspending medium, the concentration of particles, the frequency and strength of the applied field, and the elapsed time. The quantities which can be most easily varied and measured are the suspension conductivity, particle concentration, frequency, field strength and elapsed time.

The Test System

One objective of this work has been given as the study of the di-

electrophoresis of a living organism. The test system chosen was an aqueous suspension of yeast cells. A brief account of the reasoning behind this choice will now be given.

The desire to use an organism with a simple shape restricted the choice of materials to one-celled microorganisms. This in turn restricted the size and thus led to the decision of using a suspension rather than a single particle. The suspension would also tend to give more reproducible "average" results which were less dependent on the particular growth stage of each cell.

Besides being of simple shape, it was also desired that the organism be easy to grow, relatively simple to work with, non-hazardous, hardy enough to undergo the planned extremes of conditions, non-motile, and as large as possible. Baker's yeast, Saccharomyces cerevisiae which was the organism used by Pohl and Hawk (26), seemed to satisfy all of these requirements and was chosen as the test organism.

Yeast Morphology

It is appropriate at this point to give a brief description of yeasts in general and Baker's yeast in particular. For more detailed information the literature should be consulted (31, 32, 33).

Yeasts are classified as higher protists in the group of fungi. They are plants which have a well-defined nuclear membrane and chromosomes, exhibit mitotic cell division, but lack chlorophyll so that they cannot synthesize their own food. They can obtain their energy either by aerobic oxidative dissimilation or by anaerobic fermentation depending upon the circumstances. Yeasts generally occur as unicellular organisms in a variety of shapes and can reproduce vegatatively by

budding and fission and sexually by sporulation. Baker's yeast reproduces almost exclusively by budding.

In general, yeasts are larger than bacteria. Baker's yeast cells are spherical to ovoid and the average size is 6 x 9 microns. They have no organs of locomotion and thereby are non-motile. The yeast cell is surrounded by a rigid cell wall and a cytoplasmic membrane. The thickness of the membrane is approximately 80 Å and is believed to consist of two protein layers separated by a layer of lipid. This lipoprotein structure is similar to that for other types of cell membranes.

Yeasts will grow over a wide temperature range with the optimum for most yeasts being 20 to 30°C. Their nutrient requirements are minimal but they will usually grow most abundantly on complex media. The acid tolerance varies with the strain or species and ranges from pH 2.2 to 8.0. Some varieties can grow in high concentrations of salt or sugar.

Procedures for Growing Yeast

The original stock was obtained from commerical dry yeast by growing it on peptone-dextrose agar. The streak-plate method (31) was used to isolate a pure colony (one which arises from a single organism and thus, barring mutations, has the same characteristics throughout). The growth media consisted of large test-tubes of 4% dextrose-1% peptone solution which had been sterilized by autoclaving for at least 15 minutes. Initially this medium was innoculated with a sample from the pure colony. The resulting growth at room temperature was used to innoculate, via a sterile wire transfer loop, a second growth tube. The first tube was then available for use in the experiments. A third tube

was innoculated from the second before it was used, a fourth from the third, and so on. This procedure was continued, thereby maintaining a constant supply of freshly grown cells.

Equipment

Most of the equipment and procedures to be described here would be necessary for the study of any suspension, although the details might vary from one system to another. Because of this wide-ranging applicability, the descriptions will be in sufficient detail to allow the setup to be repeated elsewhere.

Electrode Design

The configuration originally chosen was that used by Pohl and Hawk (26), a pin-plate design, but was subsequently replaced by a pin-pin arrangement which produces exactly the same field. The rounded pin tips act essentially as two separated spheres. Near the tips, this field can be shown to be approximately equivalent to that produced by concentric spheres and this approximation will be made later to simplify calculations.

The pin-pin electrode arrangement is shown in Figures 3 and 4. The electrodes are made from 22 gauge, .51 mm diameter, platinum wire mounted inside a cylindrical well in a plexiglass plate. The plate dimensions are 32 x 76 x 3.4 mm, which makes it a convenient size for mounting on a microscope stage for viewing. The cylindrical well, which holds the suspension, is 1.7 mm deep and 4.0 mm across. The pin tips were made approximately spherical by applying abrasive paper to them while they were being turned in a high speed drill. When the tips

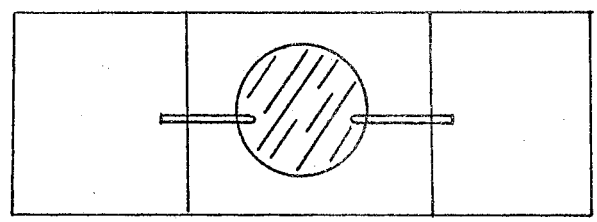

Top View

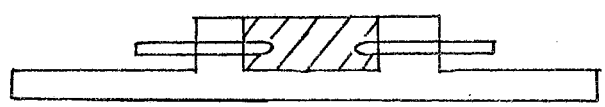

Side View

Figure 3. Diagram of Pin-Pin Dielectrophoresis Cell.

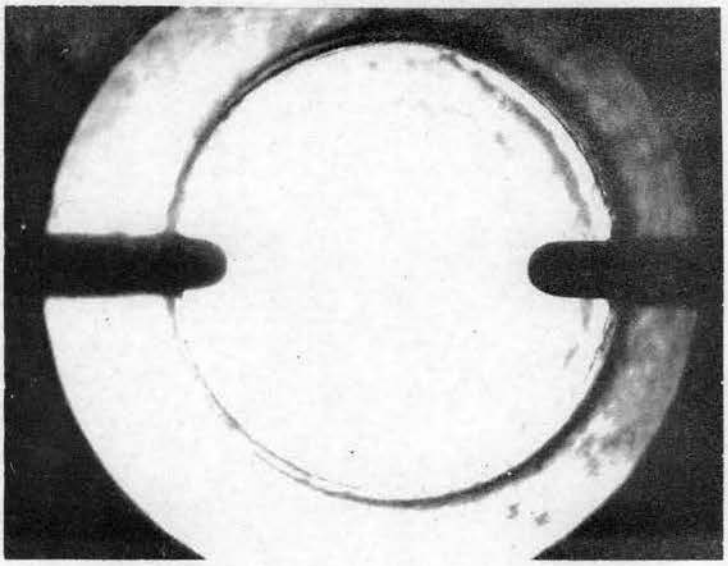

Figure 4. Photograph of Pin-Pin Cell

were sufficiently rounded, they were polished to remove any sharp edges by using increasingly finer grades of abrasive paper. A final polishing using 1/4 micron diamond dust brought the electrodes to a sufficiently smooth finish. The pins were cemented in place with a plexiglass solvent, ethylene dichloride, and were separated by 2.75 mm tip to tip. Electrical connections were made by soldering a wire to the exposed end of each pin. When the electrode well is filled with a suspension and mounted on a microscope stage, the response of its contents to an applied voltage can be viewed and measured.

The pin-pin arrangement is preferred over the pin-plate design because of its easier construction. It is preferable to the more exact and also easily constructed vertical concentric cylinder combination because it offers better optics. Since the yield measurements depend on estimating the amount of material collected at the strong field electrode, the view of this region must be as clear as possible. In the concentric cylinder design, the strong field region runs the full length of the central wire. For a vertical wire, the light seen through the microscope must travel through this entire thick region of concentrated cells and is considerably distorted by the diffraction and refraction of the light passing around and through the many collected cells. On the other hand, the regions of high field near the spherical pin tips are in radial planes, so that the viewing of the axial plane normal to the light is not obstructed by a great number of cells above and below the plane.

Voltage Supplies

One of the keys to successful studies with dielectrophoresis is

the availability of moderate voltages over a wide range of frequencies. In our studies, several different instruments were used to provide voltages over the range from 5 Hz to 150 MHz. The instrument used most often was a Hewlett-Packard 200 CD audio oscillator which was continuously variable between 5 Hz and 600 KHz. Its maximum output was about thirty volts, so that when voltages higher than that were required, a Lafayette KT615 audio amplifier was used to step up the voltage. A crystal driven oscillator which produced a 2.55 MHz signal at up to 200 volts was designed and built by the O.S.U. Electrical Engineering Department. A schematic of the electrical circuitry appears in Figure 5. It requires +300 volts and -150 volts from a power supply. In our case two Lambda C-280M power supplies were used. Higher frequencies were supplied by a Heathkit DX-60B transmitter using a 7.334 MHz crystal. The harmonics available were 14.7, 22.0, and 29.4 MHz and the maximum voltage obtainable ranged from 30 volts at 29.4 MHz to 50 volts at 7.33 MHz. The highest frequencies, 50.7 MHz and 152 MHz, were produced up to 50 volts with an Ameco TX-62 transmitter. In order to dissipate the power generated by the transmitters, it was necessary to connect the test cell in parallel with a Heathkit Cantenna 50 ohm dummy load. In one instance frequencies in the range from 260 MHz to 910 MHz at voltages of the order of 8 volts were generated with a General Radio 1209-C oscillator.

Frequency Monitoring

It turns out that the frequency is a very important parameter in dielectrophoresis studies. Thus it is critical that the frequency of the applied voltage be as monochromatic as possible. Variations about

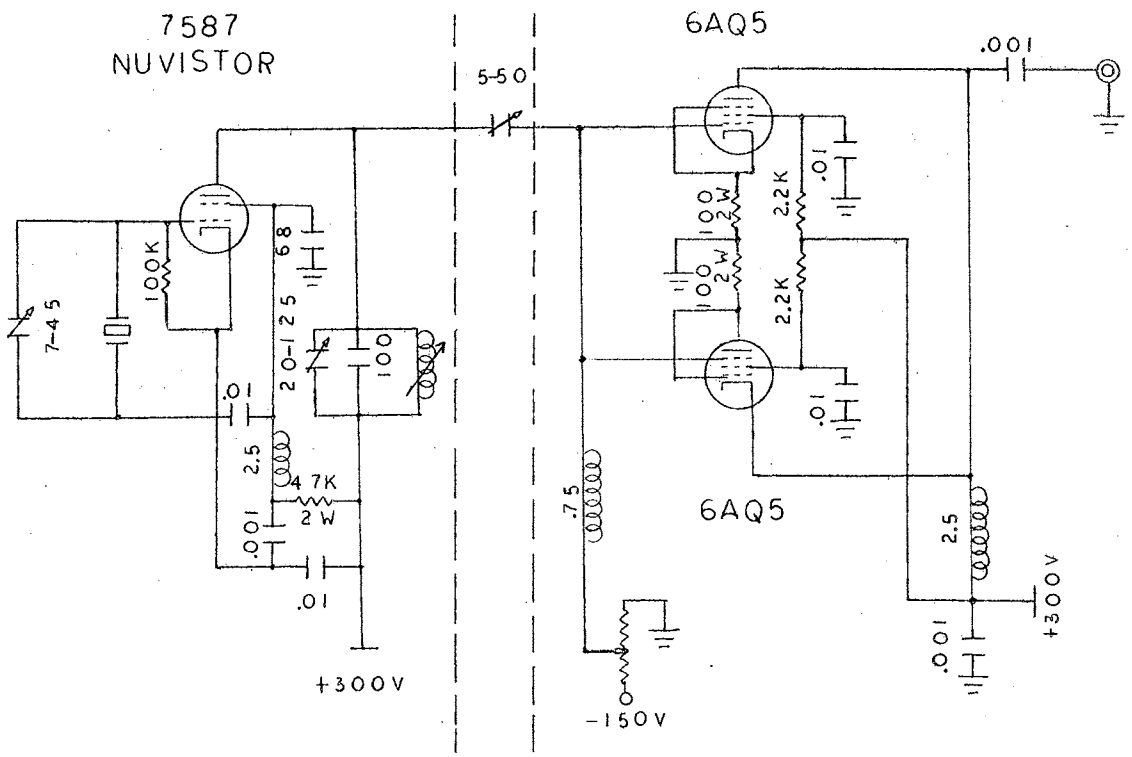

Figure 5. Schematic for 2.55 MHz Oscillator

an average frequency will not cause significant errors but the inclusion of harmonics, sub-harmonics, or sixty-cycle hum could prove disastrous. It is therefore necessary to monitor the frequency of the applied signal with an appropriate device. A good grade oscilloscope is the most convenient method of doing this. The one used in these experiments was a Hewlett-Packard 140A . An oscilloscope can also indicate whether the signal is truely sinusoidal as is assumed in the calculations.

Voltage Measurement

The wide range of frequencies involved restricts the choice of voltmeters that can be used. The one selected was a Hewlett-Packard 410B vacuum tube voltmeter. It was accurate to ±3% at frequencies below 400 MHz and gave relative indications up to a 1 GHz. The a.c. voltage limit was 300 volts.

Conductivity Measurement

It has been found that the conductivity of the yeast cell suspension has a considerable effect on cellular response to a nonuniform field. For this reason it is very important to have an accurate measurement of the conductivity.

By definition the conductivity, σ , is the proportionality factor between the current density and the field strength. For a medium between two parallel plates, it is easily shown (see Appendix A) that the conductivity is inversely proportional to the resistance. Therefore if the resistance can be measured, then σ can be calculated.

Conducting solutions present some problems to the simple calcula-

tions of σ. A direct current will produce electrolysis at the electrodes, modifying them with time, and causing the resistance to be time dependent. Therefore, alternating currents are to be preferred. However, this complicates the analysis by introducing capacitance effects. It is the accepted procedure to assume that the system can be modeled as a network consisting of a pure resistance, the solution, in parallel with a pure capacitance, the electrode capacitance. Then if the system is balanced on a bridge against a resistor-capacitor parallel combination, the measured resistance is equal to the suspension resistance and simply related to σ. If the resistance so measured is not highly frequency dependent, then the assumed model is likely to be correct. If however, the resistance varies considerably with frequency, then the measured resistance is being affected by series capacitances (polarization at the electrodes) and it no longer represents the actual resistance of the system. This problem of electrode polarization is very critical and should always be considered when making conductivity measurements. It is treated in more detail in Appendix A.

For electrode configurations other than parallel plates, if the capacitance effects are negligible the conductivity is still inversely proportional to the resistance. Rather than calculate the proportionality factor, the cell constant, from the geometry of the electrodes, it is simpler to determine it by measuring the resistance of a solution of known conductivity. The standard solutions for making these measurements are various concentrations of KCl. If a probe is operating properly, the cell constant will not vary with concentration, so that this is another way to check the validity of the results.

The bridge used throughout this study was a General Radio-1650B

impedance bridge with a resistance range of 10^{-2} to 10^{7} Ω and 1% accuracy between the frequencies 20 Hz - 20 KHz. Measurements were usually made at 1 KHz using the bridge's internal oscillator, although other frequencies were available via a Hewlett-Packard 600 CD Audio oscillator. An external nulling capacitor was connected across the variable resistance arm of the bridge, thereby simulating the R-C parallel combination.

Several dipping type conductivity probes were used. By inserting them into a test tube containing a few ml of solution, the conductivity can be obtained. The various probes included a coaxial arrangement of two platinized platinum rings and parallel plate systems with electrode materials of stainless steel, carbon, shiny platinum, and platinized platinum. The former was a commerical probe, Yellow Springs Instruments 3403, and found to give the best results at high conductivities. At very low conductivities, the shiny platinum probe was found to be the best. The stainless steel and carbon probes gave very poor results with errors being measured in orders of magnitude. For the conductivity range of interest, the Y.S.I. probe was adequate and so was used throughout the experiments. It had a cell constant of 1.1 cm^{-1}.

Concentration Measurement

One of the independent variables for cell suspensions is the concentration of cells. For this reason, an apparatus is required which will allow this measurement to be made quickly and accurately. There are several approaches that can be taken in this regard but the simplest is to use an optical technique.

If a beam of light is passed through a tube containing a suspension of cells, it will be absorbed and scattered by the cells; the amount of

light transmitted being inversely proportional to the cell concentration. This provides a rapid means with which to measure the cell concentration once the transmitted light has been calibrated in terms of it. In our early experiments, this method was used employing a Lumetron Model 401 colorimeter. The colorimeter consisted of a light source, a set of filters, an 18 mm O.D. cylindrical sample tube, and a photovoltaic cell for measuring the transmitted light.

The voltage reading was calibrated at several points by measuring the corresponding cell concentration using a direct microscopic count. This count is made by counting microscopically the number of cells in each of a large number of equal volumes contained in a counting chamber. The average number of cells per unit volume can then be calculated. A Levy No. 3304-A counting chamber, marked in volumes of $1.25 \cdot 10^{-5}$ cc, was used for this purpose.

There were several drawbacks to the use of the Lumetron colorimeter. One was the large volume of suspension, at least 7 cc, that it required. Another was its lack of sensitivity at concentrations below 10^7 cells/cc, which is the range of greatest interest. This necessitated the pereparation of a relatively large quantity of a concentrated cell suspension, determining its cell concentration, diluting it to the standard working concentration, and then needing only a small fraction of it for the experimental tests. The result was an inefficient use of time and cells.

This situation was corrected when the Lumitrom was discarded in favor of a "home-made" optical density apparatus. A cutaway view of its physical features is given in Figure 6 and a schematic of the electrical circuitry appears in Figure 7. It consists essentially of a 6 volt

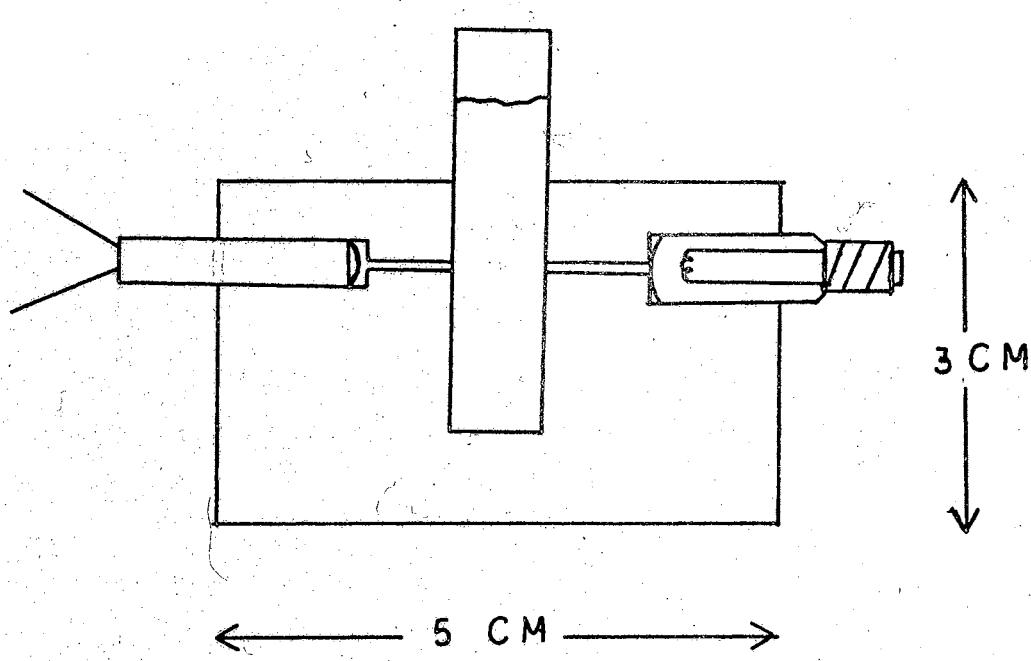

Figure 6. Cross-Section of Optical Density Apparatus

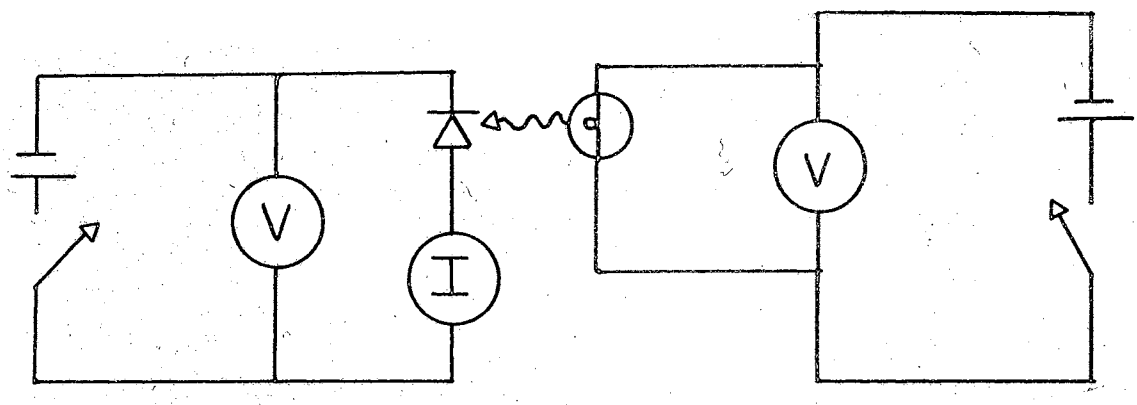

Figure 7. Schematic of Optical Density Apparatus Circuitry

lamp and a Texas Instruments LS-400 photodiode mounted in an opaque bakelite block. A 10 mm square curvette containing the suspension is placed between them. The amount of current passed by the photodiode for a given applied voltage is proportional to the light intensity falling upon it, which is in turn related to the cell concentration. The current was measured with a Keithley 610B electrometer. The conversion from photodiode current to cell concentration was made at a high concentration using the Lumetron colorimeter as a standard, and then at lower concentrations by sequentially diluting the known concentration and measuring the corresponding currents. The resulting conversion curve is shown in Figure 8. The current at infinite dilution was the same as that with the cuvette removed (1.57 Ma), and was used as a reference point. Before a cell concentration measurement was made, the light intensity was first adjusted, by varying the applied voltage across the lamp, until this reference current was obtained. This procedure corrected for any changes in lamp battery voltages and any ageing of the lamp.

The optical density apparatus in this configuration did not have the drawbacks of the Lumetron system. The total volume required was less than 1.5 cc and the optical density corresponding to a cell density of 2.10^6 cells/cc was easily readable to within ±5%. This concentration was found suitable for microscopic viewing and was used in most of the experiments.

The Microscope

The microscopic observations were made with a Bausch and Lomb PB252 photo-binocular microscope. It was equipped with a 1X-2X zoom

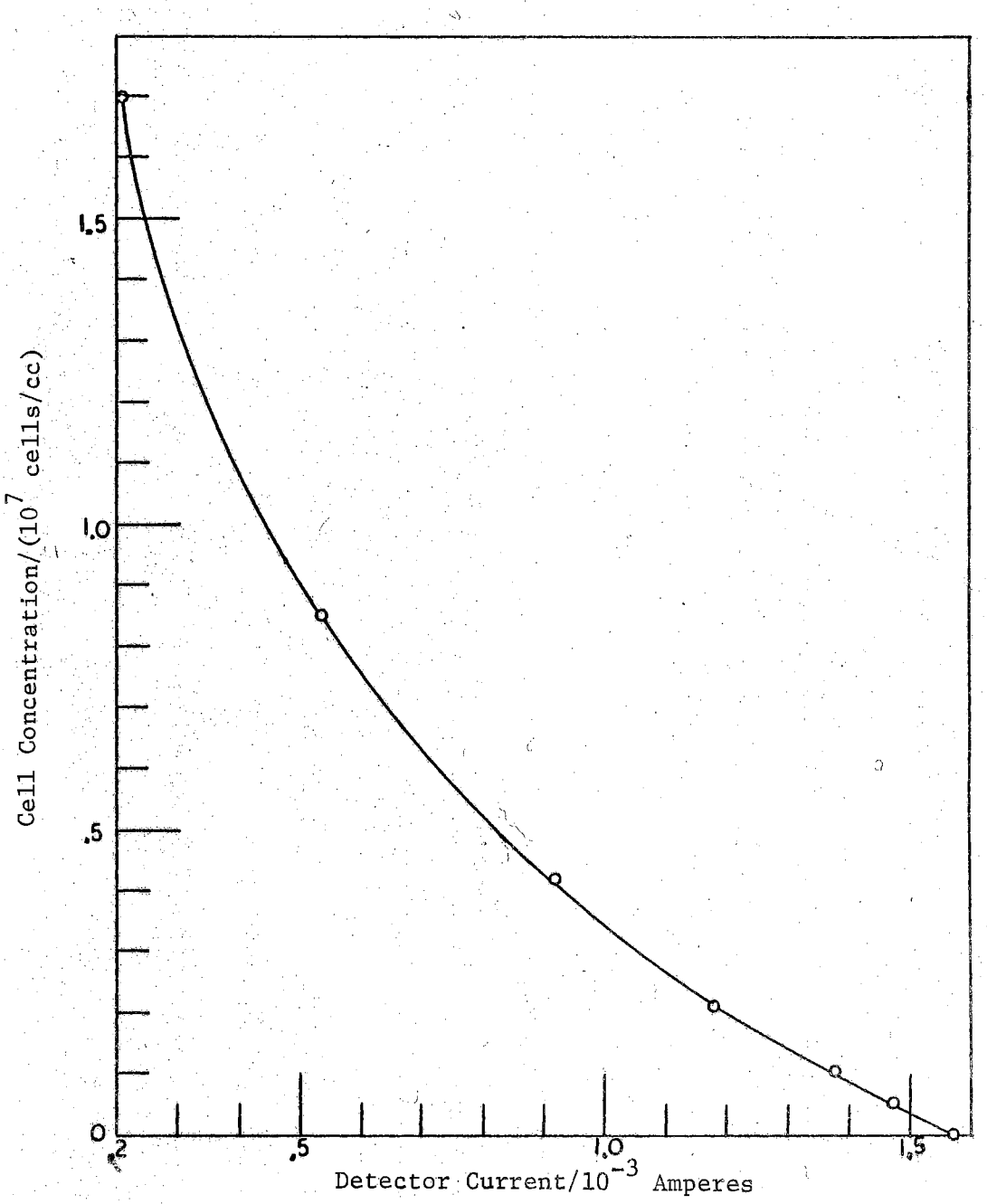

Figure 8. Conversion Curve Relating Cell Concentration to Detector Current.

which, with the proper objectives and 10X wide field eye-pieces, permitted almost continuous variation of magnification from 35 to 1940. However, due to the physical size of the electrode cells, and the small working distance of the high power objectives, the practical upper limit to the magnification was 400. This was with a 20X objective, 10X eye-pieces, and the zoom set at 2X.

A 10 mm reticle marked into 100 divisions was mounted into one of the oculars. It was calibrated with the various objectives at several zoom settings using an Edscorp standard graduated slide. The calculated distances using the reticle were within 3% of the actual distances for the 10X and 20X objectives when the zoom was either in the 1X or 2X position. For intermediate zoom positions, the accuracy was much less. Thus numerical measurements were made with the zoom only in the 1X or 2X position, although observations were made at other powers.

A Typical Run

It seems that the most efficient way to describe the procedures developed for studying yeast is to describe the step by step process of a sample measurement. Consider the determination of the yield as a function of frequency. The other variables must be assigned constant values. Typical values would be a voltage of 20 volts, a suspension conductivity of 10^{-3} mho/m, a concentration of $2 \cdot 10^{6}$ cells/cc, and a collection time of two minutes.

First the yeast cells are harvested from a growing tube via a well-rinsed bulb pipette and mixed with deionized water (distilled water passed through an ion exchange resin). The suspension is centrifuged until the cells are packed at the bottom of the centrifuge tube and the

liquid is poured off. More deionized water is added, the suspension is mixed thoroughly with the pipette, and again centrifuged. This procedure is repeated until the conductivity of the suspension, as measured with the Y.S.I. probe and impedance bridge, is at or below the desired value. In between measurements the probe is kept in a test tube of deionized water to prevent contamination by the probe. If the suspension conductivity becomes too low, it can be increased by the addition of a few drops of dilute KCl solution. (If the cells were to be studied in a solution of a specified molarity, they would be centrifuged once more and then the special solution would be added.)

The cell concentration is controlled by diluting a portion of the solution in the optical density apparatus until the desired concentration is reached. If the suspension becomes over-diluted, this can be corrected by adding a small amount of the undiluted portion to it. After the correct concentration is obtained, another check of the conductivity is made to ensure that the solution has not been contaminated.

Before the electrode chamber can be used, it must be rinsed several times with deionized water. Spraying with a water jet obtained from a squeeze bottle with an attached deionizer is the simplest and surest way to rinse the electrodes. The chamber is then dried using an air jet from a squeeze bottle. This drying is necessary to prevent a dilution of the suspension when it is placed in the chamber. Each time before the well is filled, the suspension should be thoroughly mixed to counteract any settling which might have occurred. Because of the small volume of the chamber (0.21 cc) it has been found that the most accurate method of filling it is to use a 1 cc syringe which is graduated in hundredths. This permits the same volume to be used each time with-

in about five per cent.

After the chamber has been filled, it is mounted on the microscope stage and electrical leads are connected. The frequency and voltage of the applied signal are selected and the connecting switch is thrown, applying the voltage across the electrodes. It is observed that, while the field is on the cells generally migrate to the pin electrode. They attach themselves there, in chain-like formations, commonly called pearl-chains (23), parallel to the field lines. Photographs of a typical collection are shown in Figure 9. The average length of these chains after a given time is designated as the yield and is measured using the reticle in the microscope. For this particular run the lenghts would be measured at the end of two minutes and the field would be shut off.

Once the measurement is complete, the chamber is removed from the microscope stage, rinsed with the deionized water jet, and dried with the air jets. Occasionally not all of the cells are removed from the electrode by this process. In this case a gentle brushing with a soft substance (cotton or a pipe cleaner) is necessary, after which again the chamber is rinsed and dried. It is then filled with more solution, a new frequency is selected, and the procedure is repeated. This is continued for all of the desired frequencies.

At the end of the experiment, and if necessary at selected times throughout the experiment, the conductivity and concentration of the system should be checked. The concentration is not likely to change appreciably, but the conductivity may change by 50% over a period of several hours. This is especially true if the beginning conductivity was quite low, say in the order of 10^{-6} mho/cm, and is due to CO_2

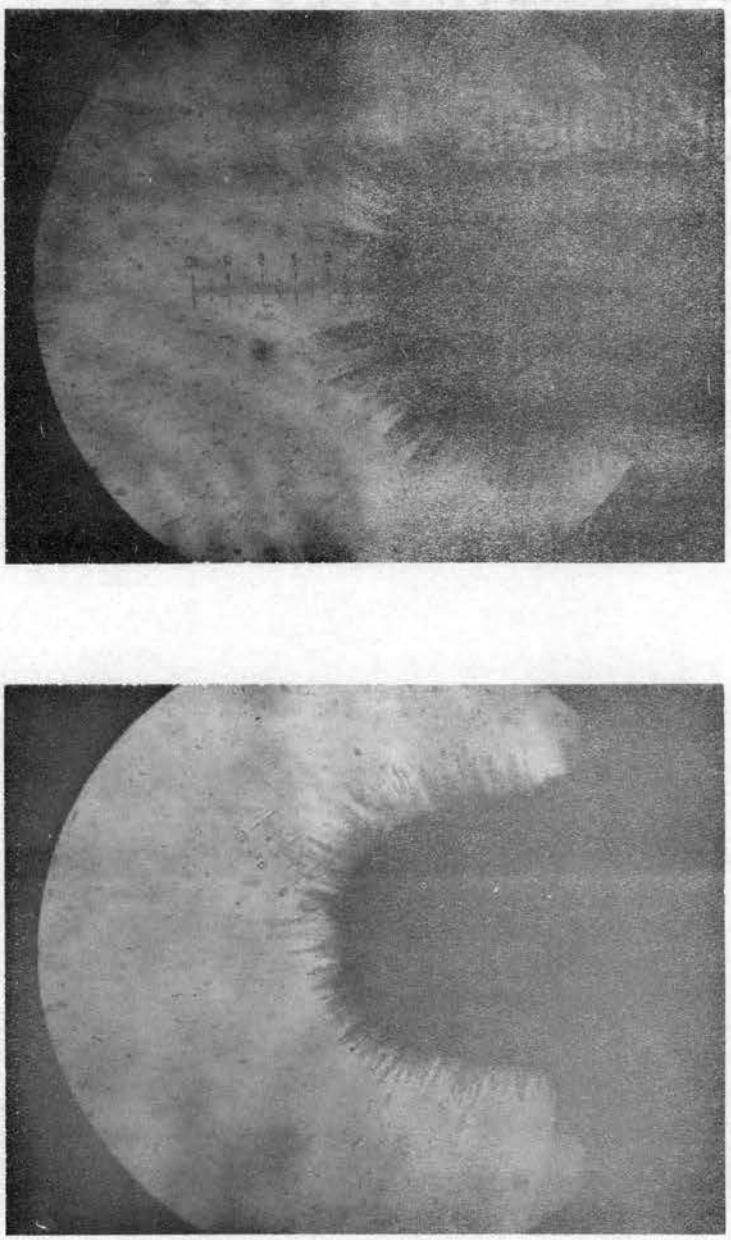

Figure 9. Photographs of Yeast Collecting

absorption from the air and also to ion leakage by the cells themselves.

The preceding procedures have been given for the sample case of determining yield as a function of frequency. For other independent variables, they are altered to fit the particular situations but these changes are for the most part only minor ones.

CHAPTER III

EXPERIMENTAL RESULTS FOR YEAST

The independent variables upon which the yield depends can be divided into two categories. The first contains the basic physical parameters. These are the quantities which would be of importance regardless of the material in suspension and are the frequency, the voltage, the particle concentration, the conductivity of the suspension, and the elapsed time. The second group contains the biological parameters which are those quantities that affect the condition and composition of the cells. These include the colony age, chemical treatment, and exposure to heat or ultraviolet light. These lists of parameters do not of course exhaust all of the possibilities. However, these are the more important ones and do serve to give an indication of what can be done with dielectrophoresis.

The variation of the yield as a function of each of the mentioned parameters will be given for selected conditions. Some of the results will be general in that the trends would be unchanged if the conditions were varied. Other results will not be general and will explicitly depend on the values of the other parameters. The generality will be pointed out in each case.

In each of the data sets to be presented, the yield is shown as a function of a selected parameter. The yield is the average length of the longest chains attached to the electrodes after a particular elapsed

time. It is measured to the nearest division of the microscope eyepiece scale when the microscope is at 100 power. One division corresponds to an object length of 10.3μ or about 1.5 yeast cell diameters. The dielectrophoretic collection rate, or DCR, is defined as the yield after a unit elapsed time.

Dependence on Physical Parameters

Voltage

Figure 10 shows the variation of yield with applied voltage at two different frequencies, 10^5 Hz and $2.55 \cdot 10^6$ Hz. The conductivity was $6 \cdot 10^{-4}$ mho/m, and the elapsed time for each measurement was 1 minute. It is seen that the response is approximately linear with moderate voltages. It deviates from linearity at high voltages primarily due to the strong stirring that results. When the stirring is moderate it brings more cells close to the pins where they can be held by the stronger field there; thus causing an increase in collection. At the highest voltages, though, this stirring becomes turbulent, rips collected cells from the pin, and hence reduces the yield. This is illustrated by the fact that the deviation begins at a lower voltage for 100 KHz which also has more attendant stirring than at 2.55 MHz. The fact that the yield is directly proportional to the voltage holds true for various sets of conditions and appears to be a general result.

Cell Concentration

The yield as a function of cell concentration is shown in Figure 11. An original concentration C_o of about 10^7 cells/cc was prepared and a yield measurement made. The suspension was then repeatedly di-

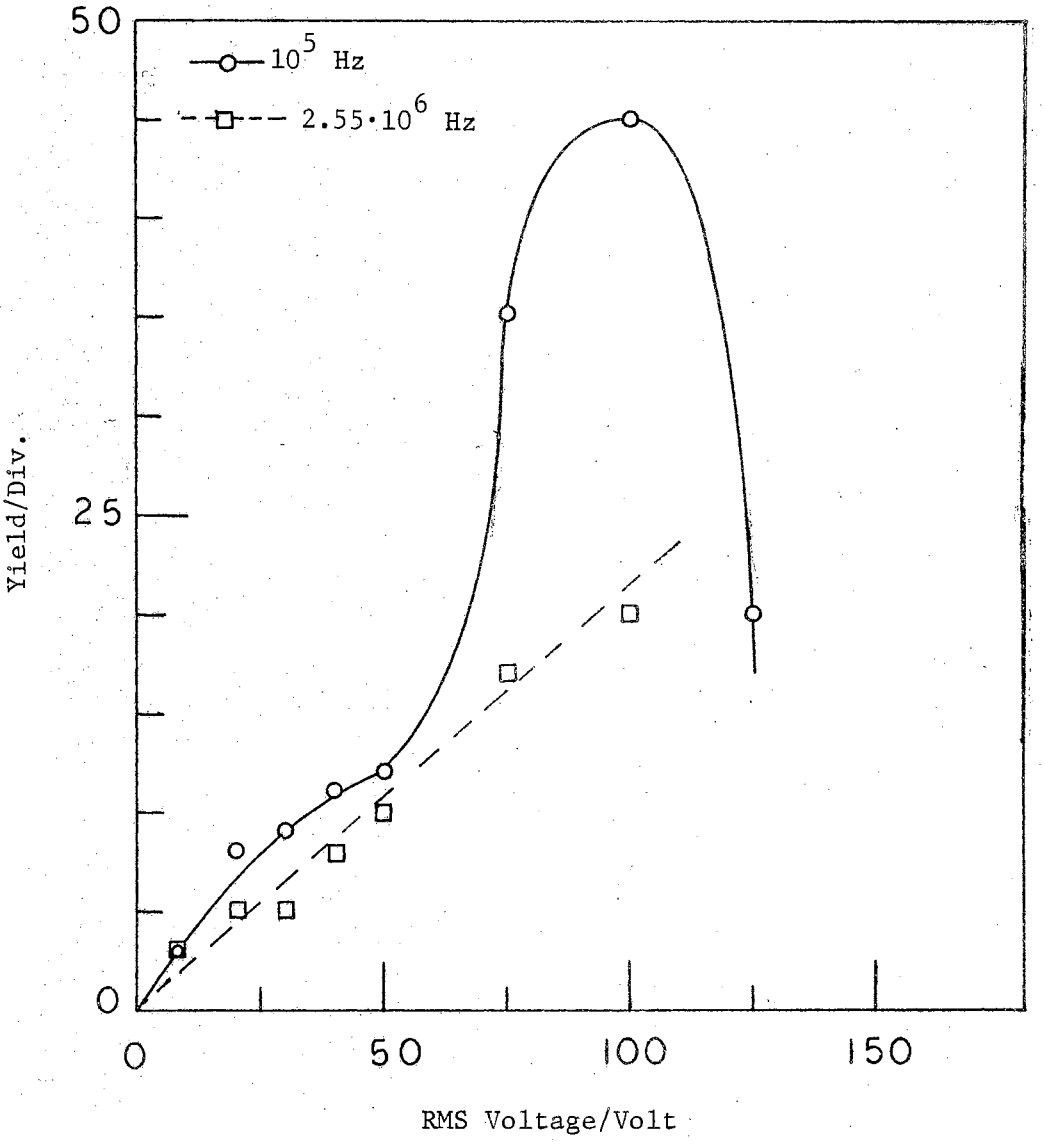

Figure 10. Voltage Dependence of Yield at Frequencies of 10^5 Hz and $2.55 \cdot 10^6$ Hz, $\sigma = 6 \cdot 10^4$ mho/m.

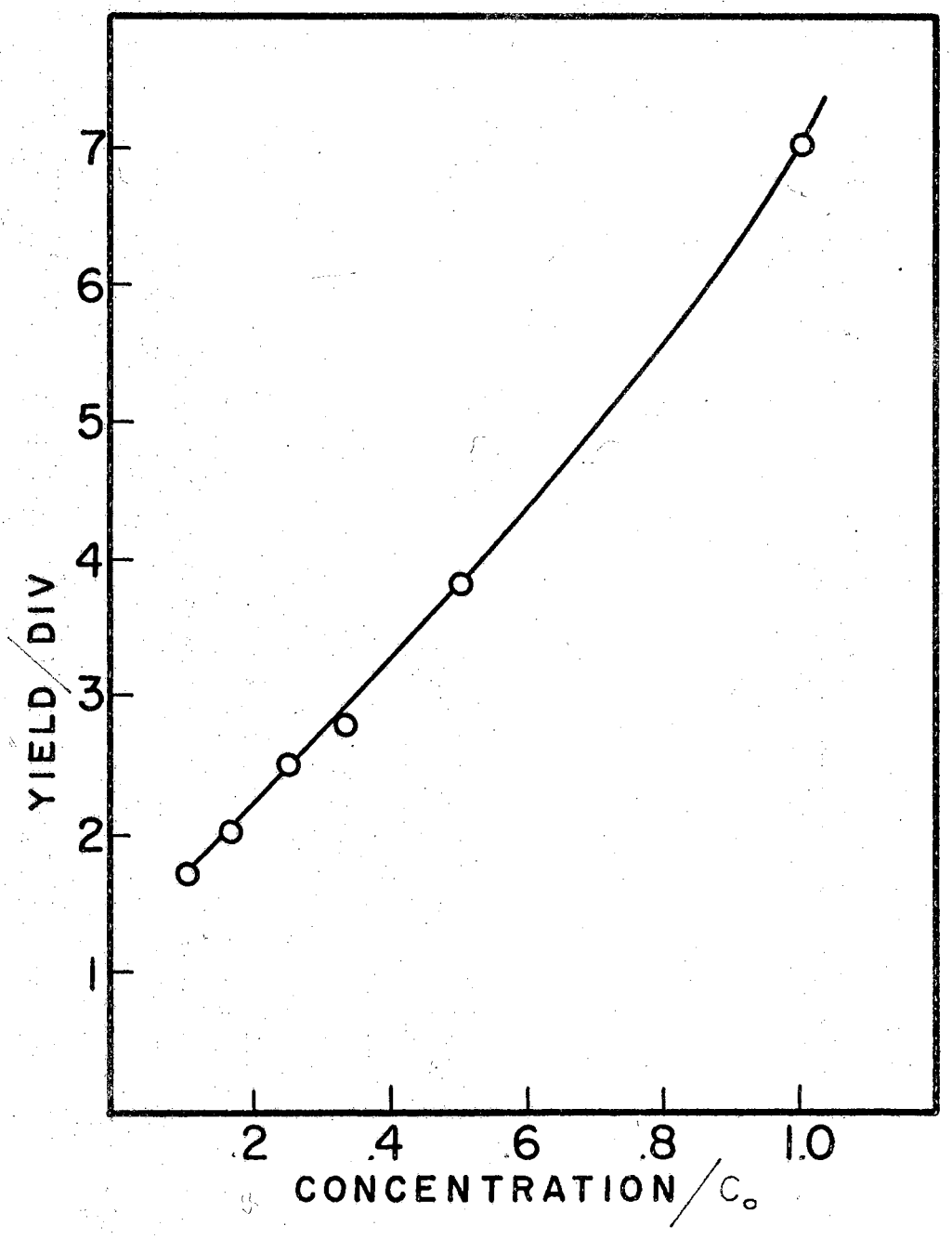

Figure 11. Dependence of Yield on Concentration. V = 10 volts, f = 10^4 Hz, $\sigma = 3 \cdot 10^{-4}$ mho/m.

luted by suitable fractions, with deionized water, a measurement being made after each dilution, until the concentration had been reduced by a factor of 10. The conductivity was about $2 \cdot 10^{-4}$ mho/m, the voltage was 10 volts at 10 KHz, and the measurement time was 1 minute. The results indicate that the yield in general is linear also with cell concentration.

Time

The length of time the voltage is applied across the electrodes will obviously affect the amount of collection. Yield was determined as a function of time by noting it at specified points during the collection. The results are depicted in Figure 12, which shows the yield plotted against the square root of the elapsed time. The reasons for this representation will become clear in Chapter VII. As can be seen a straight line results for the times less than one minute. Beyond this, the yield does not increase substantially.

One reason for this deviation is that because of the small depth of the electrode well, the settling of the cells soon reduces the concentration. The collection process itself also reduces the concentration of the suspension, but this is taken into account to obtain the $t^{1/2}$ dependence.

Frequency and Conductivity

The variation of the yield as a function of frequency of the applied voltage is shown in Figure 13. The voltage was 20 volts, the conductivity 10^{-2} mho/m, the concentration $2 \cdot 10^{6}$ cells/cc, and the time interval was 2 minutes. This shows a rather complicated dependence with

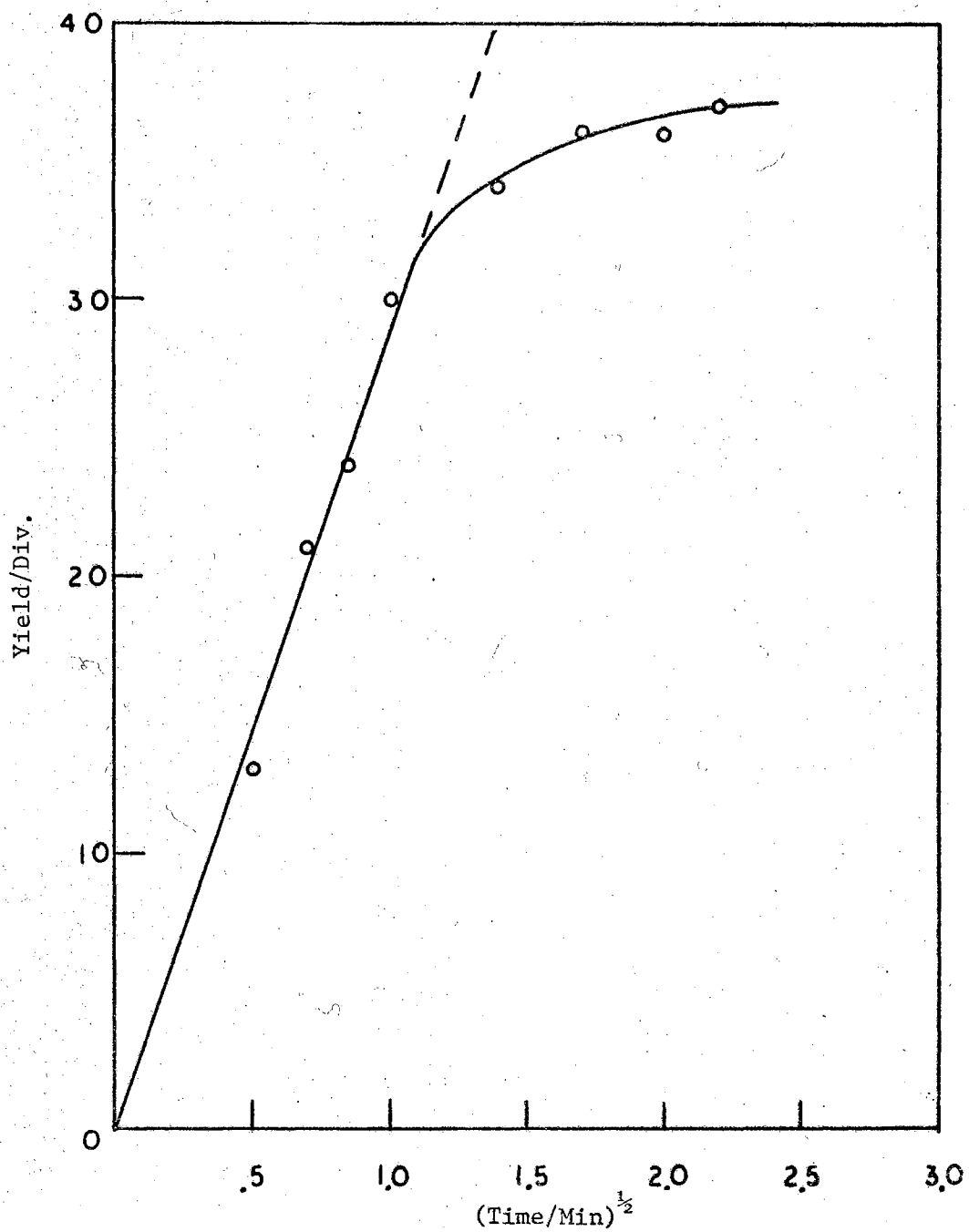

Figure 12. Variation of Collection with the Square Root of the Length of Time the Field is Applied. V = 120 volts, f = 2.55 x 10^6Hz, σ=4 x 10^{-4} mho/m.

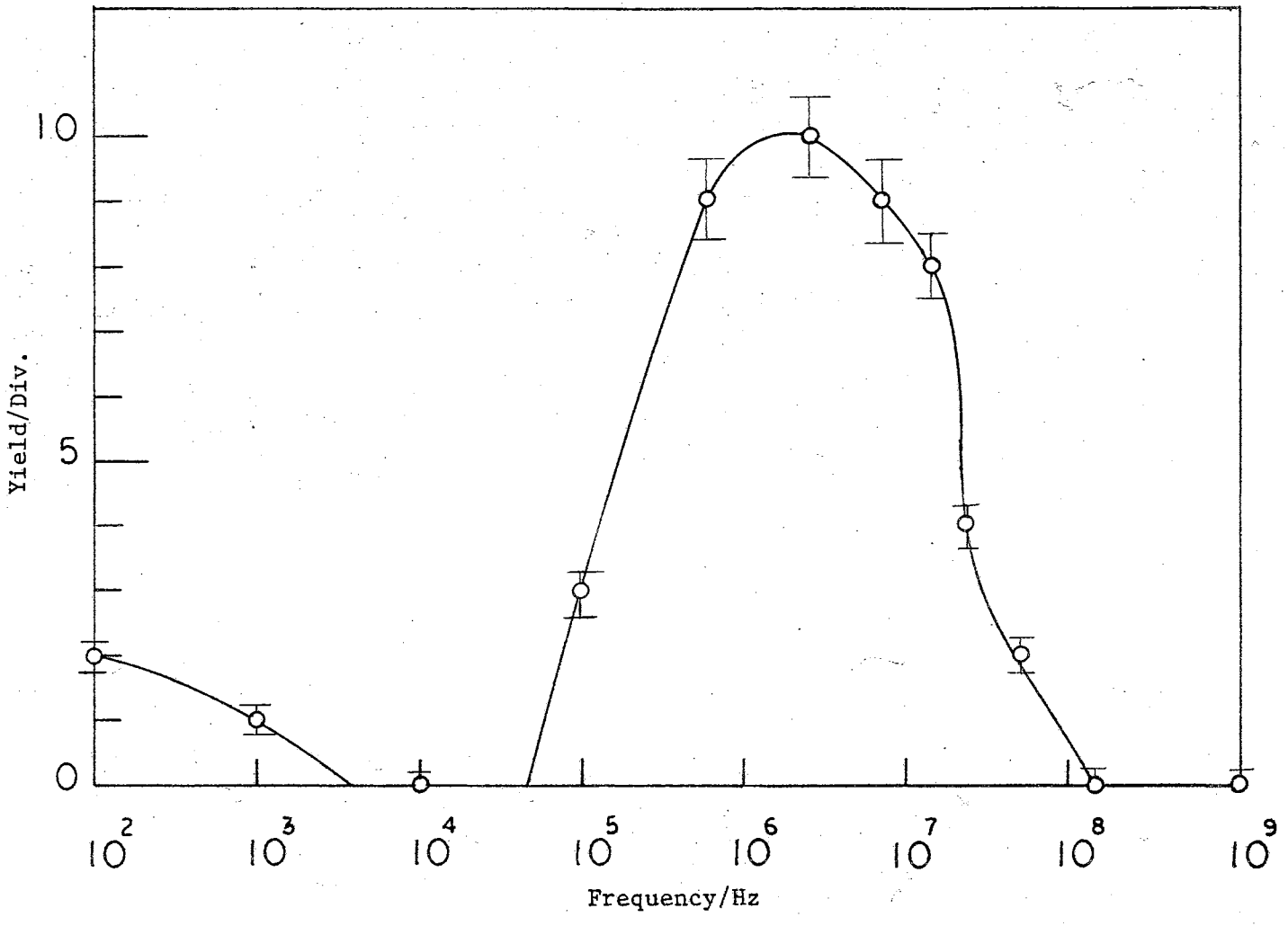

Figure 13. Frequency Dependence of Yield. V = 20 volts, $\sigma = 10^{-2}$ mho/m.

the yield being a minimum at about 10^4 Hz, a maximum around 10^6 Hz, and falling back to zero above 10^8 Hz.

If the experimental conditions are changed by changing the conductivity of the suspension, then the resulting frequency dependence is changed also. This is shown in Figure 14, where the conductivity is varied from $3 \cdot 10^{-4}$ to $9 \cdot 10^{-2}$ mho/m. As can be seen, not only do the magnitudes of the maximum and minimum yields change, but the frequencies at which these extrema occur are also shifted. This would imply that the frequency and conductivity are interrelated and not independent of each other.

Thus for the five physical parameters considered, it has been found that three of them, the voltage, the concentration, and the elapsed time, are truely independent quantities and affect the yield in particular manners irrespective of the values of the other variables. The other two physical quantities, the frequency and conductivity, however, are seen to be interrelated and so that one of these must be specified before the effect of the other can be given. The principal task of any theoretical description of the yeast suspension is to explain these yield variations with the various physical parameters.

Dependence on Biological Parameters

At this point it is not yet possible to designate various cell constituents or processes as the seat of dielectrophoretic effects. It is possible, however, to subject the organisms to various physical and chemical treatments, affecting perhaps different parts in different ways, and note the dielectrophoresis of the treated cells with the hope that eventually the important mechanisms can be isolated. It is with this

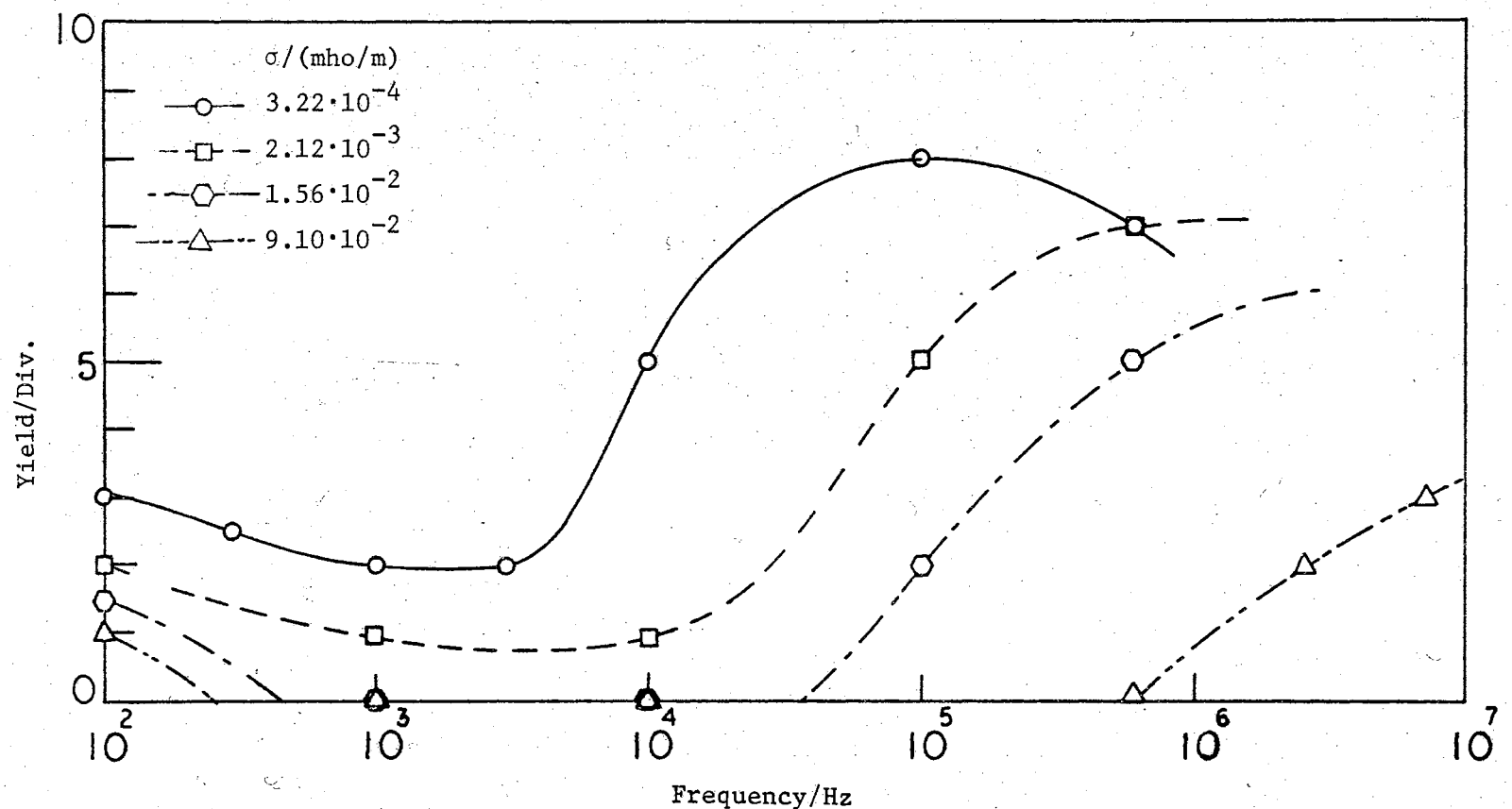

Figure 14. Variation of Yield With Frequency and Suspension Conductivity. V = 20 volts.

aim in mind that we consider the following sets of results.

Culture Age

A yeast cell changes considerably in its physical and chemical makeup as it ages. As the age of a culture increases, the average age of the constituent cells also increases, especially once the reproduction rate has slowed. The effect of the age of the cell can therefore be implied from the effect of the culture age. It usually takes about two days after innoculation before significant numbers of cells appear in the growing tubes. Rapid growth continues until about five days, after which the number of cells in the culture increases very slowly. Cells taken from cultures of ages two, five, and nine days can then be assumed to represent young, old, and very old cells respectively.

Samples from two, five, and nine day old cultures were studied under similar external conditions. The frequency dependences at low conductivity are shown in Figure 15. There is little difference in the three at the lower frequencies, except for the lack of a minimum for the five day cells. At higher frequencies, the five and nine day old cells respond about the same; about half that of the two day old cells.

At high conductivities, Figure 16, the five and nine day old cells yields were nearly identical at the middle frequencies. The very old cells had a slightly higher yield at low frequencies and a slightly lower yield at the high frequencies. The young cells differed from the others by showing no collection at 100 Hz and a nonzero minimum in the middle frequencies.

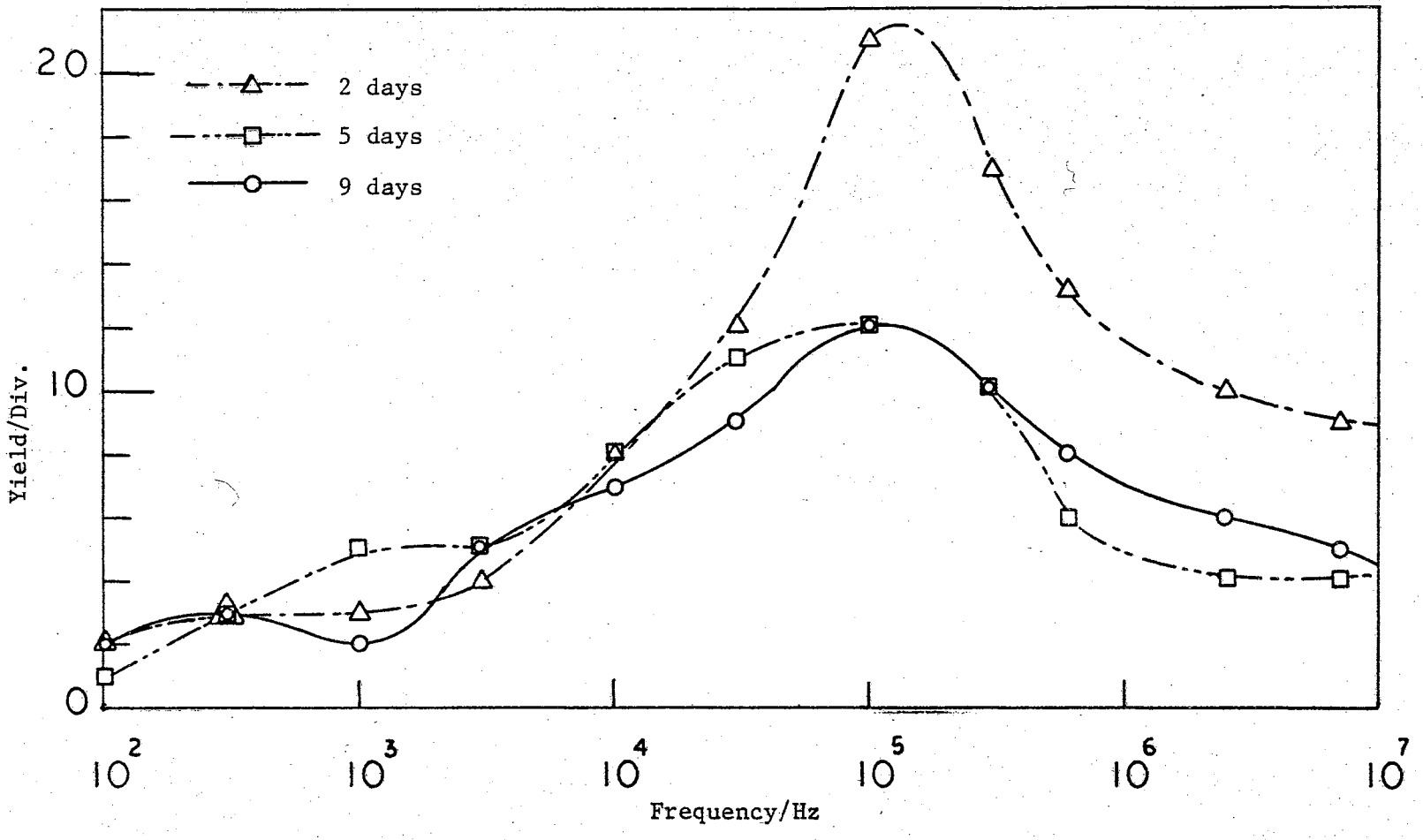

Figure 15. Low Conductivity Collection for Cells From Cultures of Different Ages. V = 20 volts, $\sigma = 2.2 \cdot 10^{-4} - 8.3 \cdot 10^{-4}$ mho/m.

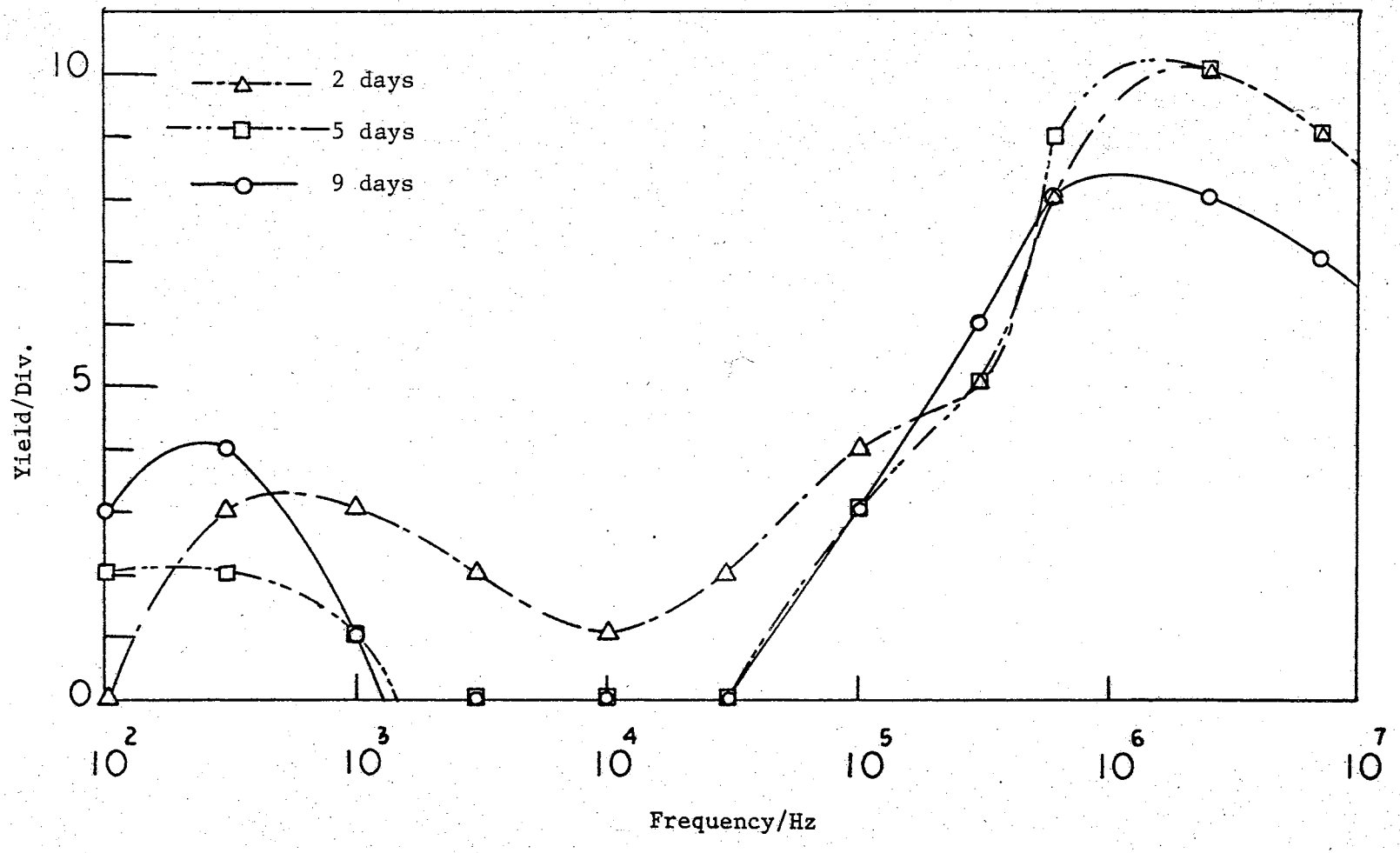

Figure 16. High Conductivity Collection for Cells From Cultures of Different Ages. V = 20 volts, $\sigma = 1.1 \cdot 10^{-2}$ mho/m.

Heat Treatment

According to Pohl and Hawk (26) yeast cells killed by treatment with crystal violet will not produce a yield at 2.55 MHz whereas generally live ones will. This suggests the treatment by other killing methods to determine the generality of that result. One of the methods chosen for killing the cells is the use of heat. In this case, the dead cells were produced by autoclaving, for at least 15 minutes, a test tube containing a growing culture. They were prepared for observation in the same manner as live cells. The concentration chosen was that which gave the same optical density as the live cell concentration of $2 \cdot 10^6$ cells/cc.

The yield for dead cells was measured as a function of voltage, time, and concentration and found to be similar to the results for live cells. That is, the yield was linear with applied voltage and concentration, and proportional to the square root of the elapsed time. This again implies that these relations are independent of the sample body.

The relations which are dependent on the body, the variation with frequency and conductivity, were not the same as for the live cells. It is difficult to get reproducible results even in terms of general trends as the sample sets shown in Figures 17 and 18 demonstrate. The striking differences between these results and those for live cells from Figure 14 are the lack of a minimum in the mid-frequency range and the occurrence of the high-frequency cutoff at a much lower frequency. The shift with increasing conductivity is toward lower frequencies in Figure 17 and toward higher frequencies in Figure 18, indicating the lack of reproducibility. This may be due to uncontrolled differences in preparation such as; the age of the cells to be autoclaved, the washing proce-

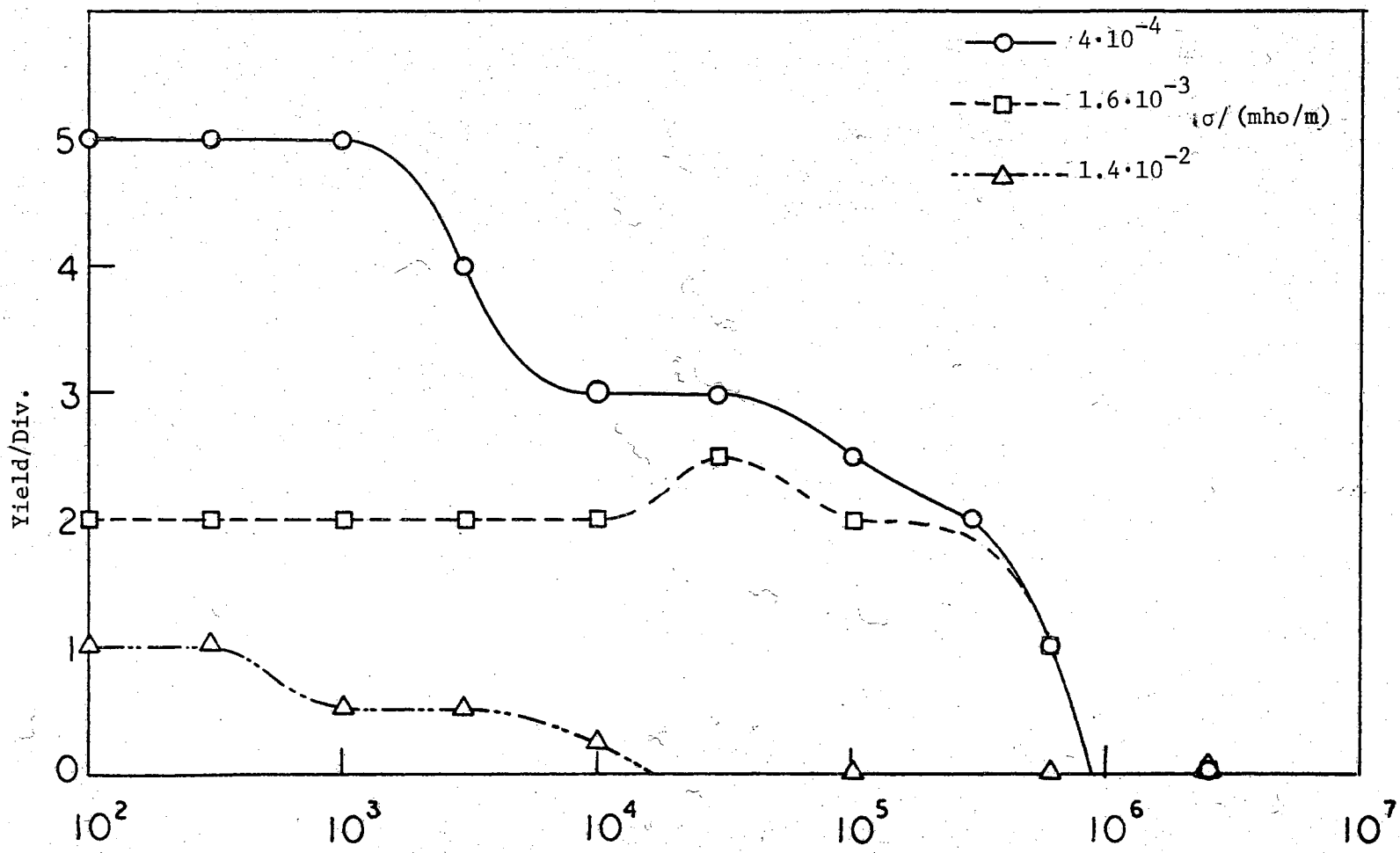

Figure 17. Collection of Dead Cells. V = 20 volts

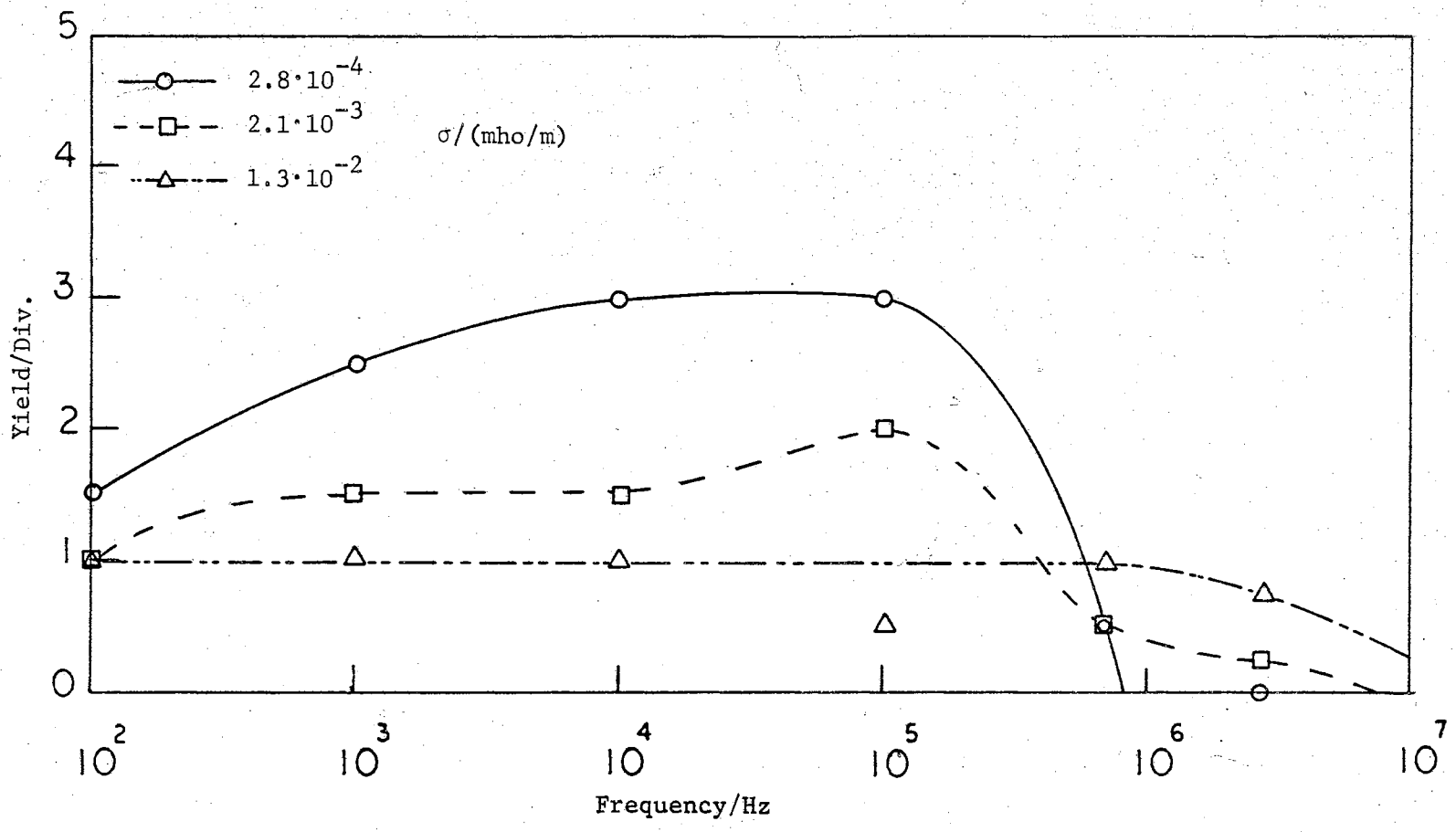

Figure 18. Collection of Dead Cells; Repeat. V = 20 volts.

dure before autoclaving, and the length of time in the autoclave. This is one area which needs more detailed and controlled study.

Exposure to Ultraviolet Light

Another effort was made to check the response of a cell which might be defined as dead. In cooperation with Dr. K. Haefner of the Southwest Center for Advanced Studies in Dallas, Texas, yeast cells were studied which had been irradiated with selected ultraviolet light. The light at the wavelength chosen (λ = 2537Å) had inflicted nuclear damage, causing the nucleus to appear granular, and resulted in the cells being unable to reproduce (71). In the strictest sense, the cells were not living, although they did continue to metabolize. The cells were studied at f = 3 MHz, V = 50 volts, and $\sigma = 10^{-2}$ mho/m. The cells collected quite readily, appearing to be normal. No detailed studies were made for these particular cells.

Treatment With Herbicides

Two well known herbicides were chosen with which to treat the yeast cells. They were 2, 4, 5-trichlorophenoxy acetic acid and 2, 2'-dipyridyl diquaternary bromide. They were used in concentrations of 10^{-3} M and $2 \cdot 10^{-5}$ M respectively for two hours. After treatment the cells were rinsed, prepared in the usual manner, and studied at 2.55 MHz.

The results were that those cells treated with 2, 4, 5-T. would not collect, just as expected for dead cells at this frequency. However the cells treated with 2, 2'-D. collected readily, appearing very much like live cells. Longer treatment times gave the same results. Finally a medium consisting of dextrose, peptone, and 10^{-5} M 2,2'-D. was innocu-

lated with yeast and subsequently a good culture developed. Thus the treated cells were indeed living, being unaffected by the "poison", and therefore collected as they should. The dependence of the yield on the frequency and conductivity was not determined for these treated cells.

Ion Treatment

It is well known that living microorganisms have a net charge distributed over their surface, this being the basis for electrophoresis (31). It is conceivable that these charges could be partly responsible for the charge layer known to be surrounding the particle, in that an oppositely charged cloud would form in the medium. This would add to any excess charge which would be near as the result of ion transport into and out of the cell by the working membrane. If the surface charges could be bound up and neutralized, then the charge cloud would be diminished and a corresponding change in dielectrophoresis might occur. This effect would be manifested, as will be discussed in a subsequent chapter, as a lowering of the yield near the mid-frequency minimum, that is in the 10^3-10^4 Hz range.

A reasonable approach to the neutralization of the bound charge is to expose the cells to ions of differing valences. One might expect that the higher valence ions would be bound more strongly to the cells and thus be less able to partake in conduction. Following this reasoning, cells were studied in unbuffered aqueous solutions of the salts KNO_3, $Ca(NO_3)_2$, $La(NO_3)_3$, and $Th(NO_3)_4$, at concentrations of 10^{-5} M, 10^{-4} M, and 10^{-3} M.

The cells were prepared by rinsing them to a high resistivity and then after pouring off all the water possible, adding the proper amount

of the desired solution to obtain the standard cell concentration. Measurements were made over the frequency range 10^2 - 6 x 10^5 Hz. The results were plotted as a function of frequency and as a function of conductivity. There were no general trends for the whole frequency range when comparing yields.

One example of this is Figure 19 which contains the yield as a function of frequency for a suspension conductivity of $2 \cdot 10^{-3}$ mho/m. The frequent crossings of the curves discourage a simple analysis (except maybe for the explanation that the variations are all due to experimental error). However the critical area for the effect of the charge layer is between 10^3 and 10^4 Hz. At 10^3 Hz, it is seen that except for the low yield of Th^{+4}, the expected order of K^+, Ca^{++}, La^{+3}, and Th^{+4}, is just reversed. However at 10^4 Hz the order is the expected order. A graph of yield against conductivity for this frequency, Figure 20, shows that this order is maintained for other conductivities.

A repeat of the experiment with Mg^{++} substituted for Ca^{++} showed the above trends to be accidental. Figure 21 shows these results for the same conditions as in Figure 20. Thus there does not seem to be any appreciable effect due to ion treatment.

There are several conclusions that might be drawn from the above lack of effect. One is that the charge layer does not exist. Another is that it does exist but that its strength is not important for dielectrophoresis. A third is that there is no more neutralization of the bound charge by multi-valent ions than by single-valent ions. Finally one could conclude that for living cells, the charge layer is due only partly to bound charge and the rest is produced by some cell mechanism, say charge transfer. The one that seems most likely is the last one.

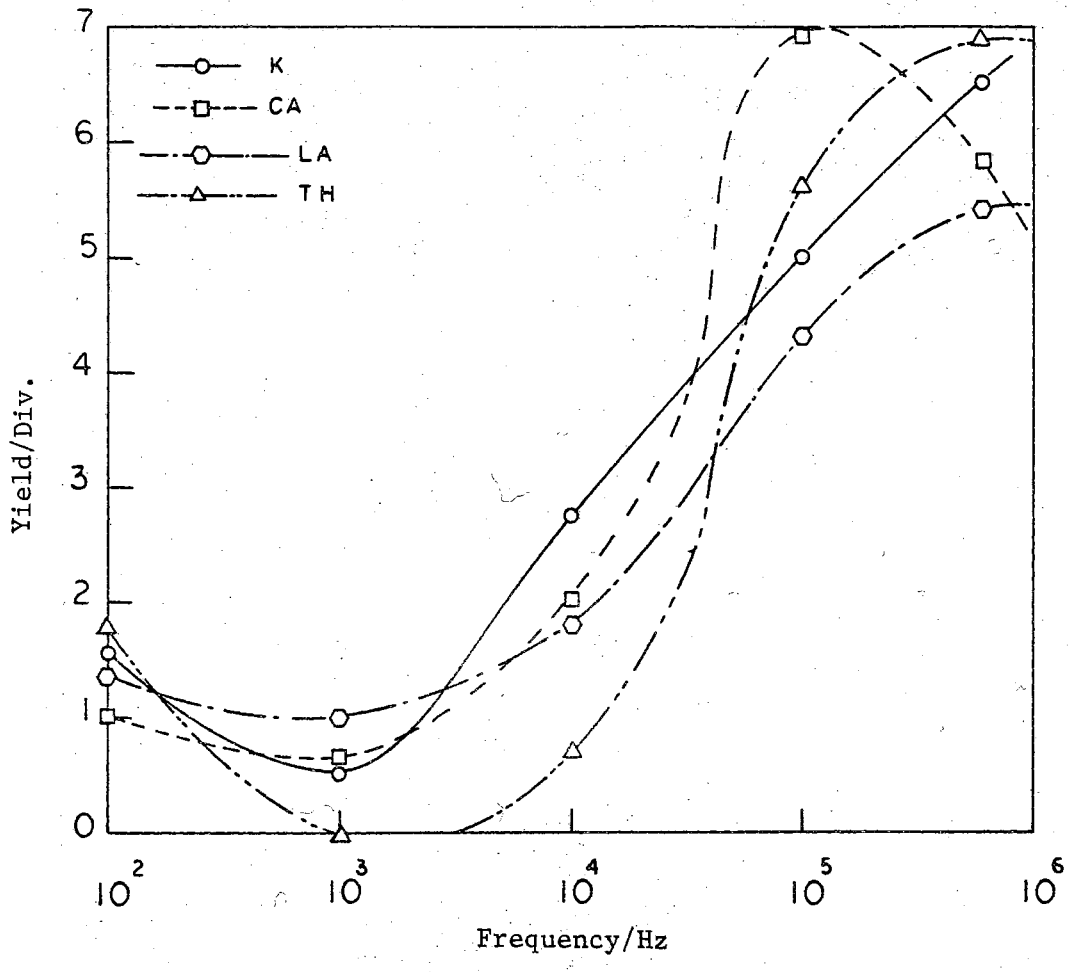

Figure 19. Effect of Ion Valence on Yield. V = 20 volts, $\sigma = 2 \cdot 10^{-3}$ mho/m (Note: All solutions have been corrected to the same conductivity by the addition of KCl).

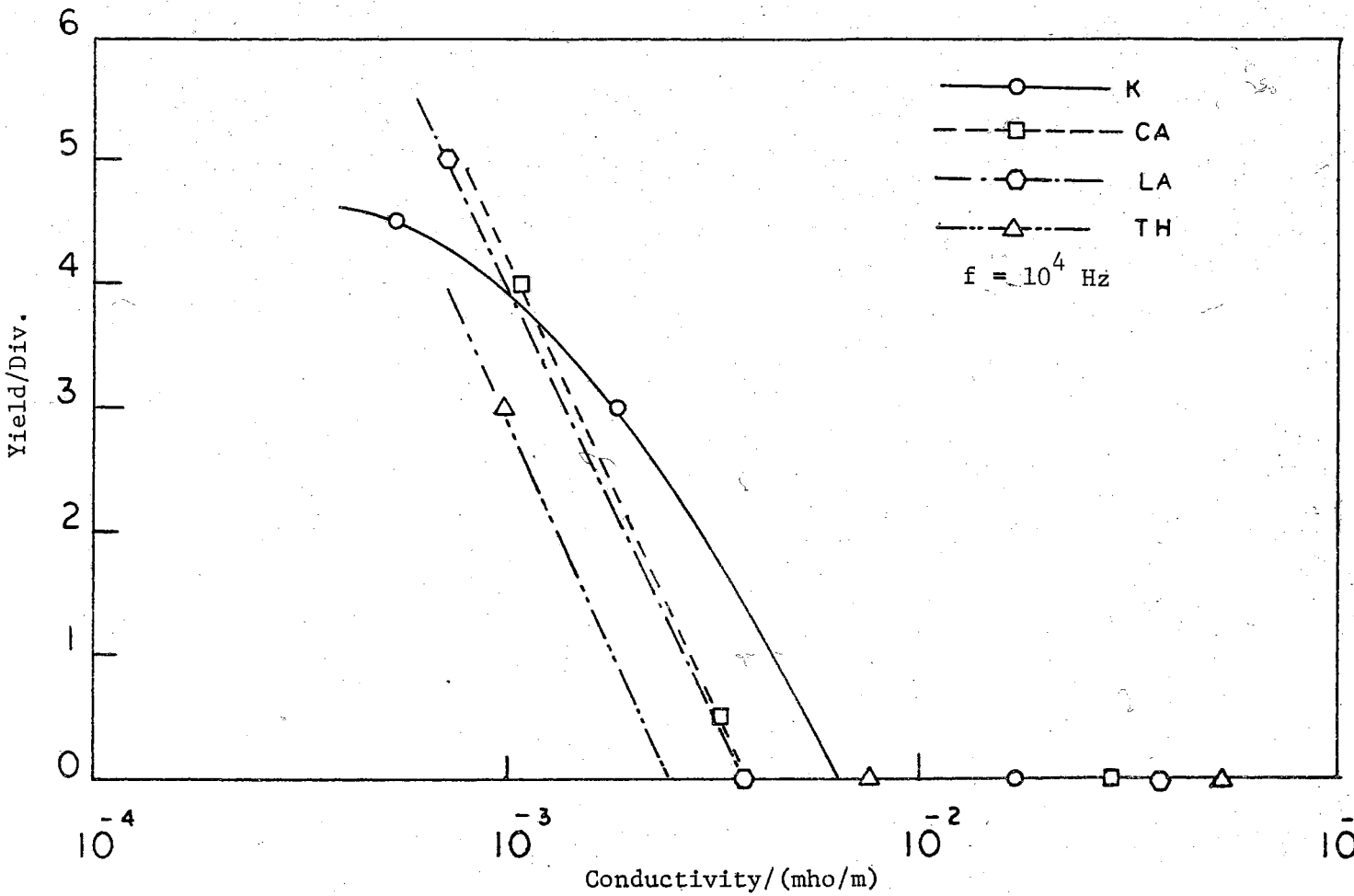

Figure 20. Ion Effect as a Function of Ion Concentration as Expressed Through Resulting Conductivities. V = 20 volts, f = 10^5 Hz. (Note: KCl not added.)

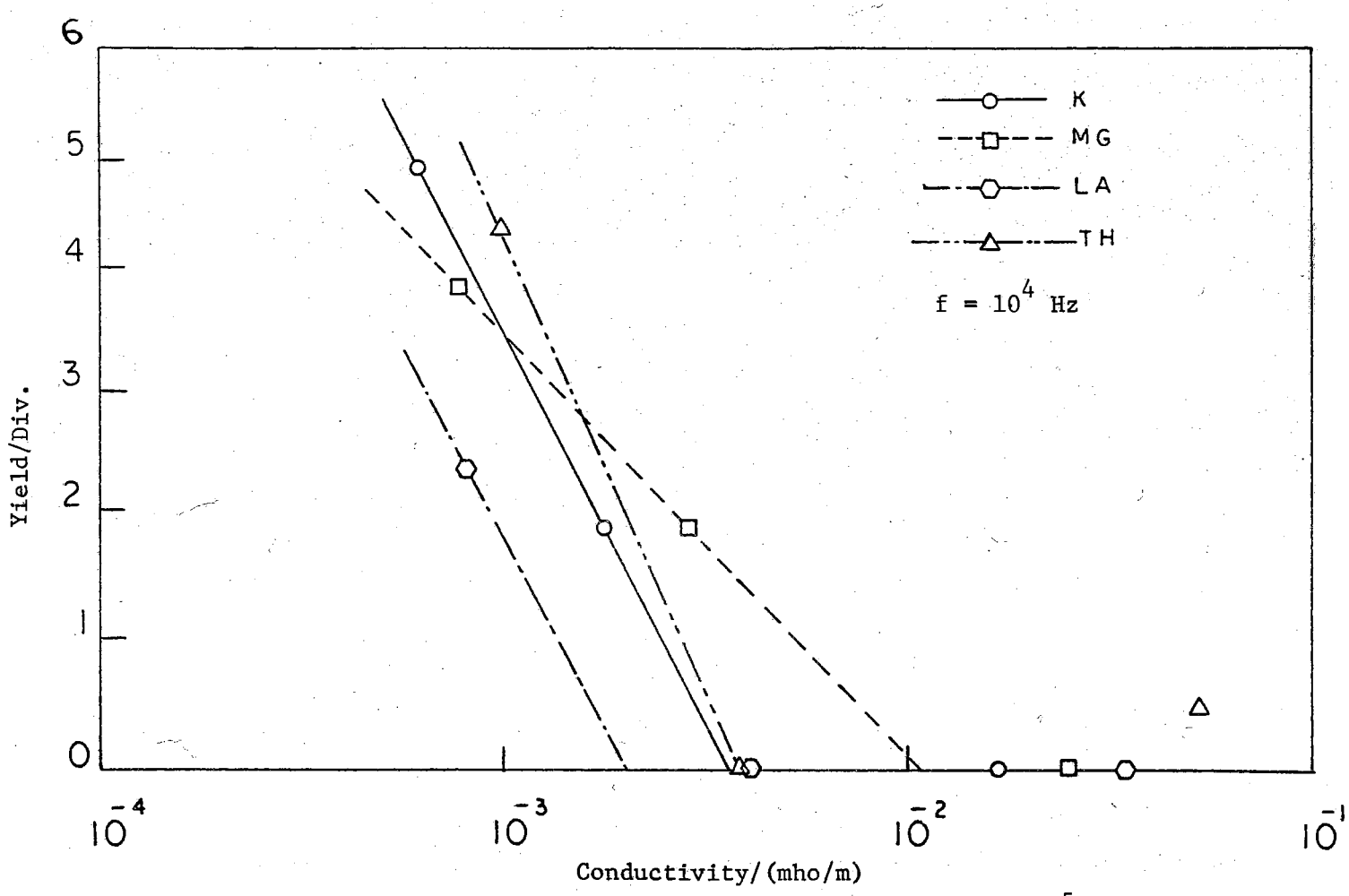

Figure 21. Ion Effect; Repeat. V = 20 volts, f = 10^5 Hz.

This could be tested by making yield measurements on inanimate particles which have no charge transfer mechanisms.

Suggested Parameters for Future Study

As was stated earlier the above parameters by no means form an all inclusive list. There are other parameters and treatments which would be interesting to examine. Most of these would fall into the biological category in that they would be concerned with altering the conditions and hence the electrical properties of the cells. A few, however, might be considered as basic parameters.

One such basic parameter is the size of the particle. Another is the particle shape. For spherical particles, the size would be indicated by the radius. For ellipsoidal cells, the values of the major and minor axes would determine the size and the axial ratios would describe the shape. However, the size and shape of the cells would be difficult to control unless a group of cells in the same growth stage, and thus the same size and shape, could be obtained.

Some parameters of biological nature which might be of interest are the effects of pH, osmotic pressure, radiation treatment, and various chemicals. The effect of environment during growth could also be investigated. In this case the cells would be subjected to various changes in the environment such as changes in the composition of the growth medium and variation of the temperature. Finally, it would be of considerable significance if the cells could be studied according to their growth phase (growing, budding, or resting) and the yield could be shown to be a function of the phase. It would then be possible, under the proper conditions, to separate the different phases.

Unexpected Phenomena

During the course of the experiments, several strange and unexpected effects were noticed concerning the movement of the cells. These were stirring of the liquid, repulsion of the cells from the pin, and rotation of the cells about an axis through their centers.

Stirring

For almost all conditions there is some attendant stirring of the suspension. That is, the cells move in directions which are not coincident with the field lines. At high frequencies and low conductivities, the stirring is very slight. The cells, in this case, move along the field lines and it is easy to tell the radius at which the force becomes significant. At this point the cells are given a rapid acceleration. At lower frequencies and higher conductivities the stirring becomes more pronounced and it is not obvious where the field becomes effective.

The stirring is usually in a pattern symmetrical about the pin-pin axis. Sometimes the flow is from left to right down the axis and at other times it is opposite to this. There do not seem to be any special conditions which determine the direction of flow.

On a few occasions at high conductivity and very high frequency ($\geq 7 \cdot 10^6$ Hz) the stirring was observed to come in pulses. There would be violent stirring for about a second and then calm for several seconds, after which the cycle would repeat. The length of the cycle was voltage dependent in that an increase in voltage shortened the time of least stirring.

At low frequencies with high conductivity, the stirring often became so violent that any collection was soon torn off by the swiftness

of the current. Since the stirring effect is usually associated with high conductivity, or low frequency, its explanation probably involves a charging phenomenon.

Repulsion

Closely related to stirring is the repulsion effect. Herein particles which are moving in towards a pin to be collected, suddenly move away in a direction normal to the surface. Usually this occurs before the cell has attached itself to the electrode, but sometimes a cell which has been in contact with the electrode for several seconds will suddenly shoot away. In a few cases, at a particular point on an electrode, a few cells will be in a cycle of touching the pin, shooting away a short distance, and moving back in to touch the pin again. This might continue for the duration of the experiment. Collected cells are never repelled from the ends of chains, only from contact or near contact with the electrode. As in the case of stirring, repulsion seems to be a function of conductivity and so it too is probably due to charging effects.

Rotation

Possibly the most puzzling phenomenon is that of cell rotation. Here the cells spin about an axis normal to the field lines at a rate of a few revolutions per second. This can be seen to occur at almost any applied frequency and anywhere in the field; attached to an electrode, attached to another cell, or floating freely in the medium. It is not unusual to see several cells of a long attached chain rotating individually in their places. As the applied frequency is changed, the

speed of rotation for a particular cell will also vary. It may speed up, slow down, or stop. A cell which has stopped as a result of a frequency change many times will commence rotating again if the frequency is returned to its original value. Usually as the frequency is changed some cells will stop rotating and others will begin. The speed of rotation also seems to be voltage dependent in that an increase in applied voltage increases the revolving rate.

A brief study of cell rotation as a function of frequency and conductivity was made for the cells of different ages used in the culture age study. For each sample the frequencies were noted at which any cell could be seen to be rotating. The results are shown in Figure 22 using bar graphs. The blackened portions represent regions of rotation. These should be compared with the yield measurements for these cells shown in Figures 15 and 16. There are no obvious relations between the two phenomena.

One note of interest is that for young cells the existence of rotation at high frequencies and low conductivity and the lack of rotation at low frequencies and high conductivity distinguishes them from the older cells. It may turn out that, in the future, the rotation of the cells may be as good a diagnostic tool as the yield.

Presently, there is no satisfactory explanation for the cause of the cell rotation. Since the field is not a rotating field, pure dielectrics should not experience a torque. The answer may again lie in a charge transfer process, although it must be on a smaller scale than that causing repulsion. In support of this suggestion is the fact that all rotation occurs in a direction such that the side of the cell nearest the pin-pin axis, and hence in the strongest field, moves away

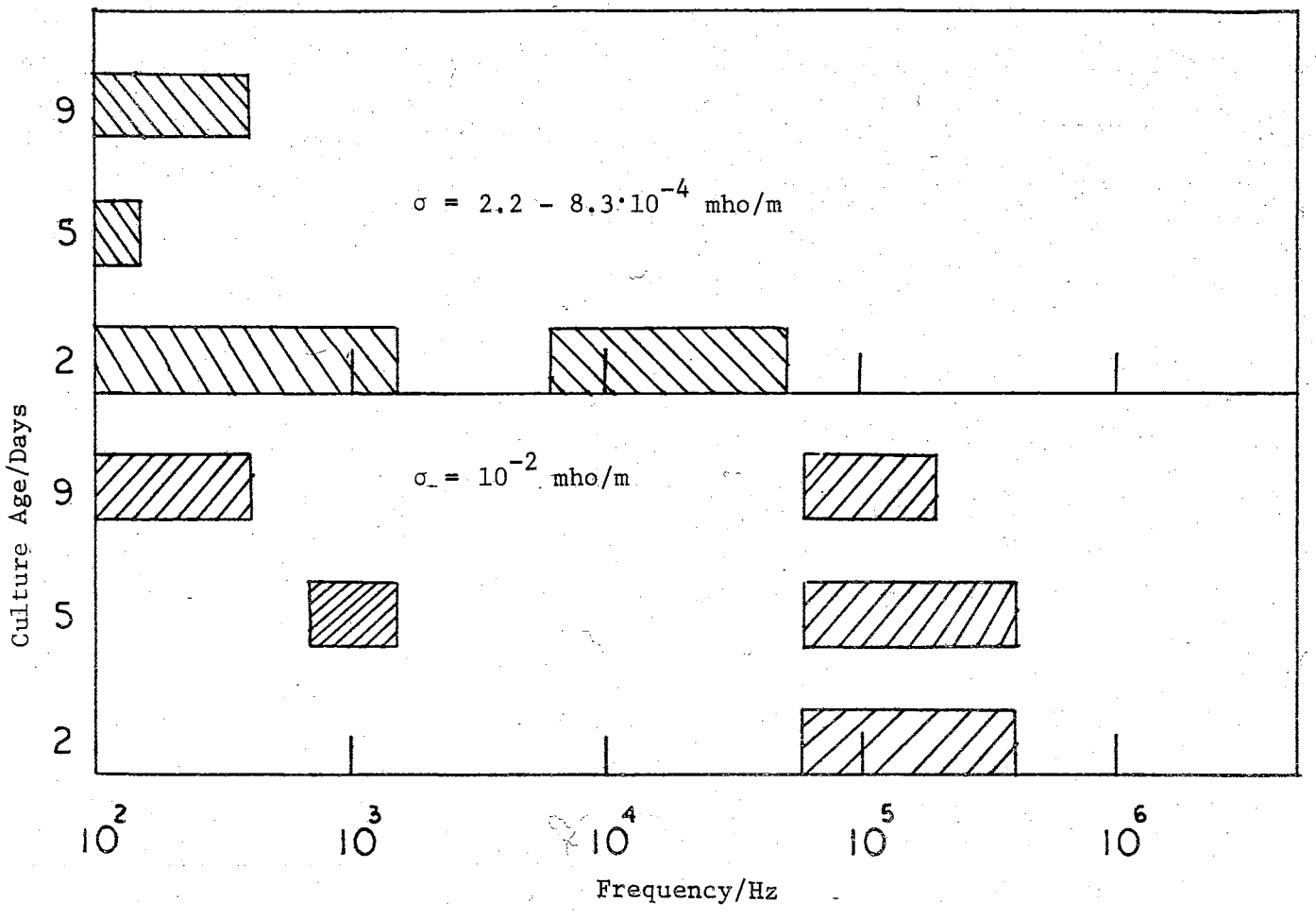

Figure 22. Occurrence of Cell Rotation as a Function of Frequency and Conductivity for Cells of Different Ages. V = 20 volts.

from the pin. This in effect is a repulsion of one side more than the other, producing a torque, but not producing a repulsive force large enough to overcome the overall attractive dielectrophoretic force.

Precautions

This section is intended for those with a physics background who wish to continue the work in this area using approximately the same equipment that has been described here. It will mention some of the "tricks" to successful study which have been discovered by one means or another.

Microbiological Techniques

It is important to use proven methods for handling the organism under study. The original stock of the organism should be kept refrigerated and thereby available at any time to start a new culture equivalent to any preceding one. Otherwise, over a long period of time, mutations could cause the cells to evolve into some with very different characteristics. Sterilization procedures should be followed closely to prevent contamination by some other organism. Thorough knowledge of the autoclave and innoculation procedures should be obtained.

Conductivity Contamination

One of the most likely sources of error to the unwary is the accidental change in the conductivity of the suspension, especially when working with low conductivities. This can occur when the suspension comes in contact with any surface where ions are present. This could be a dirty pipette, a finger, or a dirty electrode cell. Fingers are

especially troublesome. Ions can easily be transferred from them to a utensil and then to the suspension. It is a wise practice to rinse all utensils with deionized water each time before using them. Pipettes and syringes can be checked for cleanliness by rinsing them with deionized water and then measuring the conductivity of the rinse water.

Other sources of ion contamination are the atmosphere, due to CO_2 absorption, and the cells themselves. The cells, when placed in a low conductivity medium, will immediately begin to lose ions from their interior into the medium. For these reasons it is recommended that whenever possible, conductivity measurements should be made both before and after an experiment.

Settling

Yeast cells are slightly more dense than water, so as a result, over a period of time, they will settle out of suspension. This should be kept in mind when concentration measurements are being made or when cells of standard concentration and ready for study have been sitting in a test tube or syringe for several minutes. To keep the concentration as uniform as possible from one measurement to the next, the suspension should be thoroughly but gently mixed before each sample is removed.

Electrode Cleaning

To begin with, the electrodes should be as smooth as possible. They must certainly be clean. After each yield measurement there is the problem of removing the collected cells from the electrode. Merely turning off the applied field will not dislodge all of them. The best

simple method is to remove the electrode cell from the microscope stage and rinse it with a hard stream of deionized water (from a plastic squeeze bottle). This usually removes all of the old cells. If it does not, then a pipe cleaner can be lightly brushed across the electrodes. The cell will then have to be rinsed again with deionized water to remove any contamination transferred from the pipe cleaner. The cell can be dried by blowing on it with air from an empty polyethylene wash bottle.

Sources of Error

In a biological system consisting of many individual, uncontrollable, ever-changing subsystems, the sources for error are many. Some of the more obvious ones will be enumerated here.

Accuracy of Parameters

As discussed earlier it is often difficult to measure precisely the conductivity of an ionic solution because of electrode surface effects. These same effects make it difficult to be certain that the voltage being applied across the electrodes is also being applied to the solution and not being partially dropped across surface impedances. Were this occurring, the result would be a frequency dependence due solely to the frequency dependence of the effective applied voltage.

A different type of error in voltage reading is possible at very high frequencies. Above about 10 MHz, the stray capacitances become critical in determining the effective network which the voltage source "sees". There will be phase shifts and voltage variations among the different parts of the network; and for this reason, the voltage meas-

ured 30 cm from the electrode system is likely not to be the true voltage applied across the system. This error can be reduced by making the high frequency voltage measurements, directly at the electrodes.

The error in the cell concentration is composed of several parts. One is the error in the reading of the optical density of the suspension, which is about 5%. Another is the conversion from detector current to cell concentration, since in this conversion the size of the cells is not considered. The optical density is essentially proportional to the concentration of cells multiplied by the square of the cell radius, so that the larger the cells, the fewer that are required to produce the same optical density. This error is partly compensated for however, because the yield is theoretically proportional to the product of the concentration and the fourth power of the radius. This results in a greater yield for the larger cells, even though their concentration is less. Still another error in the cell concentration can result if a suspension has been allowed to stand quietly for several minutes, permitting the cells to settle to the bottom of the container. The concentration of a sample will then be a function of the height from which it was taken.

Yield Determinations

There are several factors which contribute to uncertainties in yield measurements. The first is the error in estimating the yield itself. The length of a chain is measurable to the nearest whole scale division. This is quite a large roundoff considering that the maximum on the yield curve is usually less than ten divisions and that the critical low frequency points have yields usually of less than three

divisions.

Besides the error in estimating the length of each chain, there is the error in selecting the length which most represents all the chains. This is a judgement decision since the lengths may vary by a factor of two or three around the pin. Normally the second or third longest chain was chosen. This procedure prevented the occurrence of one very long chain from giving the measurement a misleadingly large yield.

Uncontrolled Factors

Other factors which affect the accuracy of the yield measurements include the phenomena of stirring and repulsion already mentioned. It is not possible to quantitatively estimate their effect, since it is not known how to control them. In this same category would be all changes of the cells which were unknown to or uncontrollable by the experimenter. Included would be any changes in the average age, size, or internal constitution of the cells, due perhaps to the differences in colony age and experimental treatment.

CHAPTER IV

POSSIBLE MECHANISMS

The preceding chapter presented the experimental variation of the yield as a function of the various parameters. Now the task is to explain this observed behavior. For ideal spherical particles of radius a and permittivity ε_2 suspended in a medium of permittivity ε_1, the dielectrophoretic force can be shown to be (13)

$$\vec{F} = \frac{2\pi a^3 \varepsilon_1(\varepsilon_2 - \varepsilon_1) \nabla(\vec{E}^2)}{\varepsilon_2 + 2\varepsilon_1} \qquad \text{(IV-1)}$$

where $\vec{E}$ is the rms value of the applied field strength. Starting with this equation and assuming the field to be produced by concentric spheres, it is possible to show that the yield is given by

$$y = \frac{8\pi a^4 C V r_2}{9 r_1 (r_2 - r_1)} \left[\frac{2t}{\eta} \left(\frac{\varepsilon_1(\varepsilon_2 - \varepsilon_1)}{\varepsilon_2 + 2\varepsilon_1}\right)\right]^{\frac{1}{2}}, \qquad \text{(IV-2)}$$

where V is the applied rms voltage, C is the particle concentration, r_1 is the radius of the inner sphere, r_2 is the radius of the outer sphere, t is the elapsed time, and η is the viscosity of the suspending medium. (The derivation of Equation IV-2 will not be given here, but a similar derivation of the yield for a more complicated force equation will be presented in Chapter VII.) Thus even for ideal particles the linear dependence of the yield on the voltage and concentration, and the square

root dependence on time is easily shown. However, Equation IV-2 has no provision for a dependence on frequency or conductivity. It is the effects of these quantities which an adequate theory must explain.

If the permittivities of the particles and the medium in Equation IV-2 are allowed to be frequency and conductivity dependent, then these parameters can be incorporated into the yield expression. The idea of allowing the apparent permittivity to be frequency dependent is not new. Most dielectric constant measurements consist of determining the effective parallel capacitance of the material and attributing it to an apparent permittivity. As the effective capacitance changes with frequency, this permittivity must also change. The problem is then to devise a physical system which would exhibit this effective permittivity. The same type of problem must be faced in explaining the dielectrophoresis results. In this case, however, the system must also explain the conductivity dependence.

There are four mechanisms that have been proposed as possible explanations for the variation of the dielectroc constant of materials with frequency. They are (1) dipole rotation of the constituent molecules, (2) gating mechanisms operating in the cell membrane (3), Maxwell-Wagner relaxation at the various interfaces, and (4) relaxation of a surrounding ion atmosphere. We shall consider each of these and see if a conductivity dependence is or can be incorporated into the mechanism. If so, and if the mechanism is a plausible one, then it can serve as a guide in the development of the dielectrophoresis theory.

Dipole Rotation

The rotation of molecules with permanent dipole moments and their

relaxation, or failure to follow the field, at high frequencies has long been suggested as the basis for frequency dependence of the permittivity. It provides a quite satisfactory explanation for molecules which have a small relaxation time (the time required for the molecule to realign itself with the field). For a detailed review, several good texts are available (34, 35, 36).

The dipole theory was introduced by Debye (27) when he postulated a single relaxation time for a molecule with a permanent dipole moment. His theory included the concept of a complex permittivity, which merely stated that at any time the molecule would have a component of polarization in phase and a component out of phase with the applied field. These components were shown to be frequency dependent, with the in-phase part being that which would be measured as a capacitance effect. Thus it is only this frequency dependent, in-phase component which would determine the apparent permittivity.

The field which the molecule "sees" is not the same as the applied field, since it is influenced by neighboring molecules. The effective field assumed by Debye was that known as the Clausius-Mossotti field (34, p.5), which is valid only for gases at low pressures. Onsager (37) improved the expression for the effective field by reexamining the field induced by the dipole. His equation was found to be correct for many pure polar liquids. Kirkwood (38) has extended the detail to produce an even more complicated expression for the field. By the use of these better expressions for the effective field, the permittivity dispersion could be explained for a wide range of materials.

Some materials did not fit even the detailed equations correctly leading Cole and Cole (39) to introduce the possibility of having a

series of relaxation times. They also introduced a method for determining if the data could be represented by a single relaxation process. It involved plotting the imaginary part against the real part of the permittivity (Cole-Cole plot) and noting whether the center of the resulting circle lay on the real axis or below it.

Until the experiments of Oncley (40), permittivities had been measured only for the small inorganic molecules. He studied the permittivity of various protein solutions in the frequency range of 50 to $5 \cdot 10^6$ Hz and explained the relaxation behavior in terms of rotating ellipsoids. He derived the relaxation time to be

$$\tau = 4\pi\eta\, ab^2/kT \qquad \text{(IV-3)}$$

where a and b are the axes of the ellipsoid. The critical frequency corresponding to the relaxation time turned out experimentally to be in the range of $10^5 - 10^7$ Hz.

Grant (41, 42) investigated the dispersion regions of proteins, amino acids, and water above 10^8 Hz. He found the dispersion of amino acids to occur at about $7 \cdot 10^8$ Hz and that for water to be at about $2 \cdot 10^{10}$ Hz. He also noted a minor relaxation for proteins in this region.

The permittivity dispersion for the very large DNA molecules has been studied by Junger (43) and Takashima (44). Both report relaxation effects occurring in the lower frequency range ($10^3 - 10^4$ Hz). Takashima measured the permittivities of aqueous solutions of several types of DNA molecules whose molecular weights ranged from $2 \cdot 10^6$ to $7 \cdot 10^6$. He attributes the relaxation effects to rotating ellipsoids and using Oncley's formula calculates an expected relaxation time which agrees

with experiment within an order of magnitude. He presents an argument to show that the results cannot be explained by Maxwell-Wagner type effects, but he uses incorrect equations and appears to mix mks and cgs units so that his conclusions are suspect. He does indicate that part of the explanation might lie in the relaxation of a polarizable ion atmosphere.

Shortcomings of Dipole Rotation Theory

The Debye theory and its subsequent modifications provide an adequate explanation for the variation of the measured permittivity with frequency for gases and most liquids of small molecular weight. However, as the size of the body increases, the agreement between the theory and experiment decreases. It might seem desirous to explain the dielectrophoresis of yeast cells in terms of a changing permittivity due to the rotation of the whole cell or its constituents. There are, however, several arguments against this approach.

The first is the shape of the yield-frequency curves (Figure 13). Were the process one purely of rotation, then at low frequencies, the permittivity would be at its maximum since all the dipoles would be aligned. As the frequency increased, some dipoles would not follow the field and so the permittivity would decrease monotonically. There is no provision for allowing the permittivity to increase with increasing frequency. For aqueous suspensions, ε_1 of Equation IV-2 is the permittivity for water and is constant up to 10^{10} Hz. Therefore any variation of yield with frequency must be due to a variation in ε_2 only. The yield can go to zero only if ε_2 has decreased to be less than or equal to ε_1. For any frequency higher than that at which $\varepsilon_2 = \varepsilon_1$, the

yield must be zero since ε_2 cannot increase again. There is thus no explanation for the yield to go to zero in the middle frequencies and then increase again at higher frequencies as experiment shows.

There are also other arguments against selecting this mechanism exclusively. It is difficult to see how one could introduce a conductivity dependence to explain the variation of yield with conductivity. Also according to Oncley's analysis for ellipsoids, the relaxation time τ should be inversely proportional to the temperature. But Schwan (25, p.180) states that for lysed erythrocytes, τ has the same temperature dependence as ionic conductance. The relaxation time should also be independent of the pH of the suspension, but for proteins pH dependence has been observed (45).

A strong argument against the dipole rotation mechanism is the fact that the changes in permittivity are too small to account for the very large permittivities of suspensions at low frequencies. The dielectric constant, the ratio of the permittivity of the material to that of free space, has been estimated to be as high as 10^6 for such suspensions (25, p.150). The maximum dielectric constant for molecular solutions is that found for DNA, which for a fairly concentrated .2% solution is about 1200 (44). The rotating dipole picture then can at best only account for a dielectric constant which is too small by a factor of 10^3.

One final note is the fact that the critical frequency, the frequency at which relaxation occurs, is higher than 10^5 Hz for all molecules except DNA. Thus the rotational effect of almost all of the cell constituents should not be seen in the region below 10^5 Hz where most of the yield variation occurs.

Gating Mechanism

An alternate process which might explain the conductivity and frequency dependence of the yield is concerned with the makeup of the yeast cell membrane. It is well known that conduction occurs across the membrane. It has been postulated that the conduction might occur at specific conduction sites and be controlled by some sort of ion-exchange mechanism (46, 25, 47). As the frequency is increased, this mechanism may begin to lag behind the field. This lag in conduction can be treated in terms of a complex conductivity just as the lag in polarization implied a complex dielectric constant. The imaginary part of the conduction behaves as a polarization and so appears as an increase in permittivity. This would provide a mechanism for increasing the effective permittivity with increasing frequency and also introduce a dependence on suspension conductivity, two results not obtainable with the pure rotation theory. There are some experimental results on membranes which are compatible with this approach (25, p.180).

Layered Structure of Membrane

A different type of mechanism dealing with the cell membrane might also be responsible for the observed dielectrophoretic effects. As stated earlier, the membranes of practically all types of cells are thought by many to consist of a three layered, protein-lipid-protein, structure (73). Since each layer has its own conductivity and permittivity the combination of them in series results in an effective capacitance and conductance which are combinations of the individual parameters. The treatment of such systems involves the standard Maxwell-Wagner (48) approach and produces an effective capacitance and conduct-

ance which are frequency dependent. This is so even if the individual parameters are frequency independent. For conductivities and permittivities which are of the order of those found in cell membranes, the capacitance (or permittivity) of the combination shows a relaxation in the frequency range of 10 to 10^3 Hz (25, p.181). This is also an important range for dielectrophoresis studies, so that this type of process must be kept in mind.

Ionic Atmosphere

A final mechanism which might explain the variation of the yield with frequency is the concept of an ion atmosphere surrounding the cell. This atmosphere can then be polarized and add considerably to the permittivity and also exhibit relaxation. It was introduced by Miles and Robertson (49) and treated by them as a concentric conducting shell. The Maxwell-Wagner approach applies to this situation also and is very similar to the layered membrane approach except that a conducting shell is used instead of one composed of protein. For a very thin ion atmosphere, the conducting shell can be replaced by a surface conductivity (50). This approach correlates well with experiment in several respects. The relaxation frequency can be shown to be inversely proportional to the radius of the particle which is approximately true experimentally. It can also be used to explain the very high dielectric constants of suspensions at low frequencies (51). It is interesting to note that very high effective permittivities also exist at low frequencies for suspensions of polystyrene spheres (52). Polystyrene itself has a low dielectric constant which is frequency independent at these frequencies. This is strong evidence in support of this mechanism.

Finally, the results of Takashima on DNA have been reexamined by Pollak (72) in terms of a Maxwell-Wagner approach using conductivities and permittivities consistent with the highly elongated nature of the DNA molecules. This approach gives relaxation times which agree well with experiment.

Review of Mechanisms

Four mechanisms have been discussed which might be considered as possible explanations for the dependence of the yield on frequency and conductivity. Rather than regarding the effect in living cells as being due to only one of the processes, we consider it more likely that all of them could be acting simultaneously, with their relative importance being determined by the experimental conditions such as frequency and conductivity. At high frequencies the dominant effect is likely to be dipole rotation whereas at the lower frequencies, the gating mechanism or ion layer might be more important.

The trend is to explain the low frequency results for large particles in terms of the ion atmosphere concept. As has been mentioned, this position has been taken by Miles and Robertson, O'Konski, Schwan, and Schwarz. It is also the approach of Dintzis, Oncley, and Fuoss (53) in their explanation of the dispersion for polyelectrolytes ($M = 2 \cdot 10^6$ and comparable to DNA). This lends considerable support to the preference of this approach over the rotating dipole approach since it is Oncley who explains protein relaxation in terms of rotating ellipsoids.

Although the trend is to explain low frequency behavior in terms of ion atmospheres, the other processes cannot be ruled out completely

and their effects should be considered in any general treatment of the problem. Since the latter two mechanisms involve Maxwell-Wagner type approaches, the whole problem can be considered from this approach with the dipole rotation and gating mechanism being accounted for by allowing the appropriate conductivities and permittivities to vary.

CHAPTER V

GENERAL EXPRESSION FOR DIELECTROPHORETIC FORCE

In the preceding chapter, several mechanisms were considered which could be responsible for the observed dependence of the yield or DCR on frequency and conductivity. To determine the correct mechanisms, it is first necessary to have a theoretical expression for the yield. There are two approaches that can be taken to obtain this expression for a particular mechanism. One is to derive a general relation for the yield and then apply the conditions appropriate to the given mechanism. An alternate method is to calculate a general force expression, apply the proper conditions to it, and then derive a particular expression for the collection rate corresponding to that mechanism. The latter is the simpler of the two methods and is the one which will be followed here. That is, a general expression for the dielectrophoretic force will be obtained, a plausible model incorporating most of the mechanism will be chosen, and a relation giving the theoretical yield for this model will be calculated. The general force relation will be derived in this chapter, while the other two steps will be treated in the next two chapters.

Complex Quantities

As was mentioned in Chapter IV, the consideration of materials as perfect dielectrics leads to a force expression that is not compatable

with the experimental results. We must therefore determine a general expression which is applicable to real materials. These non-perfect dielectrics will in general have both dielectric constants and conductivities. If the applied field is periodic there will also be a time lag of response. This time lag is most easily expressed as a phase difference between the applied field and the resulting current and polarization.

For a sinusoidal field impressed across a simple (linear) medium, the current, charge density, polarization, and other descriptive parameters will also be sinusoidal, but not necessarily in phase with the field. That is for

$$\vec{E} = \vec{E}_o e^{j\omega t}$$

we have (see Appendix C for definitions)

$$\begin{aligned} \vec{J}_c &= \vec{J}_{co} e^{j(\omega t - \theta_J)}, & \vec{D} &= \vec{D}_o e^{j(\omega t - \theta_D)} \\ \rho &= \rho_o e^{j(\omega t - \theta_\rho)}, & \vec{P} &= \vec{P}_o e^{j(\omega t - \theta_P)} \\ \vec{B} &= \vec{B}_o e^{j(\omega t - \theta_B)}, & \vec{H} &= \vec{H}_o e^{j(\omega t - \theta_H)} \\ \vec{M} &= \vec{M}_o e^{j(\omega t - \theta_M)}, \end{aligned} \qquad \text{(V-1)}$$

where j is $\sqrt{-1}$, θ_i is the phase angle and i_o is the amplitude for the instantaneous value of the quantity i. For simple media, the relations

$$\vec{D} = \varepsilon\vec{E} \quad \text{and} \quad \vec{J}_c = \sigma\vec{E} \qquad \text{(V-2)}$$

also hold. It follows that ε and σ must be given by

$$\varepsilon = \frac{D_o}{E_o} e^{-j\theta_D} \tag{V-3}$$

and

$$\sigma = \frac{J_o}{E_o} e^{-j\theta_J} ,$$

and that they are therefore complex. An alternate way of expressing these complex quantities is to break them up into real and imaginary parts such as

$$\varepsilon = \varepsilon' - j\,\varepsilon''$$

and (V-4)

$$\sigma = \sigma' - j\,\sigma'' ,$$

The ratio of the imaginary part to the real part determines the amount by which the related quantities are out of phase. That is

$$\varepsilon''/\varepsilon' = \tan\theta_D$$

and (V-5)

$$\sigma''/\sigma' = \tan\theta_J ,$$

If these quantities are pictured in the complex plane, they can be considered as vectors which can be broken up into two components, one real and one imaginary. This is illustrated in Figure 23 where ε is shown to be broken into its real and imaginary components in a standard phasor diagram (54). With the phase of $\vec{E}$ taken as the reference, the

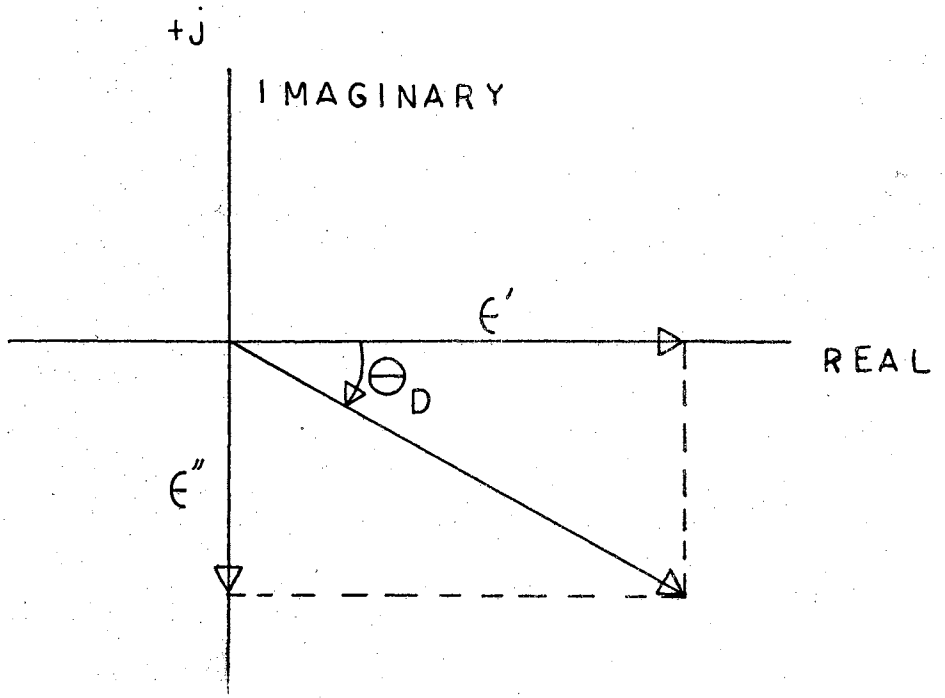

Figure 23. Phasor Diagram of Complex Permittivity in Terms of its Real and Imaginary Components.

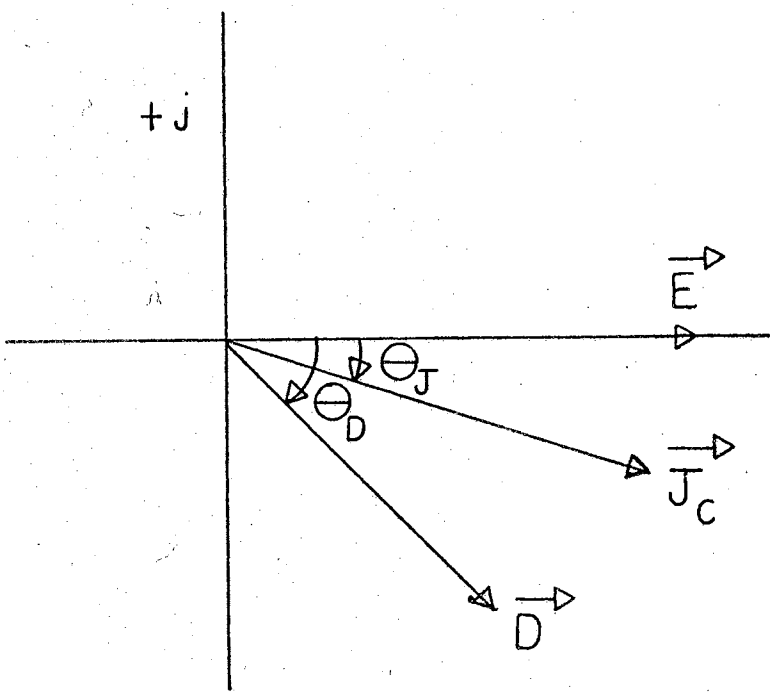

Figure 24. Phasor Representation When the Conduction Current and Displacement Lag Behind the Impressed Field.

phase of $\vec{D}$ and $\vec{J}_c$ are shown in Figure 24. The amounts of phase lag depend on the components of ε and σ respectively, since these are the quantities relating $\vec{D}$ and $\vec{J}_c$ to $\vec{E}$.

Maxwell's Equations

For sinusoidal fields of the form given in Equations (V-1), Maxwell's equations for simple media become (55),

$$\varepsilon(\nabla \cdot \vec{E}) = \rho_f \tag{V-6}$$

$$\nabla \times \vec{E} = -j\omega\vec{B} \tag{V-7}$$

$$\nabla \cdot \vec{B} = 0 \tag{V-8}$$

$$\nabla \times \vec{H} = (\sigma + j\omega\varepsilon)\vec{E}. \tag{V-9}$$

The boundary conditions at an interface between materials 1 and 2 are

$$\varepsilon_1(\vec{n}_1 \cdot \vec{E}_1) + \varepsilon_2(\vec{n}_2 \cdot \vec{E}_2) = -\eta_{1f} - \eta_{2f} \tag{V-10}$$

$$\vec{n}_1 \times \vec{E}_1 + \vec{n}_2 \times \vec{E}_2 = 0 \tag{V-11}$$

$$\vec{n}_1 \times \vec{H}_1 + \vec{n}_2 \times \vec{H}_2 = -\vec{I}_{1f} - \vec{I}_{2f} \tag{V-12}$$

$$\vec{n}_1 \cdot \vec{B}_1 + \vec{n}_2 \cdot \vec{B}_2 = 0, \tag{V-13}$$

The continuity equations for conservation of charge are

$$\nabla \cdot (\sigma\vec{E}) + j\omega\rho_f = 0 \tag{V-14}$$

and

$$\nabla \cdot (\vec{I}_{1f} + \vec{I}_{2f}) + j\omega(\eta_{1f} + \eta_{2f}) - \vec{n}_1 \cdot (\sigma_1\vec{E}_1) - \vec{n}_2 \cdot (\sigma_2\vec{E}_2) = 0. \tag{V-15}$$

In the above equations the usual meanings are given to the familiar symbols of $\vec{E}$, $\vec{B}$, $\vec{H}$, ε, ω, and σ. The less familiar symbols are defined as follows; $\vec{n}_1$ and $\vec{n}_2$ are unit outward normal vectors, ρ_f is the volume density of free charge, η_f is the surface density of free charge, and $\vec{I}_f$ is the surface density of free current (current/width), which is different from zero only for perfect conductors.

Eliminating ρ_f from Equations (V-6) and (V-14) and assuming $\nabla\sigma = 0$, gives

$$\nabla\cdot\vec{E} = 0 \tag{V-16}$$

everywhere except at the boundaries where of course $\nabla\sigma \neq 0$. Combining Equations (V-10) and (V-15) to eliminate $(\eta_{1f} + \eta_{2f})$ and restricting ourselves to non-perfect conductors gives the conditions at the boundaries as

$$(\sigma_1 + j\omega\varepsilon_1)(\vec{n}_1\cdot\vec{E}_1) + (\sigma_2 + j\omega\varepsilon_2)(\vec{n}_2\cdot\vec{E}_2) = 0. \tag{V-17}$$

It is convenient at this point to define the expression

$$K \equiv \sigma + j\omega\varepsilon \tag{V-18}$$

as the complex conduction factor and the quantity

$$\xi \equiv \frac{K}{j\omega} = \varepsilon - \frac{j\sigma}{\omega} \tag{V-19}$$

as the complex dielectric factor. Dividing Equation (V-17) by $j\omega$ then gives

$$\xi_1(\vec{n}_1\cdot\vec{E}_1) + \xi_2(\vec{n}_2\cdot\vec{E}_2) = 0. \tag{V-20}$$

Thus the boundary condition for real media and sinusoidal fields is identical with that for ideal dielectrics in static fields if the dielectric constant is replaced by the complex dielectric factor ξ.

The Physical Significance of K

It is customary to treat the quantity $(\sigma + j\omega\varepsilon)\vec{E}$ as a total current density $\vec{J}$ to be composed of a conduction current $\vec{J}_c$ and a displacement current $\vec{J}_D$. We then have

$$\vec{J}_c = \sigma\vec{E}, \tag{V-21}$$

$$\vec{J}_D = j\omega\varepsilon\vec{E} = \frac{\partial\vec{D}}{\partial t}, \tag{V-22}$$

and

$$\vec{J} = \vec{J}_c + \vec{J}_D = K\vec{E}. \tag{V-23}$$

$\vec{J}_c$ is the result of the flow of charge whereas $\vec{J}_D$ is due to a changing $\vec{D}$ field. These can be two separate and distinct processes with each having its own particular mechanism. If the mechanisms can respond instantaneously, that is if σ and ε are real, then $\vec{J}_c$ and $\vec{D}$ will be completely in phase with the impressed field and $\vec{J}_D$ will be exactly 90° ahead of $\vec{E}$. The total current will then have a real part $\vec{J}_c$ and an imaginary part $\vec{J}_D$. This is shown in Figure 25.

If, however, the mechanisms cannot respond instantaneously, then ε and σ become complex and the situation pictured in Figure 26 occurs. $\vec{J}_c$ and $\vec{D}$ both lag behind $\vec{E}$, the amount of each depending on the proper-

Thus the boundary condition for real media and sinusoidal fields is identical with that for ideal dielectrics in static fields if the dielectric constant is replaced by the complex dielectric factor ξ.

The Physical Significance of K

It is customary to treat the quantity $(\sigma + j\omega\varepsilon)\vec{E}$ as a total current density $\vec{J}$ to be composed of a conduction current $\vec{J}_c$ and a displacement current $\vec{J}_D$. We then have

$$\vec{J}_c = \sigma\vec{E}, \tag{V-21}$$

$$\vec{J}_D = j\omega\varepsilon\vec{E} = \frac{\partial\vec{D}}{\partial t}, \tag{V-22}$$

and

$$\vec{J} = \vec{J}_c + \vec{J}_D = K\vec{E}. \tag{V-23}$$

$\vec{J}_c$ is the result of the flow of charge whereas $\vec{J}_D$ is due to a changing $\vec{D}$ field. These can be two separate and distinct processes with each having its own particular mechanism. If the mechanisms can respond instantaneously, that is if σ and ε are real, then $\vec{J}_c$ and $\vec{D}$ will be completely in phase with the impressed field and $\vec{J}_D$ will be exactly 90° ahead of $\vec{E}$. The total current will then have a real part $\vec{J}_c$ and an imaginary part $\vec{J}_D$. This is shown in Figure 25.

If, however, the mechanisms cannot respond instantaneously, then ε and σ become complex and the situation pictured in Figure 26 occurs. $\vec{J}_c$ and $\vec{D}$ both lag behind $\vec{E}$, the amount of each depending on the proper-

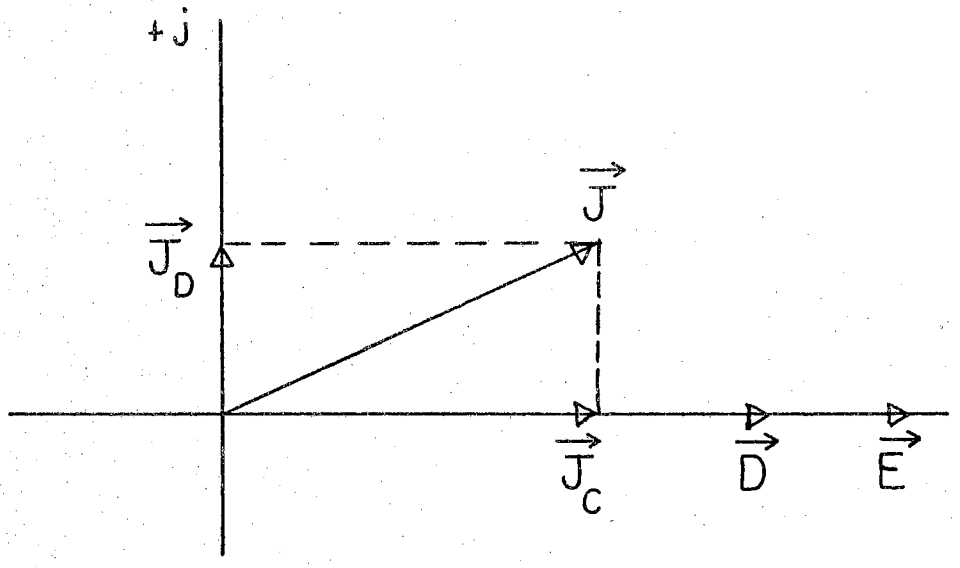

Figure 25. Total Current for the Ideal Case of No Phase Differences.

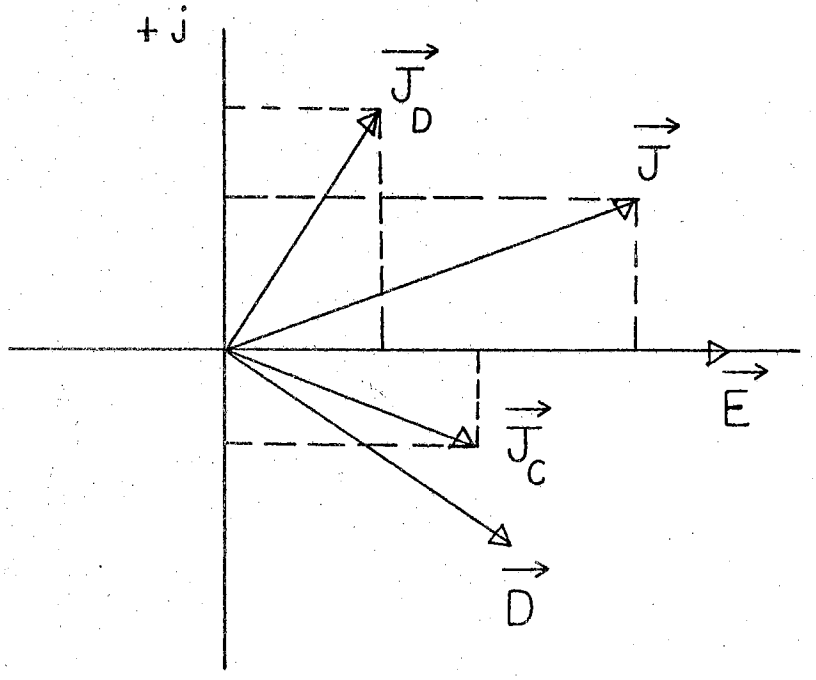

Figure 26. Total Current for the Case of Phase Differences.

ties of its own mechanism, and $\vec{J}_D$ leads $\vec{E}$ by less than 90°. Again the total current $\vec{J}$ has a real part and an imaginary part but they will not be equal to $\vec{J}_c$ and $\vec{J}_D$ respectively. Instead, the real part of $\vec{J}$ is the sum of the real parts of $\vec{J}_c$ and $\vec{J}_D$ while the imaginary part of $\vec{J}$ is given by the sum of the imaginary parts of $\vec{J}_c$ and $\vec{J}_D$.

Expressing $\vec{J}$, $\vec{J}_c$ and $\vec{J}_D$ in terms of their real and imaginary components gives

$$\vec{J} = \vec{J}' + j\,\vec{J}'' \tag{V-24}$$

$$\vec{J}_D = \vec{J}_D' + j\,\vec{J}_D'' \tag{V-25}$$

and

$$\vec{J}_c = \vec{J}_c' + j\,\vec{J}_c'' \tag{V-26}$$

Substituting for ε and σ from Equation (V-4) into (V-21) and (V-22) gives

$$\vec{J}_D = (\omega\varepsilon'' + j\omega\varepsilon')\vec{E}$$

and

$$\vec{J}_c = (\sigma' - j\sigma'')\vec{E}.$$

Comparing these results with Equations (V-24)-(V-26) gives

$$\vec{J}' = \vec{J}_c' + \vec{J}_D' = (\sigma' + \omega\varepsilon'')\vec{E} \tag{V-27}$$

and

$$\vec{J}'' = \vec{J}''_c + \vec{J}''_D = (\omega\varepsilon' - \sigma'')\vec{E}. \qquad \text{(V-28)}$$

The coefficients of $\vec{E}$ in these last two expressions are just the real and imaginary parts of the complex conduction factor K. It should be emphasized that each of these components contains terms from both a conduction and a polarization mechanism. This is illustrated in Figure 27 which is similar to Figure 26 except that the currents have been divided by E to yield conductivity units.

It is usual practice to consider the current as being produced, not by the two true currents $\vec{J}_c$ and $\vec{J}_D$, but by the two component currents $\vec{J}'$ and $\vec{J}''$. The assumption is made that the real current $\vec{J}'$ is produced by some real "effective" conductivity σ_e and that the imaginary current J'' is the result of a real effective permittivity ε_e. That is

$$\vec{J}' = \sigma_e \vec{E} \qquad \text{(V-29)}$$

and

$$\vec{J}'' = \omega\varepsilon_e \vec{E} \qquad \text{(V-30)}$$

Comparison of Equations (V-27) - (V-30) shows that these effective parameters are related to the true parameters by

$$\sigma_e = \sigma' + \omega\varepsilon'' \qquad \text{(V-31)}$$

and

$$\varepsilon_e = \varepsilon' - \frac{\sigma''}{\omega}. \qquad \text{(V-32)}$$

Also since

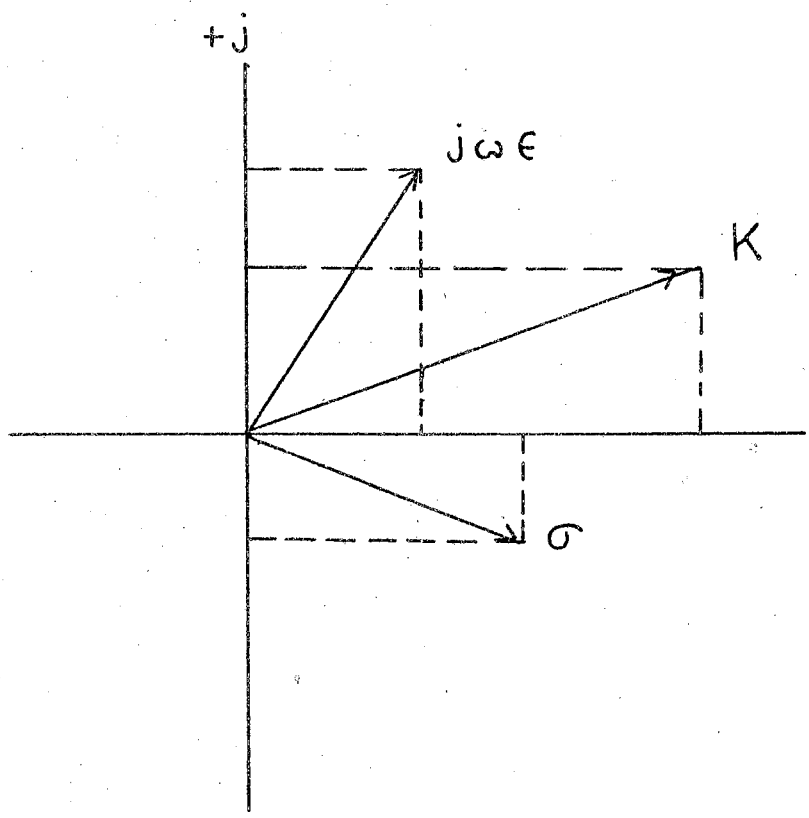

Figure 27. Illustration of Complex Conduction Factor

$$\vec{J} = (\sigma + j\omega\varepsilon)\vec{E} = (\sigma_e + j\omega\varepsilon_e)\vec{E} \qquad \text{(V-33)}$$

then

$$K = \sigma + j\omega\varepsilon = \sigma_e + j\omega\varepsilon_e \, . \qquad \text{(V-34)}$$

Alternatively,

$$\xi = \varepsilon - \frac{j\sigma}{\omega} = \varepsilon_e - \frac{j\sigma_e}{\omega} \, . \qquad \text{(V-35)}$$

In the foregoing analysis, the two basic processes of conduction and polarization were assumed to be non-instantaneous processes which leads to time lags of response and complex quantities. Maxwell's equations for this case, Equation (V-9), indicates the total current to be related to the electric field by the complex quantity K. This quantity is at all times the combination of two other complex quantities σ and ε, or it can be considered to be the complex sum of two real quantities σ_e and ε_e. Fundamentally, the former approach is the correct one, but for the taking of physical measurements, the latter is more convenient.

Experimental Determination of ε_e and σ_e

When an alternating voltage V is applied to an arbitrary sample between parallel electrodes, the resulting current I will in general be out of phase with the voltage. The material can be modeled as a pure resistance R and a pure capacitance C in parallel. The resistor current is in phase with the voltage, the capacitor current is 90° out of phase. The admittance of such a setup is

$$Y = \frac{1}{R} + j\omega C = \frac{I}{V} \, , \qquad \text{(V-36)}$$

Recalling that the resistance and capacitance for this parallel model can be defined in terms of a real conductivity and a real permittivity as

$$\frac{1}{R} = \frac{\sigma_m A}{d} \tag{V-37}$$

and

$$C = \frac{\sigma_m A}{d} , \tag{V-38}$$

where A is the crossectional area of the material and d is the plate separation, enables Equation (V-36) to be transformed to

$$\frac{V}{d} (\sigma_m + j\omega\varepsilon_m) = \frac{I}{A} . \tag{V-39}$$

But by the definitions of $\vec{E}$ and $\vec{J}$ this equation is just

$$\vec{J} = (\sigma_m + j\omega\varepsilon_m)\vec{E} \tag{V-40}$$

which is identical to Equation (V-33). Since in this case σ_m and ε_m are defined to be real quantities then they must be the effective parameters σ_e and ε_e. These quantities can be determined experimentally by balancing the sample material against a parallel combination on an impedance bridge.

Thus we see the utility of considering the material to have an effective conductivity and permittivity, since it is these quantities which are easily measured. But again it should be stressed that these quantities are not a direct measure but an implicit measure of the true conduction and polarization mechanisms occurring in the material.

General Energy and Force Equations

In order to develop a generalized force equation it is necessary to first determine a general expression for the electric energy of a system. The force can then be obtained by taking the negative gradient of this energy. For sinusoidal fields it is shown by King (55) that the time averaged electric energy in a volume τ is given by

$$\bar{U} = \tfrac{1}{4} \int_{\tau} \varepsilon_e \vec{E}^2 \, d\tau, \tag{V-41}$$

where $\vec{E}$ is the amplitide of the varying $\vec{E}$ field and <u>not</u> the rms value. Recalling from Equation (V-35) that

$$\varepsilon_e = \text{Re } (\xi) = \text{Re } (\xi^*), \tag{V-42}$$

where ξ^* is the complex conjugate of ξ and Re (ξ) is the real part of ξ, allows the energy to be expressed as

$$\bar{U} = \tfrac{1}{4} \int_{\tau} \text{Re } (\vec{E} \cdot \xi^* \vec{E}^*) d\tau \, . \tag{V-43}$$

Defining the quantity $\vec{\mathbb{D}}$ as the "total displacement vector" by (See Equations (V-2) and (V-35)

$$\vec{\mathbb{D}} = \xi \vec{E} = \vec{D} - \frac{jJ_c}{\omega} \tag{V-44}$$

gives the energy as

$$\bar{U} = \tfrac{1}{4} \int_{\tau} \text{Re } (\vec{E} \cdot \vec{\mathbb{D}}^*) d\tau. \tag{V-45}$$

To determine the energy of a body in an external field requires the intergal to be evaluated over all space. This is usually impossible

to do, so that a simpler integration is required. It is possible to develop an expression for the energy in terms of an integral over the body alone. This development is identical in approach to that used by Schwarz (74) for the non-conducting case. In that case, the conduction current is zero and $\vec{\mathbb{D}}$ is equal to $\vec{D}$.

Consider a field $\vec{E}_o$ established by charged conductors of finite extent in a linear isotropic medium of complex dielectric factor ξ_4 with a resulting total displacement of $\vec{\mathbb{D}}_o$. Now insert a body of complex factor ξ and denote the resultant field vectors by $\vec{E}$ and $\vec{\mathbb{D}}$. The change in energy will be given according to Equation (V-45) as

$$\Delta\bar{U} = \tfrac{1}{4} \int_{\text{all space}} \text{Re}\,(\vec{E} \cdot \vec{\mathbb{D}}^* - \vec{E}_o \cdot \vec{\mathbb{D}}_o^*)\,d\tau. \qquad \text{(V-46)}$$

The integrand can be modified using the identity

$$\text{Re}(\vec{E} \cdot \vec{\mathbb{D}}^* - \vec{E}_o \cdot \vec{\mathbb{D}}_o^*) = \text{Re}\{(\vec{E} + \frac{\xi_4}{\xi_4^*}\vec{E}_o)^* \cdot (\vec{\mathbb{D}} - \vec{\mathbb{D}}_o) + (\vec{E} \cdot \vec{\mathbb{D}}_o^* - \frac{\xi_4^*}{\xi_4}\vec{E}_o^* \cdot \vec{\mathbb{D}})\} \qquad \text{(V-47)}$$

Since $\vec{\mathbb{D}} = \xi_4\vec{E}$ outside the body, the second expression on the right is nonzero only inside the body.

The first term on the right can be expressed in terms of potentials as

$$(\vec{E} + \frac{\xi_4}{\xi_4^*}\vec{E}_o)^* \cdot (\vec{\mathbb{D}} - \vec{\mathbb{D}}_o) = -(\nabla\phi + \frac{\xi_4}{\xi_4^*}\nabla\phi_o)^* \cdot (\vec{\mathbb{D}} - \vec{\mathbb{D}}_o)$$

$$= -(\nabla\psi)^* \cdot (\vec{\mathbb{D}} - \vec{\mathbb{D}}_o) = -\nabla(\psi^*) \cdot (\vec{\mathbb{D}} - \vec{\mathbb{D}}_o) \qquad \text{(V-48)}$$

where

$$\psi = \phi + \frac{\xi_4}{\xi_4^*} \phi_o \, . \tag{V-49}$$

But

$$-\nabla\psi^* \cdot (\vec{\mathbb{D}} - \vec{\mathbb{D}}_o) = -\nabla\cdot(\psi^*(\vec{\mathbb{D}} - \vec{\mathbb{D}}_o)) + \psi^*(\nabla\cdot(\vec{\mathbb{D}} - \vec{\mathbb{D}}_o)) . \tag{V-50}$$

One of Maxwell's equations for simple media and periodic fields using Equations (V-9), (V-19), and (V-44) becomes

$$\nabla \times \vec{H} = \vec{J}_c + \frac{\partial \vec{D}}{\partial t} = (\sigma + j\omega\varepsilon)\vec{E} = j\omega\vec{\mathbb{D}} \, .$$

Using the vector identity that the divergence of a curl is zero gives

$$\nabla\cdot(\nabla \times H) = j\omega(\nabla\cdot\vec{\mathbb{D}}) = 0 \tag{V-51}$$

and the last term in Equation (V-50) is zero. [Note: The derivation given by Schwarz (74) asserts div $\vec{D}$ = div $\vec{D}_o$. But div $\vec{D} = \rho$ if free charge is present, hence his result is not general. The use here of div $\vec{\mathbb{D}} = 0$ is not so restricted, and gives a general result.] The volume integral of the remaining first term can be transformed by the divergence theorem into a surface integral over the enclosing surfaces, giving

$$-\int_{\text{all space}} \nabla\cdot\{\psi^*(\vec{\mathbb{D}}-\vec{\mathbb{D}}_o)\}d\tau = -\lim_{S_o \to \infty} \oint_{S_o} \psi^*(\vec{\mathbb{D}}-\vec{\mathbb{D}}_o)dS + \sum_k \oint_{S_k} \psi^*(\vec{\mathbb{D}}-\vec{\mathbb{D}}_o)dS, \tag{V-52}$$

where the S_k are the conductor surfaces and S_o is a surface which increases to infinity. Since ψ^* is established by the conductors, it is proportional to 1/r at large distances. $\vec{\mathbb{D}}$ is proportional to $\vec{E}$ and

hence to $\nabla\psi$. This gives $\vec{\mathbb{D}}$ proportional to $1/r^2$ and since the surface area is proportional to r^2 the value of the S_o integral is proportional to $1/r$ and goes to zero as $r \to \infty$. The S_k integrals are associated with the work done ΔW at the conductors upon introducing the body and so is not associated with the energy of the body per se. Thus the first term in Equation (V-47) gives the work done at the conductors and the second is nonzero only in the body. Equation (V-46) then becomes,

$$\Delta\bar{U} = \tfrac{1}{4}\int_{body} \mathrm{Re}\,(\vec{E}\cdot\vec{\mathbb{D}}_o^* - \frac{\xi_4^*}{\xi_4}\vec{E}_o^*\cdot\vec{\mathbb{D}})d\tau + \Delta W. \qquad (V\text{-}53)$$

The time averaged mean energy of the body is therefore $\Delta\bar{U} - \Delta W = \bar{w}$, or

$$\bar{w} = \tfrac{1}{4}\int_{body} \mathrm{Re}(\vec{E}\cdot\vec{\mathbb{D}}_o^* - \frac{\xi_4^*}{\xi_4}\vec{E}_o^*\cdot\vec{\mathbb{D}})d\tau$$

$$= \tfrac{1}{4}\int_{body} \mathrm{Re}(\xi_4^*(\vec{E}\cdot\vec{E}_o^* - \frac{\xi}{\xi_4}\vec{E}_o^*\cdot\vec{E}))d\tau$$

$$= \tfrac{1}{4}\int_{body} \mathrm{Re}(\xi_4^*(1 - \frac{\xi}{\xi_4})\vec{E}_o^*\cdot\vec{E})d\tau, \qquad (V\text{-}54)$$

and we have now reduced the integral to one over the body alone. This result is the same as that of Schwarz when $\xi = \varepsilon$.

It is now a simple matter to obtain the general force equation by taking the negative gradient of Equation (V-54). That operation gives

$$\vec{F} = -\tfrac{1}{4}\int_{body} \mathrm{Re}\{\nabla(\xi_4^*(1 - \frac{\xi}{\xi_4})\vec{E}_o^*\cdot\vec{E})\}d\tau\ . \qquad (V\text{-}55)$$

Before this expression can be evaluated, one must know the original impressed field $\vec{E}_o$, the resultant field $\vec{E}$ throughout the body, and the complex dielectric factor for all parts of the body. $\vec{E}_o$ will be deter-

mined by the electrode geometry, ξ will depend on the conduction and polarization mechanism involved, and $\vec{E}$ will be specified in terms of the ξ's by the boundary conditions of Equation (V-17).

If Equation (V-55) is a general force equation, then it must contain provisions for each of the mechanisms discussed in Chapter IV. This is easily shown to be the case. The rotating dipole mechanism and its relaxation effects are provided for by allowing ε to be complex. The gating mechanism and also any other conduction relaxation effects arise through the complex conductivity. The Maxwell-Wagner multi-layer membrane effects are direct results of the boundary conditions on $\vec{E}$ at the layer interfaces. And finally, the relaxation of an ionic atmosphere can be included simply by considering an extra outer layer to have a high complex conductivity.

CHAPTER VI

FORCE ON A YEAST CELL MODEL

The force equation developed in the previous chapter is general in nature. Before it can be applied to a particular body, say a yeast cell, the electrical characteristics at all points within the body must be known. Since these are not known for yeast, before any theoretical results can be calculated, some assumptions about the cell makeup and electrical behavior must be made. That is, a physical model must be chosen to represent the cell and reasonable electrical properties assigned to it.

In arriving at a suitable model from which to make calculations, we are guided by the suggestions of Fuoss (56).

> In selection of the model, the author must be guided by two principles; the model must be complicated enough to include those details which are pertinent to the problem at hand, and it must be simple enough to be amenable to treatment by the available mathematical methods. What is sought is a one-to-one correspondence between the model and the actual physical system which it represents. Obviously the more details we want the theory to describe, the more complicated must the model be.

In line with this reasoning we select a model which grossly resembles a yeast cell and contains the essential electrical mechanisms. Due to the existence of the boundary condition equation at each interface, the complexity of the mathematical treatment increases rapidly as the number of interfaces increases. Therefore, it is necessary to keep the number of distinct regions to as few as possible and still approxi-

mate a yeast cell. This leads to the choice that the model consist of three separate regions. Since yeast are spherical to ovoid, the model is chosen to be composed of three concentric spheres.

The interior of the model is meant to correspond to the yeast cell cytoplasm, the bulk of the cell. The first shell represents the cell membrane, which is assumed homogeneous. This eliminates the multilayered structure of the membrane from further consideration. The second or outer shell corresponds to an ion atmosphere surrounding the cell proper. Each of the three cell regions as well as the suspending medium are assigned a complex conductivity and a complex permittivity. This retains the possibility of having relaxation effects occurring for both the conductivity and permittivity. With the addition of the outer ionic atmosphere, the model contains provisions for the inclusion of three of the four mechanisms discussed previously.

Obviously this model is a gross oversimplification of the true state of affairs. A more desirable model would be one which also includes the multilayered membrane structure, the cell wall, the nucleus and its membrane, and various intracellular bodies. However, this leads to complications in the mathematical treatment to such a degree that the solution becomes intractable. We are concerned here more with the testing of an approach than with the exact description of the experimental behavior. Therefore, if the general features of dielectrophoresis can be obtained with this model, then the theory shall have been verified and more complicated models can be devised for more accurate descriptions.

Form of Relaxation for ε and σ

To this point no restrictions have been made on the form of the time lags of ε and σ. And it is not necessary that we make any such restrictions before going on to calculate forces and yields in a general manner. However, it is appropriate to discuss at this time the assumptions that will be made for the model system.

Complex ε

As was mentioned in Chapter IV, the simplest mechanism for permittivity relaxation was introduced by Debye (27) in terms of rotating dipoles. For a single relaxation mechanism, the complex permittivity ε is expressed by

$$\varepsilon = \varepsilon_\infty + \frac{(\varepsilon_s - \varepsilon_\infty)}{1 + j\omega\tau_\varepsilon}, \qquad \text{(VI-1)}$$

where ε_s and ε_∞ are the real parts of ε at very low and very high frequencies respectively, ω is the angular frequency, j is the $\sqrt{-1}$, and τ_ε is the relaxation time of the mechanism. Equation (VI-1) can be broken into real and imaginary parts to give

$$\varepsilon' = \varepsilon_\infty + \frac{\varepsilon_s - \varepsilon_\infty}{1 + \omega^2\tau_\varepsilon^2} \qquad \text{(VI-2)}$$

and

$$\varepsilon'' = (\varepsilon_s - \varepsilon_\infty)\frac{\omega\tau_\varepsilon}{1 + \omega^2\tau_\varepsilon^2}. \qquad \text{(VI-3)}$$

From Equation (VI-2) the relaxation time is

$$\tau_\varepsilon = \frac{1}{\omega}\sqrt{\frac{\varepsilon_s - \varepsilon'}{\varepsilon' - \varepsilon_\infty}}$$

where ω and ε' both vary in such a manner as to keep τ_ε constant. τ_ε may also be obtained from the graph of Equation (VI-3) when ε'' is a maximum,

$$\tau_\varepsilon = 1/\omega_{max} \,. \qquad \text{(VI-4)}$$

Mechanisms other than those with a single relaxation time do exist and their treatment requires the assumption of a distribution of relaxation times (39). However, these mechanisms will be excluded from our model.

Complex σ

Just as the permittivity can be assumed to be represented by a single relaxation time, the simplest description of conductivity relaxation is that which contains only one relaxation time (55, 57, 58). The forms of the appropriate equations are identical with those for permittivity. That is, the complex conductivity σ can be expressed by

$$\sigma = \sigma_\infty + \frac{(\sigma_s - \sigma_\infty)}{1 + j\omega\tau_\sigma} \qquad \text{(VI-5)}$$

whose real and imaginary components are

$$\sigma' = \sigma_\infty + \frac{\sigma_s - \sigma_\infty}{1 + \omega^2\tau_\sigma^2} \qquad \text{(VI-6)}$$

and

$$\sigma'' = \frac{(\sigma_s - \sigma_\infty)\,\omega\,\tau_\sigma}{1 + \omega^2\tau_\sigma^2} \,. \qquad \text{(VI-7)}$$

The subscripts s and ∞ again refer to static and high frequency values respectively and τ_σ is the relaxation time associated with the conduction mechanism. It should be stressed that τ_σ and τ_ε for a particular sample may be completely unrelated if the mechanisms responsible for each are different.

Form of ξ

With these assumptions for ε and σ, expressions for the real and imaginary parts of the complex dielectric factor ξ can be given. From Equations (V-31), (VI-3), and VI-6)

$$\sigma_e = \sigma' + \omega\varepsilon'' = \sigma_\infty + \frac{(\sigma_s - \sigma_\infty)}{1 + \omega^2\tau_\sigma^2} + \frac{\omega^2(\varepsilon_s - \varepsilon_\infty)\tau_\varepsilon}{1 + \omega^2\tau_\varepsilon^2} . \qquad \text{(VI-8)}$$

Equations (V-32), (VI-2), and (VI-7) give

$$\varepsilon_e = \varepsilon' - \frac{\sigma''}{\omega} = \varepsilon_\infty + \frac{(\varepsilon_s - \varepsilon_\infty)}{1 + \omega^2\tau_\varepsilon^2} - \frac{(\sigma_s - \sigma_\infty)\tau_\sigma}{1 + \omega^2\tau_\sigma^2} . \qquad \text{(VI-9)}$$

Since Equation (V-35) gives

$$\xi = \varepsilon_e - j\,\sigma_e/\omega,$$

the expression in Equation (VI-9) is the real part of ξ and Equation (VI-8) divided by $-\omega$ gives the imaginary part of ξ.

Determination of the Potential

Once the model has been chosen and electrical parameters ascribed to it, the boundary equations can be applied and the resulting potentials

and electric fields determined. From Equation (V-59) it is seen that if the electric field is known throughout the model then the force can be calculated. In the remainder of this chapter, the potentials, the fields, and finally the force will be calculated for the two-shell model.

We begin by considering a medium supporting a uniform field of strength $\vec{E}_o$ and in which is placed a sphere of radius a_1, enclosed by two concentric spheres of radii a_2 and a_3 as shown in Figure 28. The three regions of the sphere have complex dielectric factors ξ_1, ξ_2 and ξ_3, while that of the external medium is ξ_4. Recalling Equation (V-19) we have

$$\xi_i = \varepsilon_i - j\,\sigma_i/\omega \,, \tag{VI-10}$$

where ε_i and σ_i are complex. The boundary conditions for simple media are given by Equations (V-16) and (V-20) as

$$\nabla \cdot \vec{E} = 0$$

everywhere but at the boundaries and

$$\xi_i(\vec{n}_i \cdot \vec{E}_i) = \xi_j(\vec{n}_i \cdot \vec{E}_j)$$

at the boundary between media i and j where $\vec{n}_i$ is the outward normal to region i. (Note $\vec{n}_i = -\vec{n}_j$). For frequencies below the microwave region the field can be expressed in terms of a scalar potential ϕ as

$$\vec{E} = -\nabla\Phi \,. \tag{VI-11}$$

Using this relation, the boundary conditions become

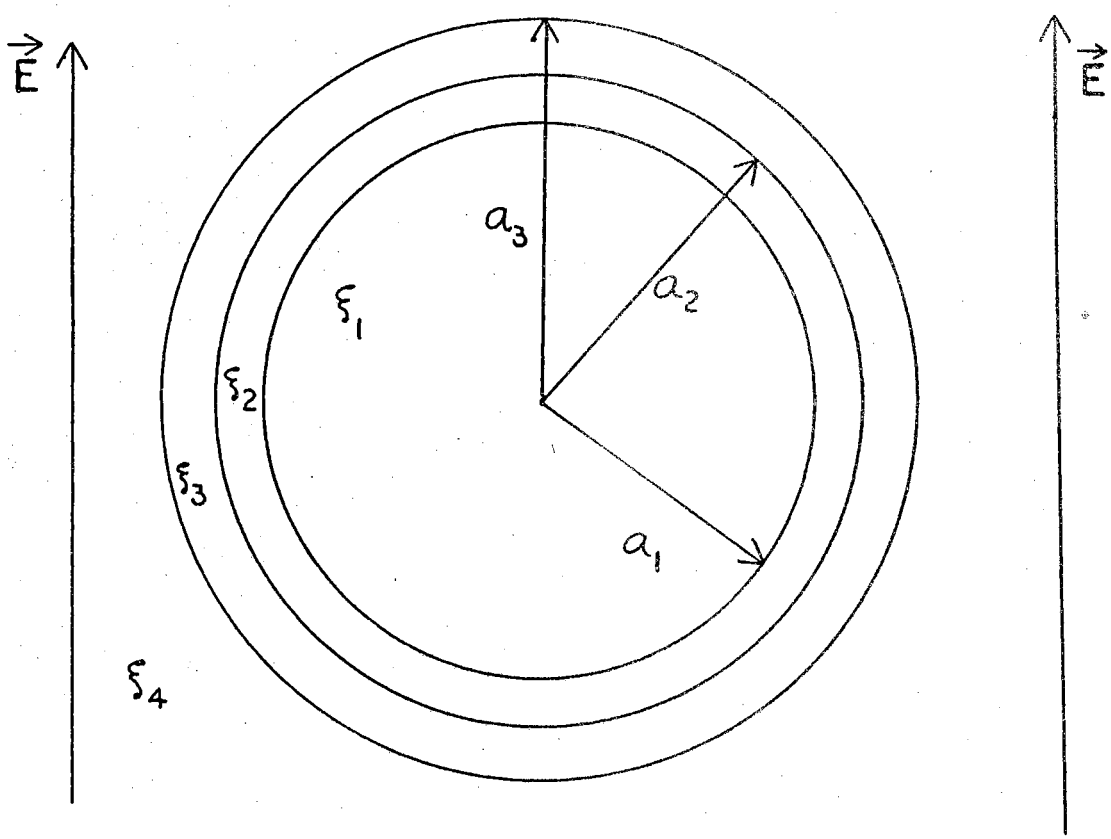

Figure 28. Two Shell Model of Yeast Cell.

$$\nabla^2 \Phi = 0 \qquad \text{(VI-12)}$$

and

$$\xi_i (\vec{n}_i \cdot \nabla \Phi_i) = \xi_j (\vec{n}_i \cdot \nabla \Phi_j). \qquad \text{(VI-13)}$$

A third condition exists and that is the continuity of the potential at the boundary or

$$\Phi_i = \Phi_j . \qquad \text{(VI-14)}$$

We must solve the three equations, Equations (VI-12), (VI-13), and (VI-14) for the particular case of a two shelled sphere. The most convenient coordinate system is obviously the polar coordinate system, with the external field directed along the z axis as shown in Figure 29. The origin is selected to be at the center of the sphere. In this case, Laplace's equation, Equation (VI-12) becomes

$$\frac{1}{r^2} \frac{\partial}{\partial r} \left(r^2 \frac{\partial \Phi}{\partial r}\right) + \frac{1}{r^2 \sin\theta} \frac{\partial}{\partial \theta} \left(\sin\theta \frac{\partial \Phi}{\partial \theta}\right) + \frac{1}{r^2 \sin^2\theta} \frac{\partial^2 \Phi}{\partial \phi^2} = 0 \qquad \text{(VI-15)}$$

For this configuration the original potential is given by

$$\Phi_o = - E_o r \operatorname{Cos} \theta . \qquad \text{(VI-16)}$$

When the sphere is placed into the field, the new fields, both inside and outside the sphere, will retain the symmetry about the z axis and thereby be independent of ϕ. For the particular case of polar coordinates and axial symmetry the term involving $\frac{\partial^2 \Phi}{\partial \phi^2}$ in Equation (VI-15) is zero and the solution involves the use of Legendre functions. In each of the four regions the potential can be expressed by (59)

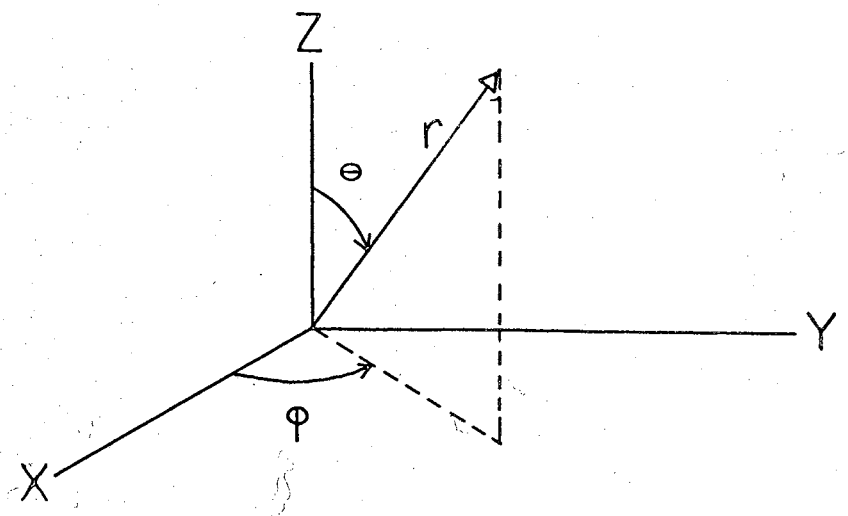

Figure 29. Polar Coordinate System.

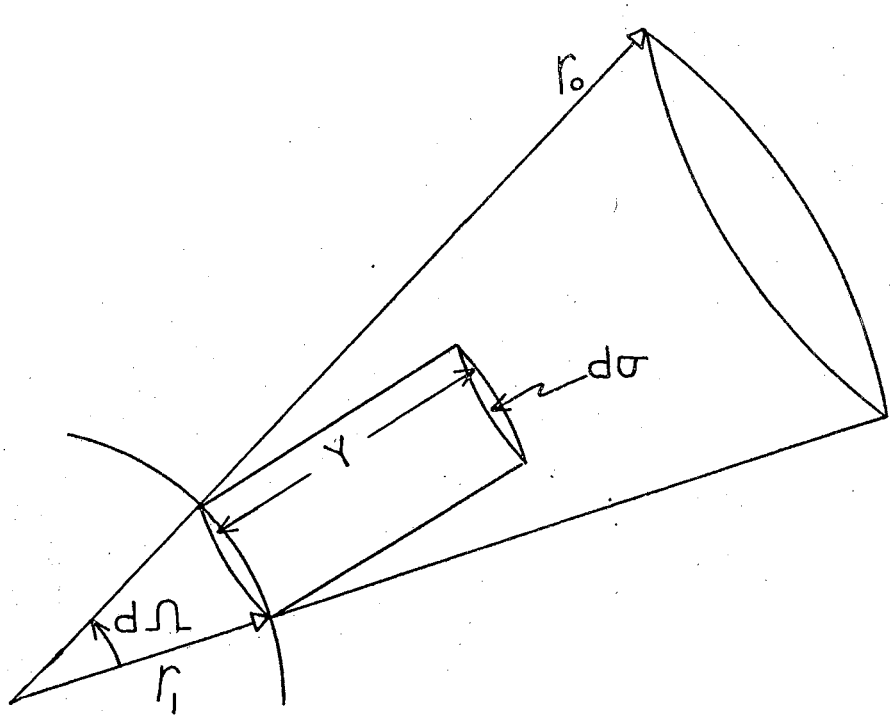

Figure 30. Relation of Volume Occupied by Cells to Volume Swept Out.

$$\Phi_i = \sum_{n=0}^{\infty} (A_{in} r^n + B_{in} r^{-(n+1)}) P_n(\text{Cos } \theta); \; i = 1 - 4, \qquad \text{(VI-17)}$$

where the $P_n(\text{Cos } \theta)$ are the Legendre functions and the A_{in} and B_{in} are constants to be determined by the application of Equations (VI-13) and (VI-14). Since the normals to the boundaries are radial, Equation (VI-13) becomes

$$\xi_i \frac{\partial \Phi_i}{\partial r} = \xi_j \frac{\partial \Phi_j}{\partial r} . \qquad \text{(VI-18)}$$

The two equations at each of the three boundaries gives a total of six equations; but there are eight sets of constants to be determined. The other two sets are determined as follows. The potential Φ_1 is required to be finite at the center of the sphere. This sets all of the $B_{1n} = 0$. The potential at a large distance from the sphere should be unaffected by the sphere and so remain uniform and equal to its original value of $- E_o \text{Cos } \theta$. This is satisfied only if $A_{41} = - E_o$ and $A_{4n} = 0$, $n \neq 1$.

The six sets of constants can now be determined by solving the six sets of boundary conditions, which are

$$\Phi_1 = \Phi_2 \text{ and } \xi_1 \frac{\partial \Phi_1}{\partial r} = \xi_2 \frac{\partial \Phi_2}{\partial r} \text{ at } r = a_1,$$

$$\Phi_2 = \Phi_3 \text{ and } \xi_2 \frac{\partial \Phi_2}{\partial r} = \xi_3 \frac{\partial \Phi_3}{\partial r} \text{ at } r = a_2, \qquad \text{(VI-19)}$$

and

$$\Phi_3 = \Phi_4 \text{ and } \xi_3 \frac{\partial \Phi_3}{\partial r} = \xi_4 \frac{\partial \Phi_4}{\partial r} \text{ at } r = a_3.$$

The appropriate forms of Φ_i and $\frac{\partial \Phi_i}{\partial r}$ are obtained from Equation (VI-17).

The algebra is somewhat involved and will not be given here. The crucial part of the solution is setting equal the coefficients of like Legendre functions. The results are:

$$A_{in} = B_{in} = 0; \quad n \neq 1, \tag{VI-20}$$

$$A_{21} = \frac{A_{11}(\xi_1 + 2\xi_2)}{3\xi_2}, \tag{VI-21}$$

$$B_{21} = \frac{A_{11}(\xi_2 - \xi_1)a_1^3}{3\xi_2}, \tag{VI-22}$$

$$A_{31} = \frac{A_{11}}{9\xi_2 \xi_3 a_2^3}\left[(\xi_1+2\xi_2)(\xi_2+2\xi_3)\ a_2^3 + 2(\xi_2-\xi_1)(\xi_3-\xi_2)\ a_1^3\right] \tag{VI-23}$$

$$B_{31} = \frac{A_{11}}{9\xi_2 \xi_3}\left[(\xi_1+2\xi_2)(\xi_3-\xi_2)\ a_2^3 + (\xi_3+2\xi_2)(\xi_2-\xi_1)\ a_1^3\right] \tag{VI-24}$$

$$A_{41} = -E_o \tag{VI-25}$$

$$B_{41} = \frac{A_{31}(\xi_4 - \xi_3)\ a_3^3}{3\xi_4} + \frac{B_{31}(2\xi_3 + \xi_4)}{3\xi_4} \tag{VI-26}$$

$$A_{11} = \frac{-27\xi_2\xi_3\xi_4 a_3^3 E_o}{L_1 + L_2} \tag{VI-27}$$

where

$$L_1 = a_3^3(2\xi_4+\xi_3)\left[(\xi_1+2\xi_2)(\xi_2+2\xi_3) + 2(\xi_2-\xi_1)(\xi_3-\xi_2)\frac{a_1^3}{a_2^3}\right] \tag{VI-28}$$

$$L_2 = 2(\xi_4-\xi_3)[(\xi_1+2\xi_2)(\xi_3-\xi_2)\, a_2^{\,3} + (\xi_3+2\xi_2)(\xi_2-\xi_1)\, a_1^{\,3}] \qquad \text{(VI-29)}$$

and

$$B_{11} = 0. \qquad \text{(VI-30)}$$

The solutions for the potentials are then

$$\Phi_1 = A_{11}\, r \cos\theta, \quad \Phi_2 = (A_{21}\, r + \frac{B_{21}}{r^2}) \cos\theta$$
$$\Phi_3 = (A_{31}\, r + \frac{B_{31}}{r^2}) \cos\theta, \quad \Phi_4 = (A_{41}\, r + \frac{B_{41}}{r^2}) \cos\theta, \qquad \text{(VI-31)}$$

since

$$P_1(\cos\theta) = \cos\theta\ . \qquad \text{(VI-32)}$$

Determination of $\vec{E}$ Fields

From Equation (VI-11), it is a simple matter to derive the $\vec{E}$ fields in each region. Since the constants are all proportional to $-E_o$, it is convenient to introduce a new set of constants defined by:

$$A_{11} = -A_1E_o \quad B_{21} = -B_2E_o$$
$$A_{21} = -A_2E_o \quad B_{31} = -B_3E_o \qquad \text{(VI-32)}$$
$$A_{31} = -A_3E_o \quad B_{41} = -B_4E_o\ .$$

In spherical coordinates the del operator is

$$\nabla = \hat{r}\frac{\partial}{\partial r} + \hat{\theta}\frac{1}{r}\frac{\partial}{\partial\theta} + \hat{\phi}\frac{1}{r\sin\theta}\frac{\partial}{\partial\phi}\ , \qquad \text{(VI-33)}$$

where $\hat{r}$, $\hat{\theta}$, and $\hat{\phi}$ are the appropriate unit vectors. Since the potentials

are independent of ϕ, the third term is zero and we have

$$\vec{E} = -\hat{r}\frac{\partial \Phi}{\partial r} - \hat{\theta}\frac{1}{r}\frac{\partial \Phi}{\partial \theta} . \qquad \text{(VI-34)}$$

Applying this equation to each of the potentials in Equations (VI-16) and (VI-31) gives the original field and those in each region as

$$\begin{aligned}
\vec{E}_o &= E_o (\hat{r} \cos\theta - \hat{\theta} \sin\theta) \\
\vec{E}_1 &= E_o A_1 (\hat{r} \cos\theta - \hat{\theta} \sin\theta) \\
\vec{E}_2 &= E_o \left[\hat{r}\left(A_2 - \frac{2B_2}{r^3}\right) \cos\theta - \hat{\theta}\left(A_2 + \frac{B_2}{r^3}\right) \sin\theta\right] \qquad \text{(VI-35)} \\
\vec{E}_3 &= E_o \left[\hat{r}\left(A_3 - \frac{2B_3}{r^3}\right) \cos\theta - \hat{\theta}\left(A_3 + \frac{B_3}{r^3}\right) \sin\theta\right] \\
\vec{E}_4 &= E_o \left[\hat{r}\left(1 - \frac{2B_4}{r^3}\right) \cos\theta - \hat{\theta}\left(1 + \frac{B_4}{r^3}\right) \sin\theta\right] .
\end{aligned}$$

Evaluation of the Energy Integral

Now that the electric fields are known in all three regions of the model, the time averaged energy of the body can be determined by evaluating the integral given in Equation (V-54). It is the sum of integrals over each of the three volumes; v_1 of the inner sphere, v_2 of the first shell, and v_3 of the second shell. That is

$$\bar{W} = \tfrac{1}{4} \mathrm{Re}\left\{\int_{v_1} \xi_4^* \left(1 - \frac{\xi_1}{\xi_4}\right) \vec{E}_o^* \cdot \vec{E}_1 \, dv + \int_{v_2} \xi_4^* \left(1 - \frac{\xi_2}{\xi_4}\right) \vec{E}_o^* \cdot \vec{E}_2 \, dv \right.$$

$$\left. + \int_{v_3} \xi_4^* \left(1 - \frac{\xi_3}{\xi_4}\right) \vec{E}_o^* \cdot \vec{E}_3 \, dv\right\}. \qquad \text{(VI-36)}$$

From Equations (VI-35)

$$\vec{E}_o^* \cdot \vec{E}_1 = E_o^2 A_1,$$

$$\vec{E}_o^* \cdot \vec{E}_2 = E_o^2 [A_2 - \frac{B_2}{r^3} (2 \cos^2 \theta - \sin^2 \theta)] \qquad \text{(VI-37)}$$

$$\vec{E}_o^* \cdot \vec{E}_3 = E_o^2 [A_3 - \frac{B_3}{r^3} (2 \cos^2 \theta - \sin^2 \theta)].$$

The integral over the inner sphere becomes

$$\int_{v_1} \xi_4^* (1 - \frac{\xi_1}{\xi_4}) E_o^2 A_1 dv = \xi_4^* (1 - \frac{\xi_1}{\xi_4}) E_o^2 A_1 \cdot v_1 = \frac{4}{3} \pi a_1^3 \xi_4^* (1 - \frac{\xi_1}{\xi_4}) A_1 E_o^2. \qquad \text{(VI-38)}$$

The integral over the first shell is

$$\int_{a_1}^{a_2} \int_o^{\pi} \int_o^{2\pi} \xi_4^* (1 - \frac{\xi_2}{\xi_4}) (A_2 - \frac{B_2}{r^3} (2 \cos^2 \theta - \sin^2 \theta)) E_o^2 r^2 \sin \theta \, dr d\theta d\phi$$

$$= \xi_4^* (1 - \frac{\xi_2}{\xi_4}) (\frac{4\pi (a_2^3 - a_1^3)}{3}) A_2 E_o^2 . \qquad \text{(VI-39)}$$

It should be noticed that the portion containing the B_2 term and the θ dependence integrates to zero and so has no effect on the energy of the body. Similarly the second shell integral is

$$\int_{a_2}^{a_3} \int_o^{\pi} \int_o^{2\pi} \xi_4^* (1 - \frac{\xi_3}{\xi_4}) (A_3 - \frac{B_3}{r^3} (2 \cos^2 \theta - \sin^2 \theta)) E_o^2 r^2 \sin \theta \, dr d\theta d\phi$$

$$= \xi_4^* (1 - \frac{\xi_3}{\xi_4}) (\frac{4\pi (a_3^3 - a_2^3)}{3}) A_3 E_o^2 . \qquad \text{(VI-40)}$$

Upon substitution of Equations (VI-38), (VI-39), and (VI-40) into Equa-

tion (VI-36) the energy of the body is seen to be

$$\bar{w} = \frac{\pi E_o^2}{3} \mathrm{Re}\left\{\frac{\xi_4^*}{\xi_4}\left[(\xi_4 - \xi_1)A_1 a_1^3 + (\xi_4 - \xi_2)A_2(a_2^3 - a_1^3) + (\xi_4 - \xi_3)A_3(a_3^3 - a_2^3)\right]\right\}. \quad \text{(VI-41)}$$

Force in Nonuniform Field

The preceding derivation has been based on the assumption of a uniform field prior to insertion of the body. Since the very nature of dielectrophoresis requires that the field be nonuniform, it is legitimate to question the validity of applying these results. The use of the uniform field results is certainly an approximation but if the field does not change radically over the dimension of the body then the approximation is a good one, with the correction being small. This can be shown by comparing the potential inside a sphere in a uniform field to that inside a sphere in the radial field of a point charge as given by Stratton (59). The first correction term is smaller than the main term by at least the factor a/d, where a is the sphere radius and d is the distance of the center from the charge. For practical applications this ratio is usually quite small, so that the uniform field boundary conditions may be applied. Had the original field been assumed nonuniform, the evaluation of the volume integrals would have been much more complicated.

The force on the two-shelled sphere is obtained by taking the negative gradient of Equation (VI-41). Since the media are assumed isotropic that gives

$$\vec{F} = -\nabla\bar{w} = -\frac{\pi(\nabla E_o^2)}{3}\,\mathrm{Re}\,\{\frac{\xi_4^*}{\xi_4}[(\xi_4-\xi_1)A_1a_1^3+(\xi_4-\xi_2)A_2(a_2^3-a_1^3)$$

$$+(\xi_4-\xi_3)A_3(a_3^3-a_2^3)]\} \quad \text{(VI-42)}$$

The values of A_1, A_2, and A_3 are obtained from Equations (VI-21),(VI-23), (VI-27) and (VI-32) and substituted into (VI-42) to give, after some rearrangement,

$$\vec{F} = -\pi\,(\nabla E_o^2)\,\mathrm{Re}\,\{\xi_4^*(\frac{N1 + N2 + N3}{D1 + D2})\} \quad \text{(VI-43)}$$

with

$$N1 \equiv 9\xi_2\xi_3(\xi_4 - \xi_1)a_1^3a_2^3a_3^3 \quad \text{(VI-44)}$$

$$N2 \equiv 3\xi_3(\xi_1 + 2\xi_2)(\xi_4 - \xi_2)(a_2^3 - a_1^3)a_2^3a_3^3 \quad \text{(VI-45)}$$

$$N3 \equiv a_3^3(\xi_4 - \xi_3)(a_3^3 - a_2^3)\,X1 \quad \text{(VI-46)}$$

$$D1 \equiv a_3^3(\xi_3 + 2\xi_4)\,X1 \quad \text{(VI-47)}$$

and

$$D2 \equiv 2a_2^3(\xi_4 - \xi_3)\,X2 \quad \text{(VI-48)}$$

where

$$X1 \equiv a_2^3(\xi_1 + 2\xi_2)(\xi_2 + 2\xi_3) + 2a_1^3(\xi_2 - \xi_1)(\xi_3 - \xi_2) \quad \text{(VI-49)}$$

$$X2 \equiv a_2^3(\xi_1 + 2\xi_2)(\xi_3 - \xi_2) + a_1^3(\xi_3 + 2\xi_2)(\xi_2 - \xi_1). \quad \text{(VI-50)}$$

Equation (VI-43) gives the force on a two-shelled sphere in a non-uniform electric field. The following assumptions have been made

during the derivation.

1. The applied field varies sinusoidally in time.

2. The media are isotropic. That is, ε and σ are scalars rather than tensors and are therefore not a function of field orientation.

3. The media are linear which means that ε and σ are not functions of the field strength $\vec{E}$.

4. The media can exhibit time lags of response implying that ε and σ can be complex scalars dependent on frequency.

5. The frequency of the field is assumed to be low enough to permit the $\vec{E}$ field to be derived from a scalar potential alone.

6. The potential inside the sphere is assumed to be approximately that of a sphere in a uniform field.

Equation (VI-43) may be more easily evaluated if it is written in terms of dielectric constants (or relative permittivities) rather than in terms of permittivities. A relative dielectric factor ξ_r can be defined by

$$\xi = \xi_r \circ \varepsilon_o \qquad \text{(VI-51)}$$

where ε_o is the permittivity of free space. Since ξ appears three times in both the N terms and the D terms of Equation (VI-43), the value of (N1 + N2 + N3)/(D1 + D2) remains unchanged if ξ_r is everywhere substituted for ξ. When $\xi_{4r}\varepsilon_o$ is substituted for ξ_4 then Equation (VI-43) becomes

$$\vec{F} = -\pi\varepsilon_o \nabla E_o^2 \, \mathrm{Re}\left\{\xi_{4r}^* \frac{(N1_r + N2_r + N3_r)}{D1_r + D2_r}\right\}, \qquad \text{(VI-52)}$$

where the subscript r indicates that ξ_r is used in place of ξ everywhere it appears.

CHAPTER VII

DERIVATION OF YIELD FOR A RADIAL FIELD

In the previous chapter, a force expression was obtained for the two-shell model in any nonuniform electric field. By specifying the electrode geometry, one can determine the resulting field and the corresponding force for a particular case. Once the force on the body is known, its motion is predictable and the rate of collection of a suspension of similar bodies can be found. Since the experimental studies utilized a pin-pin field, this geometry will be assumed for the calculations.

Force in a Radial Field

The electric field between two pins is essentially that between two separated spheres. The field strength is a complicated function of position, depending on both angle and distance. However, near one of the spheres, the field is approximately the same as that produced by concentric spheres, so that this will be the geometry considered.

The potential at some radius r between two concentric spheres of radii r_1 and r_2 ($r_2 >> r_1$), is

$$\Phi_o = \frac{\Phi_1 r_1}{(r_2 - r_1)} \frac{(r_2 - r)}{r} \qquad \text{(VII-1)}$$

where Φ_1 is the peak A.C. potential of the inner sphere, and $\Phi_2 = 0$.

Since

$$\vec{E}_o = -\nabla\Phi_o = \frac{\Phi_1 r_1}{r^2}\left(\frac{r_2}{r_2 - r_1}\right)\hat{r} \qquad \text{(VII-2)}$$

$$E_o^2 = \frac{\Phi_1^2 r_1^2 r_2^2}{r^4 (r_2 - r_1)^2} \qquad \text{(VII-3)}$$

and

$$\nabla(E_o^2) = -4\left[\frac{\Phi_1 r_1 r_2}{r_2 - r_1}\right]^2 \frac{\hat{r}}{r^5}, \qquad \text{(VII-4)}$$

then it follows from Equation (VI-43) that the force on a two-shelled sphere placed in this field is

$$\vec{F} = \frac{-4\pi\Phi_1^2 r_1^2 r_2^2 \chi \hat{r}}{r^5 (r_2 - r_1)^2}. \qquad \text{(VII-5)}$$

where $\hat{r}$ is the radial unit vector and χ is defined as

$$\chi = -\text{Re}\left\{\xi_4^* \frac{(N1 + N2 + N3)}{D1 + D2}\right\}. \qquad \text{(VII-6)}$$

The negative sign in $\vec{F}$ indicates that the force is inward towards the region of strongest field when χ is positive.

Yield for a Radial Field

As the particle moves under the action of the dielectrophoretic force given in Equation (VII-5), it will experience a viscous drag force opposing its motion. The viscous force on a spherical particle is given by the Stokes relation

$$\vec{F}_d = -6\pi\eta a_2 \vec{v}, \qquad \text{(VII-7)}$$

where η is the viscosity of the suspending fluid, $\vec{v}$ is the particle velocity, and all quantities are in MKS units. Assuming the particle to be in equilibrium means that

$$\vec{F} + \vec{F}_d = 0 .$$

Substituting in this equation for $\vec{F}$ and $\vec{F}_d$ and solving for the instantaneous velocity gives

$$\vec{v} = -\frac{2}{3}\frac{\Phi_1^2 r_1^2}{\eta a_2 r^5}\frac{r_2^2 \chi \hat{r}}{(r_2 - r_1)^2} . \qquad \text{(VII-8)}$$

The time required for a particle to move from a radius r_o to the center electrode is given by

$$t = \int_o^t dt = \int_{r_o}^{r_1} \frac{\hat{r}\, dr}{\vec{v}} . \qquad \text{(VII-9)}$$

Substitution for $\vec{v}$ from Equation (VII-8) results in

$$t = \frac{\eta a_2 (r_2 - r_1)^2 (r_o^6 - r_1^6)}{4\Phi_1^2 r_1^2 r_2^2 \chi} . \qquad \text{(VII-10)}$$

For $r_o > 2r_1$ then $r_o^6 > 64 r_1^6$ and

$$t \approx \frac{\eta a_2 (r_2 - r_1)^2 r_o^6}{4\Phi_1^2 r_1^2 r_2^2 \chi} . \qquad \text{(VII-11)}$$

The pearl-chains, into which the cells form, are approximately cylindrical in shape. The volume of a pearl-chain is then approximately

$$V_c = yd\sigma = yr_1^2 d\Omega \qquad \text{(VII-12)}$$

where y is the length of the chain (yield) and $d\sigma$ is its cross sectional area which at the point of attachment subtends a solid angle $d\Omega$ at the center of the electrode. If $r_o >> c$ the volume of suspension swept out to form the chain during time t is just the volume of the cone of solid angle $d\Omega$ extending to a distance of r_o as shown in Figure 30. This volume is

$$V_s = \frac{r_o^3 - r_1^3}{3} d\Omega \simeq \frac{r_o^3}{3} d\Omega \ . \qquad \text{(VII-13)}$$

The volume of cells in this cone is given by

$$V_c = \frac{4\pi a_2^3}{3} CV_s \qquad \text{(VII-14)}$$

where C is the cell concentration (cells/volume). Combining Equations (VII-12), (VII-13), and (VII-14) gives the yield as

$$y = \frac{4\pi a_2^3 C r_o^3}{9r_1^2} \ . \qquad \text{(VII-15)}$$

Solving Equation (VII-11) for r_o^3 and substituting gives

$$r_o^3 \simeq \frac{2\Phi_1 r_1 r_2}{(r_2 - r_1)} \left[\frac{\chi t}{\eta a_2}\right]^{\frac{1}{2}} . \qquad \text{(VII-16)}$$

Substituting this in the previous expression gives the yield as

$$Y = \frac{8\pi C \Phi_1 r_2}{9r_1(r_2 - r_1)} \left[\frac{a_2^5 \chi t}{\eta}\right]^{\frac{1}{2}} . \qquad \text{(VII-17)}$$

This shows that the yield is linear with voltage and cell concentration and is proportional to the square root of the elapsed time. These results agree with experiment as already discussed in Chapter III and shown in Figures 10, 11, and 12. Equation (VII-17) also indicates that the yield is related to the square root of the quantity containing the permittivity, conductivity, and frequency terms. It remains to be seen whether χ as defined in Equation (VII-6) can predict the proper experimental behavior.

CHAPTER VIII

CALCULATED FREQUENCY AND CONDUCTIVITY DEPENDENCE OF YIELD

In the previous chapter, a theoretical equation was derived which expressed the yield for a spherical electrode system. It correctly predicted the observed dependence of the yield on the voltage, cell concentration, and time. It will now be determined whether or not it also correctly predicts the observed frequency and conductivity dependence. To make this check, the quantity χ, defined in Equation (VII-6), must be evaluated in terms of the physical parameters which describe our model yeast cell in aqueous suspension. This means that numerical values must be supplied for the various permittivities, conductivities, and cell dimensions.

The fact that χ is the real part of a complex expression which itself is a complicated combination of complex quantities means that the evaluation of χ for a particular set of parameters is a very involved computation algebraically. The use of a digital computer is therefore to be recommended, particularly if the computer can handle complex operations. Even with the help of a computer it is desirable to simplify the expression as much as possible, based on the experimental data available concerning the various parameters.

Restrictions, Simplifications, and Chosen Values

In general, we have permitted the quantities ε and σ to be complex.

However, this is not necessarily a requirement for the frequency range in which we are interested. If some of the mechanisms are such that appreciable relaxations do not occur until much higher frequencies, then it is justifiable to assume that the corresponding parameters are real. It should be emphasized that even though ε and σ may be real and have no frequency dependence themselves, their combination to form ξ is still complex, and is frequency dependent; and it is the ξ's which appear in the equation for χ.

Permittivities

With the aim of simplifying the calculations, we examine the behavior of the permittivities in each of the various regions of the model cell. In each case, the polarization will be assumed to be produced by rotating dipoles.

The suspending medium is essentially a dilute solution of salt ions in water. As discussed in Chapter IV, the relaxation for water occurs above 10^{10} Hz while that for ionic solutions is also in this range. Thus for measurements involving frequencies below 10^{8} Hz, ε_4 can be considered constant and real. By the same argument the permittivity of the ion shell and that of the interior, which is also essentially a salt solution, can be considered real. On the other hand, the membrane is composed primarily of proteins and lipids. According to Oncley (40), the relaxation frequency for these materials is in the range 10^{5} - 10^{7} Hz; so that this relaxation falls in the high frequency end of the frequencies investigated. However, for simplicity, this relaxation will be assumed to have a negligible effect so that ε_3 may be also considered real. Since this assumption is not completely justified, any deviation

of the predicted results from the experimental results in the 10^5-10^7 Hz frequency range could well be due to ε_3 relaxation.

Conductivities

The relaxation times for the conductivity of ionic solutions have been treated in detail by Falkenhagen (60). The relaxation time can be approximately related to the conductivity by

$$\tau_\sigma \sim \frac{10^{-11}}{\sigma} \qquad \text{(VIII-1)}$$

when σ is expressed in mho/m. The critical frequency is then given approximately by

$$f_\sigma = \frac{1}{2\pi\tau_\sigma} \sim 2\sigma \cdot 10^{10}. \qquad \text{(VIII-2)}$$

Generally the conductivities of ionic solutions are greater than 10^{-4} mho/m, which implies that

$$f_\sigma > 2 \cdot 10^6 \text{ Hz}. \qquad \text{(VIII-3)}$$

Since the majority of the measurements are taken below 10^7 Hz, Equation (VII-3) allows the conductivities of the ionic regions (σ_1, σ_3, and σ_4) to be considered real and frequency independent.

Again the membrane presents a different set of conditions. As a rule, the conductivity of membranes is quite low, ranging from 10^{-7} to 10^{-4} mho/m (25). If the mechanism is assumed to be ionic conductance, then Equation (VII-2) shows the relaxation frequency to lie in the range from $2 \cdot 10^3$ to $2 \cdot 10^6$ Hz. The conduction mechanism is probably not a pure ionic conduction so that f_σ is not restricted to this range, but

this analysis does show that the relaxation of the membrane conduction may well occur in the frequency range of interest. For this reason, σ_2 must remain complex.

Typical Values

By considering all of the permittivities and conductivities except σ_2 to be real, we have reduced the number of quantities which require a numerical value to the following thirteen: σ_1, σ_{2s}, $\sigma_{2\infty}$, $\tau_{\sigma 2}$, σ_3, σ_4, ε_1, ε_2, ε_3, ε_4, a_1, a_2, and a_3. For some of these quantities, experimental values are available while the others will have to remain unknown and serve as variables in the calculations.

Some typical cell characteristics are given by Schwan (25) as:

$$\begin{aligned} \varepsilon_{1r} &\sim 60 \\ \varepsilon_{2r} &\sim 9 \\ \sigma_1 &\sim .5 - 1 \\ \sigma_{2s} &\sim 10^{-7} - 10^{-4} \\ a_2 - a_1 &\sim 10^{-8} \text{ m} \end{aligned} \qquad \text{(VIII-4)}$$

where the conductivites are in mho/m, $a_2 - a_1$ is the membrane thickness, and the relative permittivity or dielectric constant is defined in terms of ε_o, the permittivity of free space, as

$$\varepsilon_r = \varepsilon/\varepsilon_o. \qquad \text{(VIII-5)}$$

The suspending medium, being an aqueous salt solution, has

$$\varepsilon_{4r} \sim 80 \qquad \text{(VIII-6)}$$

and a conductivity which is approximately that measured as the suspension conductivity. It will therefore vary from 10^{-4} to 10^{-1} mho/m depending on the salt concentration and will be a controllable variable.

There are no accepted experimental values for the permittivity, conductivity, and thickness of the ion layer. Hence, these will be assigned what appear to be reasonable values. Since the ion layer is essentially a more concentrated solution of the suspending medium, it would be expected that the permittivity would be somewhat less than that of pure water and that the conductivity would be higher. The dielectric constant is set at 40, and the conductivity is assumed to be proportional to the suspension conductivity. That is

$$\varepsilon_3 = 40$$

and (VIII-7)

$$\sigma_3 = h\sigma_4$$

where the proportionality constant h is also a variable for the calculations. The thickness of the ion layer is chosen to be

$$a_3 - a_2 = 4 \cdot 10^{-9} \text{ m.} \qquad \text{(VIII-8)}$$

There are no known methods of isolating a purely conduction relaxation in cell membranes, and as a result there are no experimental values for $\sigma_{2\infty}$ and τ_2. These also, will have to be determined after some initial calculations have been made.

The final parameter to be specified is a_1, the radius of the inner

sphere, which is essentially the radius of a typical yeast cell. From microscopic observation, the average radius has been determined to be

$$a_1 = 4 \cdot 10^{-6} \text{ m.} \qquad \text{(VIII-9)}$$

Numerical values have now been assigned to all of the parameters except $\sigma_{2\infty}$, $\tau_{\sigma 2}$, h, and σ_4. For a particular experimental value of σ_4, these three quantities are assigned values and χ is calculated as a function of frequency. The results are then plotted and compared to the experimental yield curve for that σ_4 since according to Equation (VII-17) the yield is proportional to χ. Changes are made in $\tau_{2\infty}$, $\tau_{\sigma 2}$, and h and the process is repeated. When the graphs agree as closely as possible over the entire frequency range used, $\sigma_{2\infty}$, $\tau_{\sigma 2}$, and h are assumed to be correct and are fixed at these values. A different experimental conductivity is then chosen and with all of the parameters at their previous values, the frequency dependence of χ is again calculated. If the theory, the model, and the chosen values are correct, then this distribution should compare favorably with the experimental results.

The above procedure has been carried out for the experimental conductivities given in Figure 14. The numerical calculations were made utilizing an IBM-360-50 digital computer. For a discussion of the specific program used and its operation, see Appendix B. The values used for the parameters are shown in Table I, and the graphs of the results are presented in Figure 31. These should be compared with Figure 14. There are two important similarities between the sets of data. One is the corresponding shapes; the low frequency maximum, the

TABLE I

VALUES OF PARAMETERS USED IN CALCULATIONS

FOR LIVING YEAST CELLS

Quantity	Value
a_1	$4 \cdot 10^{-6}$ m
$a_2 - a_1$	10^{-8} m
$a_3 - a_2$	$4 \cdot 10^{-9}$ m
ε_{1r}	60
ε_{2r}	9
ε_{3r}	40
ε_{4r}	80
σ_1	1.0 mho/m
σ_{2s}	10^{-6} mho/m
$\sigma_{2\infty}$	$9.9 \cdot 10^{-7}$ mho/m
τ_σ	10^{-3} sec
h	$4.9 \cdot 10^{3}$

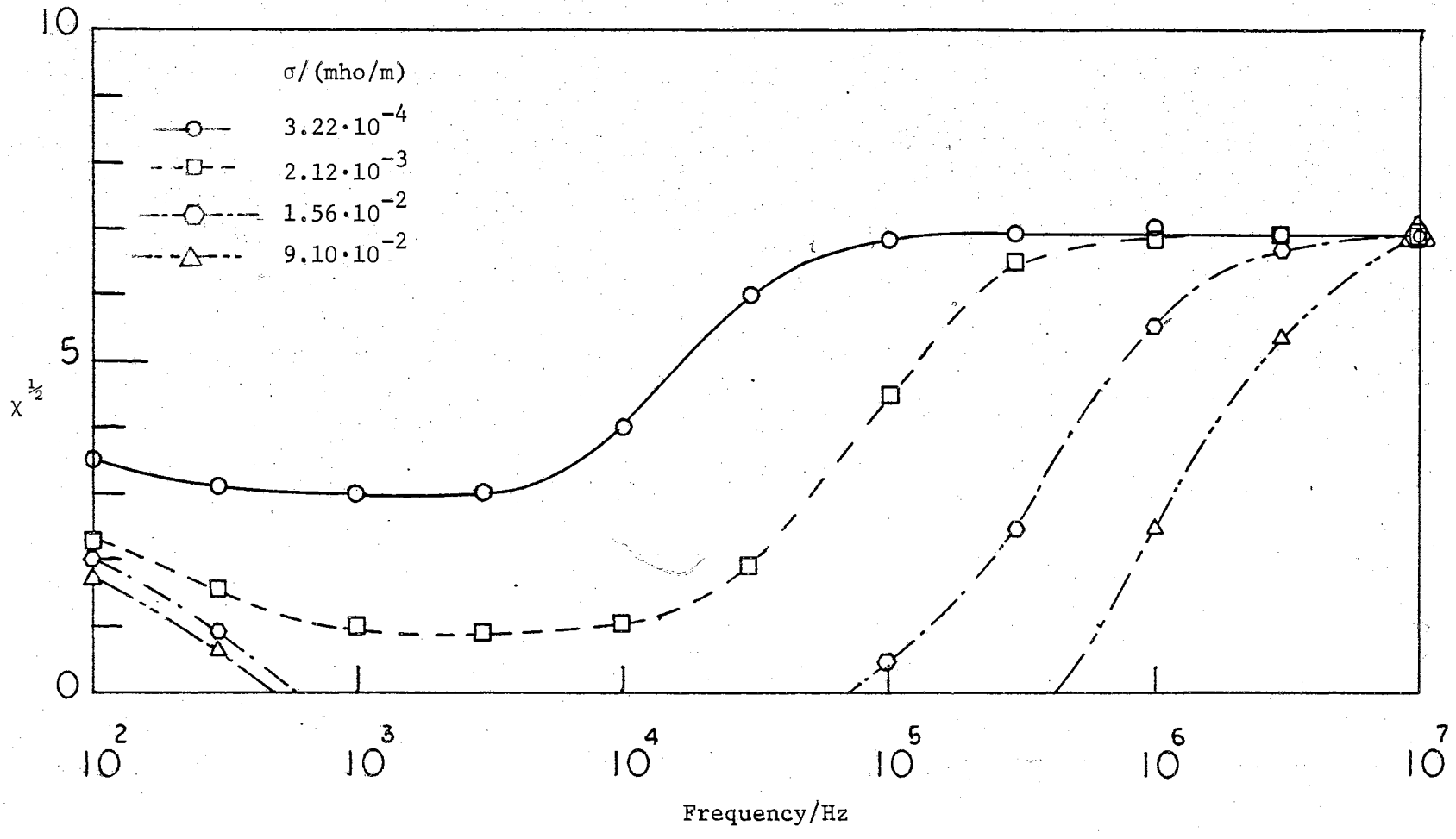

Figure 31. Theoretical Variation of $\chi^{\frac{1}{2}}$ With Frequency at Various Experimental Conductivities for Two Shell Model.

mid-frequency minimum, and the high frequency maximum for each case. The other is the shift of the curves to the right as the suspension conductivity is increased.

A comparison of the theoretical and experimental results over a wider frequency range is shown in Figure 32. Here the experimental results of Figure 13 are reproduced along with those calculated for σ_4 equal to 10^{-2} mho/m. Although the fit is not perfect, it is seen that the general shapes are the same, including a high frequency cutoff at about 10^8 Hz.

In succeeding calculations the various parameters were allowed to change to see which part of the theoretical curve was affected by each and in what manner. It was found that the high frequency cutoff point was largely determined by the conductivity of the inner sphere. An increase in σ_1 increased this frequency. The low frequency response was found to be largely an effect of the relaxation of the membrane conductivity. Without this relaxation, the yield did not pass through a minimum and for the high conductivity suspensions, was zero at all low and medium frequencies such as shown in Figure 33. The frequency at which the relaxation effect became important was determined by the relaxation time. The magnitude of χ at the mid-frequency minimum is controlled by both the conductivity and relative thickness of the ion layer. As its conductivity is increased (or its thickness increased), the minimum becomes less pronounced and the curve flattens out. The high frequency peak can not be attributed to any particular parameter so it is likely a result of the entire model. The experimental data in Figure 32 shows that in the neighborhood of 10^7 Hz, the yield levels

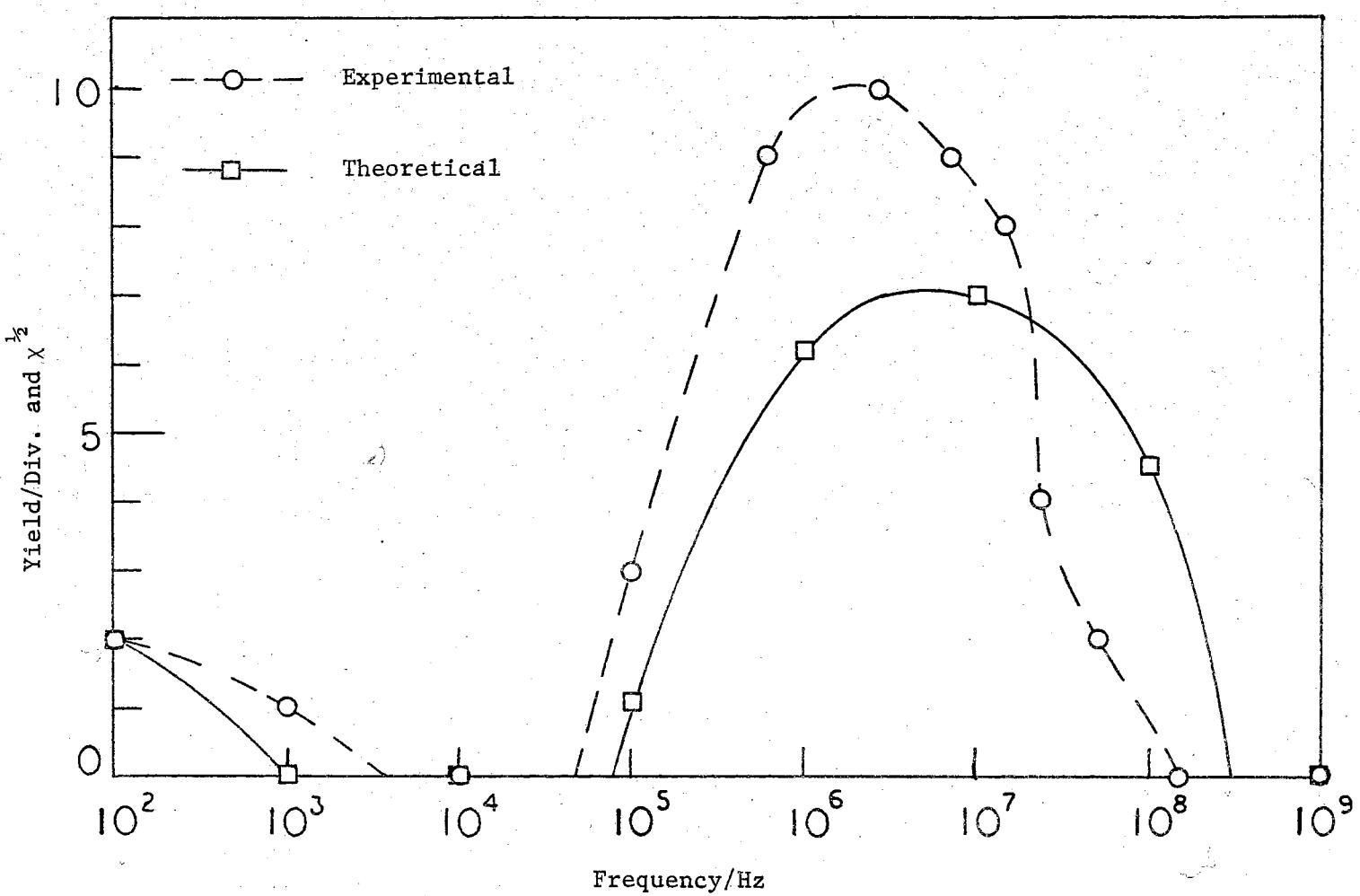

Figure 32. Comparison of Experimental and Theoretical Frequency Dependences for $\sigma = 10^{-2}$ mho/m.

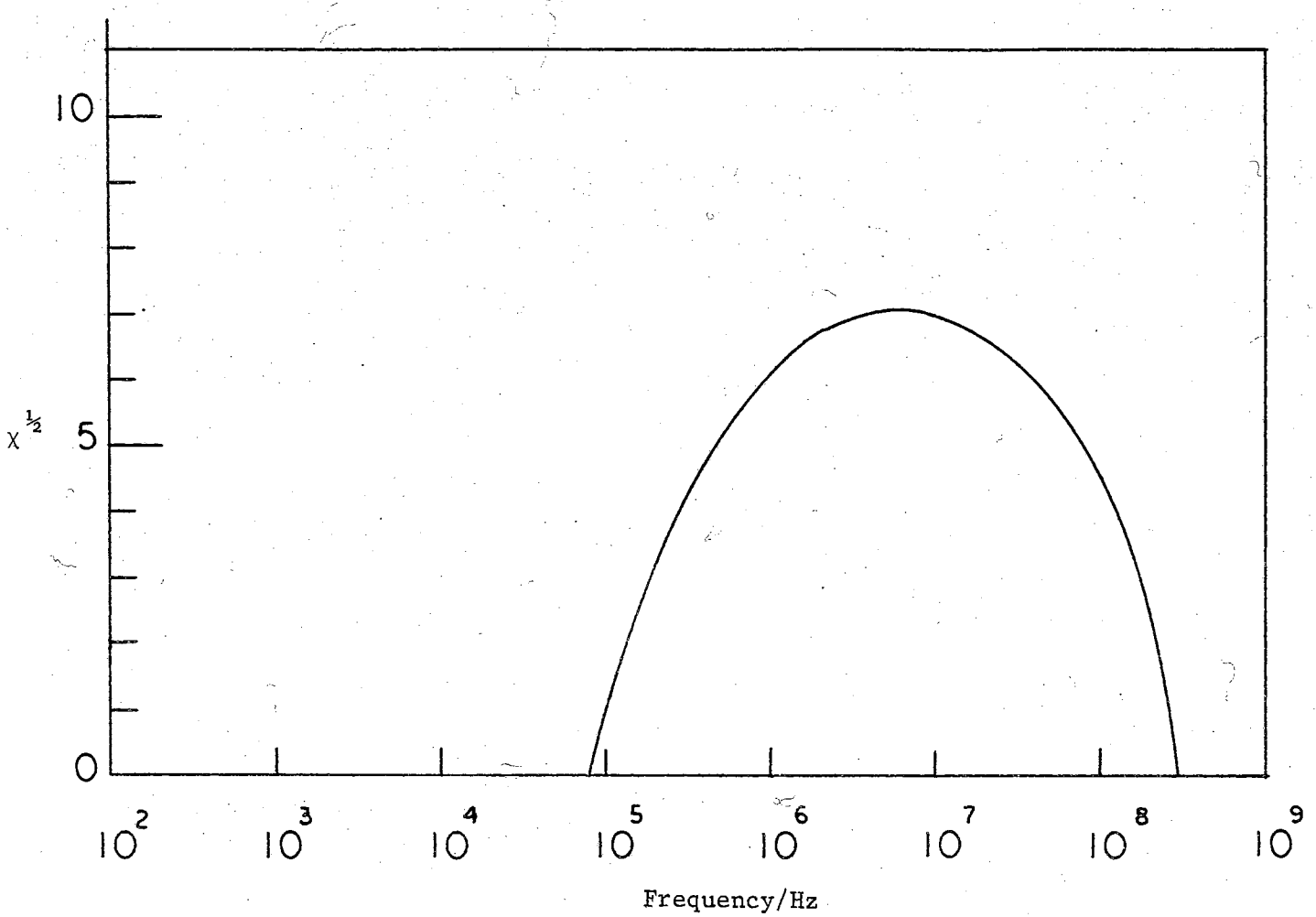

Figure 33. Theoretical Calculations of $\chi^{\frac{1}{2}}$ Assuming all Permittivities and Conductivities to be Real and Frequency Independent, $\sigma_4 = 10^{-2}$ mho/m.

off somewhat before dropping to zero. This same result has been seen for other data taken in this laboratory by W. Chen. Since the theoretical curve does not predict such a response, it could be due to a relaxation process not considered. As was mentioned earlier, the relaxation of the large organic molecules in the membrane is in this region and could be responsible for this deviation of theory from experiment.

Application to Dead Cells

It is interesting to apply the theoretical method to a model for dead yeast cells and compare the results with experiment. This would lend considerable support to the theory if it could also predict the response of dead cells using reasonable assumptions for their electrical parameters.

Toward this effort, calculations of $\sqrt{\chi}$ were made with the following assumptions: the cell radius was reduced to $2 \cdot 10^{-6}$ m as supported by microscopic measurements; the membrane was assumed to have been made slightly porous by the killing process, allowing the conductivity of the central sphere to be equal to that of the suspending medium; all other parameters were unchanged from those used in live cell calculations. Computations were made for values of σ_4 corresponding to the experimental data of Figure 18, and the results are shown in Figure 34. The two essential characteristics, no low-frequency minimum and a lower cutoff point, are predicted. The shift with increasing conductivity is to the right, just as in Figure 22; but the yield does not decrease in magnitude as experiment shows it should.

These results are encouraging, especially in light of the difficulty of reproducing the experimental data. The prediction of the gen-

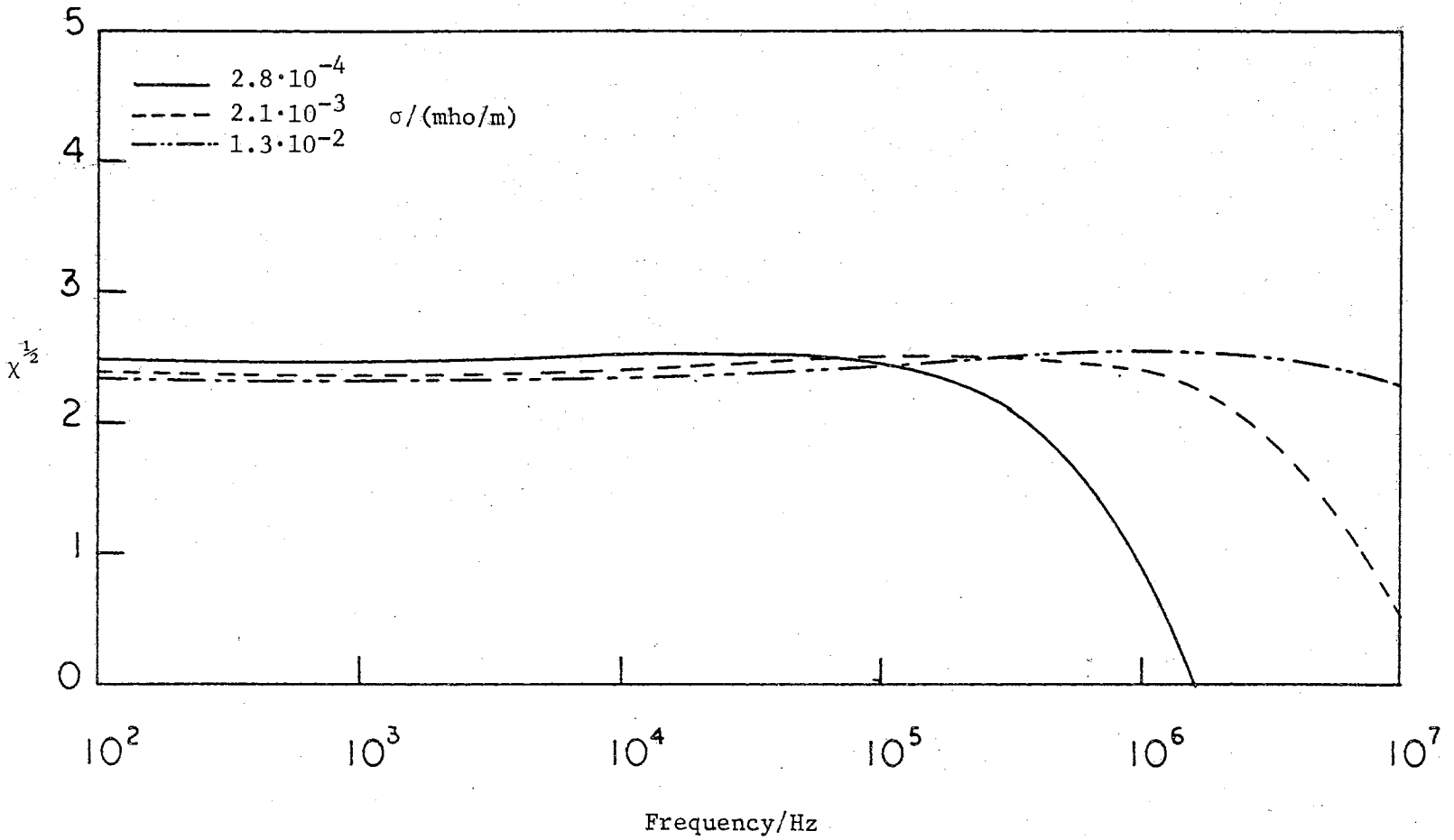

Figure 34. Theoretical Calculation of $\chi^{\frac{1}{2}}$ Using Two Shell Model to Represent Autoclaved Cells.

eral characteristics indicates that at least the theory is headed in the right direction, perhaps needing refinements in the models as more is learned about the electrical properties of the cells. Once these properties are known and a suitable theory is applied, dielectrophoresis will truly become a useful tool for microbiological research. By studying the cell behavior before and after the application of some external agent, the effect of the agent and its sight of action might be quickly determined.

CHAPTER IX

SUMMARY AND DISCUSSION

Summary

It has been known for some time that dielectrophoresis could be used to study the electrical properties of materials. Recently it has been applied successfully to living organisms. The work presented here describes the investigation in considerable detail of the behavior of yeast cells in nonuniform electric fields. The experimental procedures and necessary equipment have been described. The "yield" was selected as the best descriptive dependent variable. It expresses the length of the stacks or chains of cells collected on the electrode in a given time. The experimental variation of the yield has been reported as a function of various physical and biological parameters. It was found to be linear with voltage and cell concentration, proportional to the square root of the time, and to be a complicated function of frequency, suspension conductivity, and biological parameters.

The question arises as to how a particle such as a yeast cell, whose major constituents have dielectric constants each less than that of water can experience a stronger dielectrophoretic force than an equivalent volume of water. Simple theory concerning insulating materials does not allow this result but requires the stronger force to be experienced by the material of the higher dielectric constant. Clearly the observations call for a deeper analysis than that for the

simply polarizing dielectrics. We have in fact to deal with a composite system which contains both conductive and polarizable materials. Just as clearly then, both polarization and conduction must be included in the analysis.

There are two approaches which can be taken toward answering this question when both polarization and conduction must be considered. One is the "effective" polarization viewpoint which attributes an overall effective polarizability to the particle, and thus arrives at an "effective dielectric constant". This approach leaves some doubt as to how the force should be calculated.

The second approach is through energy considerations, wherein the energy in the system is considered before and after the particle is introduced. This can be broken down as follows: When the charge on the conductors producing the electric field does not remain constant, not all of the change in energy of the system goes into work done on the test body. Part also goes into work done at the electrodes in the movement of charge. It is therefore necessary to have an expression for the energy associated with the body only. The force may then be easily obtained by taking the negative gradient of the energy function. The advantage of this approach is its straightforwardness. All that must be known are the electric field, the permittivity, and the conductivity throughout space.

The energy approach has been selected here and a derivation has been given for the force on an arbitrary particle in an arbitrary suspending medium. The result is general to the extent that sinusoidal fields are considered and all of the constitutive parameters are allowed to be complex. This permits the conductivity σ and permittivity

ε to each be associated with a separate physical mechanism, having its own frequency dependence; i.e., a dual mechanism approach.

In order to apply the force expression to a yeast cell in aqueous suspension, a model was chosen which could be given properties comparable to that of a suspended cell. The model consisted of a sphere enclosed by two thin shells placed in an external medium. The inner sphere was to represent the cell corpus proper, the first shell represented the cell membrane, and the second shell was to approximate a surrounding ionic atmosphere. To facilitate the derivation of the electric fields for this particular model, some simplifying but reasonable assumptions were made. These were that the parameters σ and ε were field independent, were not functions of direction, but could be functions of frequency, that the frequency was low enough to permit the field to be derived from a scalar potential function, i.e., magnetic forces were neglected, and that the potential throughout the sphere was approximately equal to that for a sphere in a uniform field.

Having obtained an expression for the force on the model cell, a derivation was then made to obtain the expected yield for a suspension of these particles in a field of spherical geometry. The result showed the yield to be linear with voltage and concentration, and proportional to the square root of the elapsed time; exactly the experimental results. The frequency dependence of the yield was seen to be contained in the real part of a complex expression involving the complex dielectric factor of each region. Assuming reasonable numerical values for the model parameters, and assuming all of them non-complex except σ_2, the membrane conductivity, the dependence of the yield on frequency and suspension conductivity was calculated using a digital computer. It

was found to have the same general features as the experimental results and to furnish a gratifyingly good description of the observations. With only minor changes in the values of the parameters, the theory was also shown to apply to yeast cells which had been killed by autoclaving.

Discussion

Several conclusions may be drawn from this work. It has experimentally demonstrated the applicability of dielectrophoresis to living organisms. A detailed theoretical analysis has shown that the frequency and suspension conductivity are the two parameters which elucidate the dependence of the yield on the particular organism.

The qualitative agreement between the experimental and theoretical results supports the energy approach to the explanation of dielectrophoresis. It also implies that the frequency dependence is due in most part to the variation of the average values of the electric fields in the different regions, rather than due largely to the general frequency dependence of the conductivities and permittivities themselves throughout the cell and medium.

The only frequency dependent quantity found necessary in our theoretical model was that of a conductivity relaxation in the cell membrane which provides for the low frequency collection. It is expected that the inclusion of other parameters would only change the details of the results and not the overall behavior. It might still be desirable to consider the more general case of all of the parameters being complex in order to obtain information about a specific region, but that is left for the future.

Certainly the two shell model used is not expected to describe

exactly an organism so complex as a living cell. In fact, more detailed models can easily be envisioned. One which would maintain the spherical symmetry, and thus only complicate the algebra, would be a model with three shells. In this case the extra shell could be considered as a charge layer inside the membrane. Or the extra layer might be given the properties of the cell wall and considered to lie between the membrane and the outer ion layer. More complicated models could be constructed to take into account the eccentricity of the cell, or to represent various cytoplasmic bodies. Carried to the ultimate, each molecular species in each region could be given its particular electrical characteristics; but the corresponding model and its mathematical solution would quite possibly be hopelessly complex.

The attractive part of the present model approach to representing the behavior is that it gives a physical insight into the problem. It allows separate characteristics to be ascribed to the different major parts of the cell, which is much more pleasing than to try to represent the entire cell by some empirically "effective" parameters as has been done by some authors (49, 61). The division of the conduction and polarization into two distinct physical processes is also satisfying to the purist who prefers that mathematical constructs be expressions with physical meaning.

The future for dielectrophoresis seems bright indeed. Now that the experimental techniques have been devised and a workable theory developed, the investigation of other organisms can begin in earnest. The response of other organisms may be different from that of yeast, but probably only in detail, since the gross electrical characteristic of most microorganisms are approximately the same. With the inevitable refine-

ment of techniques, such as the study of cells all in the same growth phase or the study of a single cell, many of the errors and nonreproducibilities of this work will be eliminated, and these details will be more easily observable. The cause and effect relationships between the treatment and response of a cell will then be quickly determinable, thus making dielectrophoresis a very handy tool for the microbiologist.

BIBLIOGRAPHY

1. Pohl, H. A., J. Appl. Phys., 22, 869 (1951).
2. Gilbert, W., De Magnete, Peter Short, London (1600).
3. Quincke, G., Ann. Phys., Lpz., 62, 1 (1883).
4. Clark, A. L., Physiol. Rev., 6, 120 (1898).
5. Pellat, H., C. R. Acad. Sci., 123, 691 (1896).
6. Fortin, C., C. R. Acad. Sci., 140, 576 (1905).
7. Gyemant, A., Wiss. Veroff. Siem. Konz., 5, No. 2, 55 (1926).
8. Greinacher, H., Helv. Phys., 21, 261 (1948).
9. Pickard, W. F., J. Appl. Phys., 32, 1888 (1961).
10. Soyenoff, B. C., J. Phys. Chem., 35, 2993 (1931).
11. Wenslow, W. M., J. Appl. Phys., 20, 1137 (1949).
12. Pohl, H. A. and J. P. Schwar, J. Appl. Phys., 30, 69 (1959).
13. Pohl, H. A., J. Appl. Phys., 29, 1182 (1958).
14. Pohl, H. A., Sci. American, 203, 107 (1960).
15. Pohl, H. A. and C. E. Plymale, J. Electrochem. Soc., 107, 390 (1960).
16. Verschure, R. H. and L. Ijlst, Nature, 619 (1966).
17. Hawk, I. L., "Effects of Non-uniform Electric Fields on Real Dielectrics in Water" (unpub. M.S. thesis, Oklahoma State University, 1967).
18. Feeley, C., "Dielectrophoresis of Solids in Liquids of Differing Dielectric Constant and Conductivity" (unpub. M.S. thesis, Oklahoma State University, 1969).
19. Chen, K. W. L., "Dielectrophoresis of Solids in Aqueous Solutions" (unpub. M.S. thesis, Oklahoma State University, 1969).
20. Muth, E., Kolloid Z., 41, 97 (1927).

21. Liebesny, P., Arch. Phys. Therapy, 19, 736 (1939).

22. Heller, J. H., et al., Exp. Cell Res., 20, 548 (1960).

23. Saito, M. and H. P. Schwan, Proc. Conf. Biol. Effects of Microwave Radiation, 1, 85 (1960).

24. Saito, M., H. P. Schwan, and G. Schwarz, Biophys. J., 6, 313 (1966).

25. Schwan, H. P., Advan. Biol. Med. Phys., 4, 147 (1957).

26. Pohl, H. A. and I. Hawk, Science, 152, 647 (1966).

27. Debye, P., Polar Molecules, Chemical Catalog, New York (1929).

28. Wiley, K., (unpub. M.S. thesis, Oklahoma State University, 1970).

29. Pohl, H. A. and J. P. Schwar, J. Electrochem. Soc., 107, 383 (1960).

30. Pohl, H. A., J. Electrochem. Soc., 107, 386 (1960).

31. Pelczar, M. J. and R. D. Reid, Microbiology, McGraw-Hill, New York (1965).

32. Cook, A. H., The Chemistry and Biology of Yeasts, Academic Press, New York (1958).

33. Roman, W., Yeasts, Academic Press, New York (1957).

34. Smyth, C. P., Dielectric Behavior and Structure, McGraw-Hill, New York (1955).

35. Bottcher, C. J. F., Theory of Electric Polarization, Elsevier, Houston (1952).

36. von Hippel, A. R., Dielectrics and Waves, John Wiley, New York (1954).

37. Onsager, L., J. Am. Chem. Soc., 58, 1486 (1936).

38. Kirkwood, J. G., J. Chem. Phys., 7, 911 (1939).

39. Cole, K. S. and R. H. Cole, J. Chem. Phys., 9, 341 (1941).

40. Oncley, J. L., Chem. Rev., 30, 433 (1942).

41. Grant, E. H., T. J. Buchanan, and H. F. Cook, J. Chem. Phys., 26, 156 (1957).

42. Shepherd, J. C. W. and E. H. Grant, Proc. Roy. Soc., A, 307, 335 (1968).

43. Junger, I., Acta. Physiol. Scand., 20, Suppl. 69 (1950).

44. Takashima, S., J. Molec. Biol., 7, 455 (1963).

45. Grant, E. H., Solid State Biophysics, Ch. 9, Ed. S. J. Wyard, McGraw-Hill, New York (1969).

46. Cole, K. S., Cold Spring Harbor Symposia Quant. Biol., 8, 110 (1940).

47. Schwan, H. P. and K. S. Cole, Medical Physics, 3, 52 (1960).

48. Maxwell, J. C., A Treatise of Electricity and Magnetism, Oxford University Press, London (1873).

49. Miles, J. B. and H. P. Robertson, Phys. Rev., 40, 583 (1932).

50. O'Konski, C. T., J. Phys. Chem., 64, 605 (1960).

51. Schwarz, G., J. Phys. Chem., 66, 2636 (1962).

52. Schwan, H. P., et al., J. Phys. Chem., 66, 2626 (1962).

53. Dintzis, H. M., J. L. Oncley, and R. M. Fuoss, Proc. Natl. Acad. Sci., 40, 62 (1954).

54. Peck, E. R., Electricity and Magnetism, McGraw-Hill, New York (1953).

55. King, R. W. P., Electromagnetic Engineering, Vol. 1, New York (1945).

56. Fuoss, R. and F. Accascina, Electrolytic Conductance, Interscience, New York (1959).

57. Javid, M. and P. M. Brown, Field Analysis and Electromagnetics, McGraw-Hill, New York (1963).

58. Slater, J. C. and N. H. Frank, Electromagnetism, McGraw-Hill, New York (1947).

59. Stratton, J. A., Electromagnetic Theory, McGraw-Hill, New York (1941).

60. Falkenhagen, H., Electrolytes, Oxford University Press, London (1934).

61. Sher, L. D., Nature, 220, 695 (1968).

62. Kohlrausch, F., Wied. Ann., 58, 514 (1896).

63. Jones, G. and S. Christian, J. Am. Chem. Soc., 57, 272 (1935).

64. Jones, G. and G. M. Bollinger, J. Am. Chem. Soc., 57, 280 (1935).

65. Feates, F. S., D. J. G. Ives, and J. H. Pryor, J. Electrochem. Soc., 103, 580 (1956).

66. Nichol, J. C., and R. W. Fuoss, J. Phys. Chem., 58, 696 (1954).

67. Metcalf, W. S., J. Sci. Instrum., 42, 742 (1965).

68. Felici, N. J., Revue Generale de l'Electricite, 76, 786 (1967).

69. Schwan, H. P., Biophysik, 3, 181 (1966).

70. Robinson, R. A., and R. H. Stokes, Electrolyte Solutions, Academic Press, New York (1959).

71. Harm, W. and K. Haefner, Photochem. Photobiol., 8, 179 (1968).

72. Pollak, M., J. Chem. Phys., 43, 908 (1965).

73. Casey, E. J., Biophysics, Reinhold, New York, p. 140 (1962).

74. Schwarz, G., J. Chem. Phys., 39, 2387 (1963).

75. Wilson, E. B., An Introduction to Scientific Research, McGraw-Hill, New York (1952).

APPENDIX A

CONDUCTIVITY CONSIDERATIONS

It has been seen that conductivity plays a very important role in dielectrophoresis. This is so because it helps to determine the boundary conditions on the $\vec{E}$ fields at the material interfaces. It is therefore important to be able to determine experimentally accurate values for conductivities at various frequencies.

For solid materials, the measurements are rather simple and straightforward. On the other hand, determining conductivities in moderately and even poorly conducting liquids presents some prominent obstacles. For D.C. voltages, especially, and less importantly for high frequency A.C., electrolysis occurs at the electrodes. For low frequency A.C. voltages, capacitance effects in the form of electrode polarizations enter into the analysis. At high frequencies stray capacitances and inductances must be considered. It is only in the radio frequency range of 10^3 - 10^6 Hz that a somewhat simple approach can be taken. The problem becomes one of trying to determine the properties of the test material without introducing large errors due to the measuring devices themselves.

Background Theory

The conductivity σ is defined for a particular medium in terms of the current denstiy and the electric field by

$$\vec{J} = \sigma\vec{E} . \tag{A-1}$$

If the media are isotropic then these vectors can be replaced by their scalar magnitudes. For a rectangular sample element of thickness ℓ and cross-sectional area A, the current I passing through the element can be expressed in terms of the potential V dropped across the element by

$$\frac{I}{A} = \sigma \frac{V}{\ell} . \tag{A-2}$$

Then

$$\sigma = \frac{I}{V}\frac{\ell}{A} = \frac{\ell}{RA} \tag{A-3}$$

since the resistance R is equal to V/I.

Similarly the permittivity is defined as

$$\vec{D} = \varepsilon\vec{E} \tag{A-4}$$

and from Gauss' Law for an element between two charged plates

$$q = DA = \varepsilon EA = \varepsilon \frac{VA}{\ell} \tag{A-5}$$

where q is the charge on one of the plates. Since the capacitance C is defined as q/V, the following relation for ε is obtained,

$$\varepsilon = \frac{C\ell}{A} . \tag{A-6}$$

For a parallel plate configuration then, ε and σ can be determined from the capacitance, resistance, and the geometrical dimensions of the sample. The usual method for determining R and C is to use an impedance bridge and balance the sample against a parallel arrangement of a variable capacitance and a variable resistance. The measured values do

not ordinarily correspond to the true values because of the introduction of the errors already cited; electrolysis, electrode polarization, as well as stray capacitances and inductances.

Case of Electrode Polarization

As an example of the difficulties in obtaining the true parameters from the measured ones, consider the simple case of the sample capacitance and resistance in parallel, combined with electrode capacitances in series as shown in Figure 35. C is the sample capacitance, R is the sample resistance and C' and C" are surface capacitances at the liquid-electrode interfaces. The impedance of the R-C network at an angular frequency ω is

$$Z_{RC} = \frac{R}{1 + \omega^2 R^2 C^2} - j \frac{\omega R^2 C}{1 + \omega^2 R^2 C^2} . \qquad (A-7)$$

The impedance of the total network is

$$Z = \frac{R}{1 + \omega^2 R^2 C^2} - j \left(\frac{\omega R^2 C}{1 + \omega^2 R^2 C^2} + \frac{1}{\omega C_s}\right), \qquad (A-8)$$

where

$$C_s = C' + C" \qquad (A-9)$$

is the total series capacitance.

If the impedance is measured as a parallel R-C combination as shown in Figure 36, then it is

$$Z_M = \frac{R_m}{1 + \omega^2 R_m^2 C_m^2} - j \left(\frac{\omega R_m^2 C_m}{1 + \omega^2 R_m^2 C_m^2}\right) . \qquad (A-10)$$

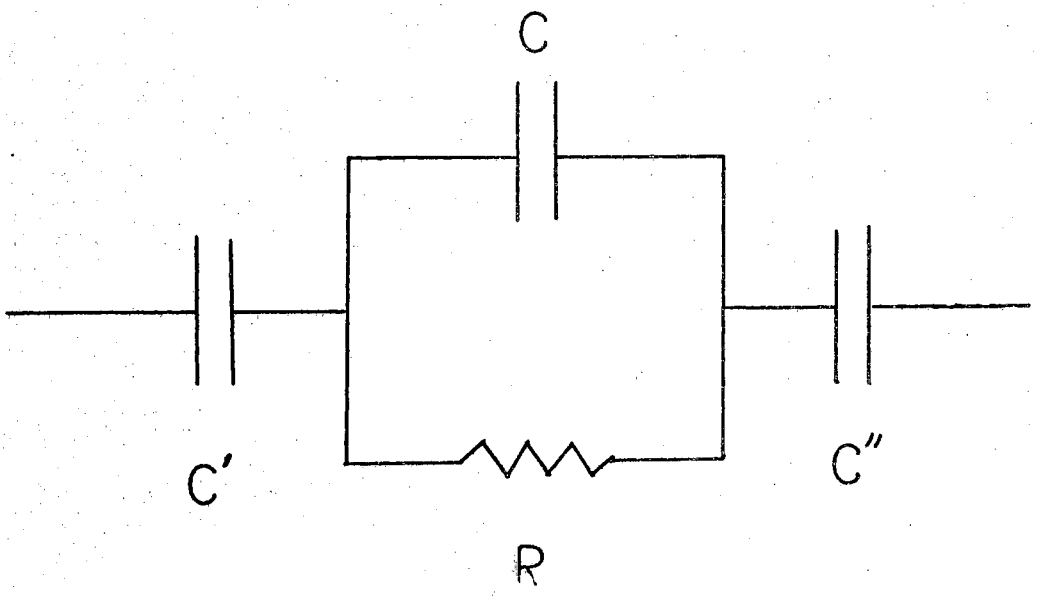

Figure 35. Electrical Model for Conductivity Measuring Device Including Electrode Polarization.

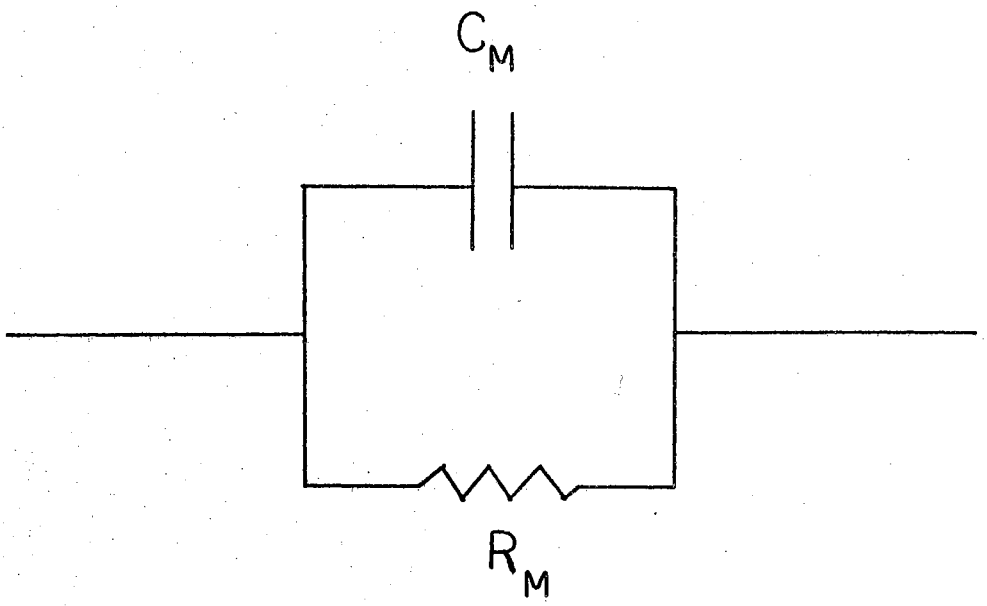

Figure 36. Equivalent Circuit as Measured on an Impedence Bridge.

Equating real and imaginary parts gives

$$R = R_m\left(\frac{1 + \omega^2 C^2 R^2}{1 + \omega^2 C_m^2 R_m^2}\right) \tag{A-11}$$

and

$$C = \frac{R_m}{R}\left[C_m - \frac{(1 + \omega^2 C_m^2 R_m^2)}{\omega^2 R_m^2 C_s}\right] . \tag{A-12}$$

For conducting solutions at low frequencies,

$$\omega CR << 1 \tag{A-13}$$

and Equation (A-11) becomes

$$R_m \simeq R + \omega^2 C_m^2 R_m^2 R \tag{A-14}$$

Solving this equation for R_m and assuming that

$$\omega R C_m << 1 \tag{A-15}$$

gives

$$R_m = \frac{R}{\omega^2 R^2 C_m^2} . \tag{A-16}$$

Since $\omega^2 R^2 C_m^2 << 1$ for many cases of interest, the measured value of the resistance can be much higher than the true value.

In the same manner, the true capacitance can be quite different from the measured capacitance. In fact, as stated by Slater and Frank (58, p.106)"...there is no experimental way of finding the dielectric constant of a good conductor at low frequencies", indicating that for these conditions it is impossible to relate the true capacitance to the

measured capacitance.

As an example of the magnitude of the possible error in resistance measurements, Figure 37 shows the resistance of a standard 10^{-2}N solution of KCl as measured using parallel stainless steel plates over the frequency range $2.5 \cdot 10^{2}$ - $5 \cdot 10^{4}$ Hz. As can be seen, the measured resistance changes by 50% over this range. For more concentrated solutions, the results are even more erroneous.

Experimental Solutions

Although in the above case the sample parameters cannot be easily related to the measured quantities, there are some experimental tricks which can be used to get around this problem. One is to make the interfacial capacitance as large as possible. Then the contribution of this quantity to the total impedance can be made small enough to be neglected as can be seen in Equation (A-8). This is most often done by adding a coating of platinum black to a set of platinum electrodes, a procedure which was introduced by Kohlrausch (62).

Another method of sorting out the sample effects from the electrode effects is to vary the interelectrode spacing. This changes the bulk parameters without altering those at the interfaces. This type of approach has been used by Jones (63).

Other variations have been used and a considerable number of papers have appeared discussing them (64 - 67). An excellent review with emphasis on biological suspensions has been given by Schwan (69). Several texts also treat the problems involved in making conduction measurements (34, 45, 70), so that further detail is not necessary here. Suffice it to say that the measurement method being used is possibly causing ser-

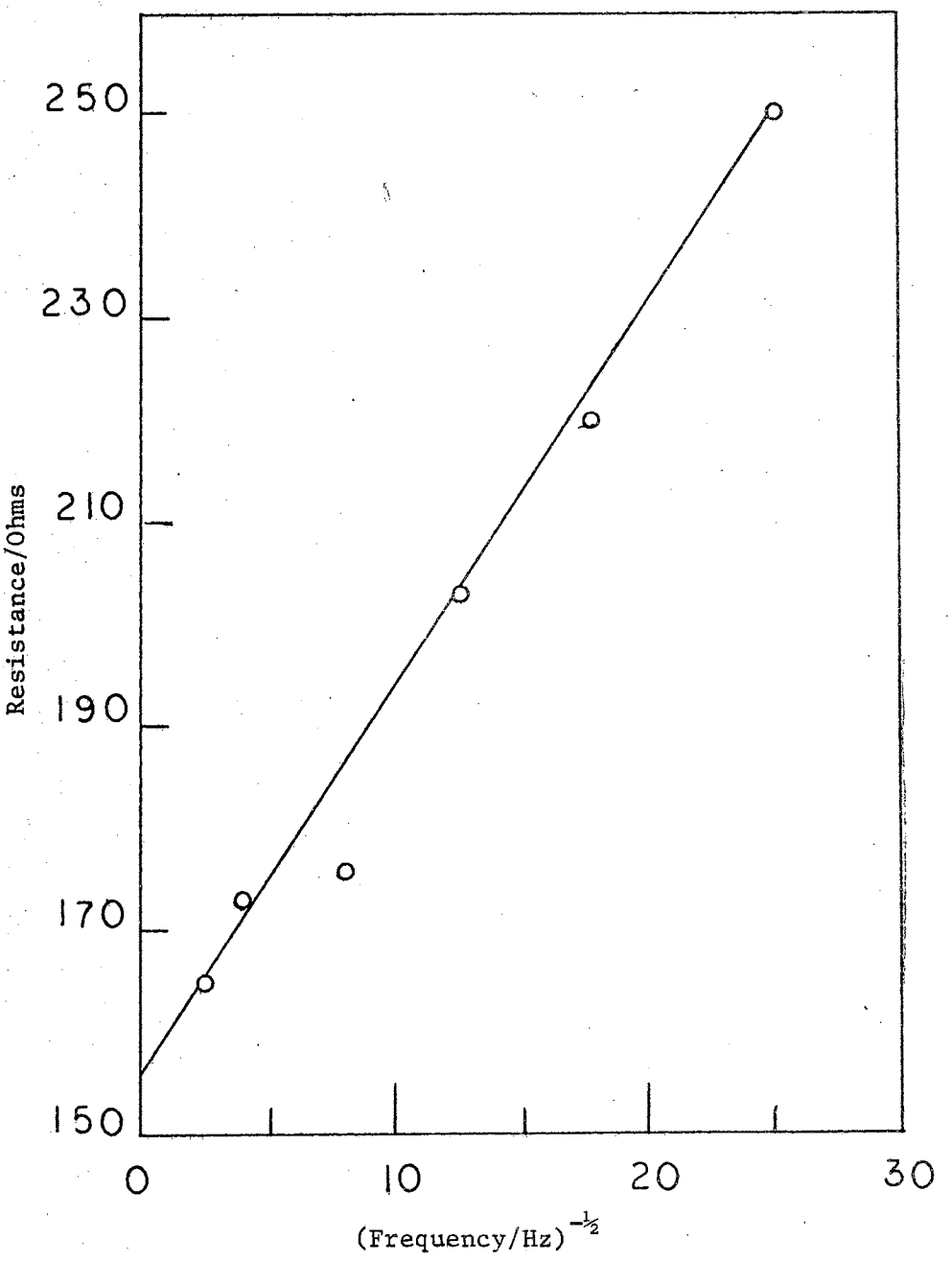

Figure 37. Resistance at Different Frequencies of a Standard 10^{-2}N KCl Solution as Measured With Stainless Steel Electrodes.

ious error if either of the following tests on standard solutions fail: (1) The measured resistance of a particular solution must be frequency independent; (2) The geometrical "conversion factor" for changing from resistance to conductivity must not vary with the conductivity of the standard solutions.

APPENDIX B

COMPUTER PROGRAM FOR CALCULATING FORCE AND YIELD FOR A TWO-SHELL SPHERE

The general force expression for a sphere with two shells is given in terms of relative parameters by Equation (VI-52) as

$$\vec{F} = -\pi \varepsilon_o \nabla E_o^2 \{Re [\xi_{4r}^* \frac{(N1_r + N2_r + N3_r)}{(D1_r + D2_r)}]\}, \qquad (B-1)$$

where the terms are defined in Equations (VI-44-51). Making the definition

$$W = -\xi_{4r}^* (\frac{N1_r + N2_r + N3_r}{D1_r + D2_r}), \qquad (B-2)$$

gives

$$\vec{F} = \pi\varepsilon_o \nabla E_o^2 \, Re\,(W). \qquad (B-3)$$

Comparing Equation (B-2) with Equation (VII-6) shows that

$$\chi_r = \chi/\varepsilon_o = Re\,(W). \qquad (B-4)$$

For a field produced by spherical electrodes, Equation (VII-17) shows that the yield is proportional to $\chi^{\frac{1}{2}}$. This implies that the yield is also proportional to $[Re\,(W)]^{\frac{1}{2}}$. The evaluation of Re (W) as a function of frequency then permits the calculation of the frequency dependence of both the force and the yield. The latter can be compared

with experimental yield determinations.

To facilitate the computation of W at various frequencies, an IBM-360-50 computer was used. The program used was written in FORTRAN IV and is shown in Figure 38 for the particular case of dead cells. The calculations are done in double precision, giving 16 significant digits to each number. The general flow of the program is as follows:

1. Define the size of those quantities which are to be arrays.

2. Define those real quantities which are to be double precision.

3. Define those quantities which are to be complex double precision.

4. Denote the real part of W by R through an EQUIVALENCE statement.

5. Read from data cards and print the values for the sphere and shell dimensions, the dielectric constants of the four media, the D.C. conductivities of the four media, and the high frequency conductivity and relaxation time for the membrane.

6. Form the effective dielectric constants and conductivities, DCA(K) and SA(K) respectively, for the four model regions at a particular frequency.

7. Compute the relative complex dielectric factor ξ_{ri} denoted in the program by C(1).

8. Calculate W.

9. Take the square root of R, the real part of W, if it is positive. This quantity Y is proportional to the yield.

10. Print the conductivities of the suspending medium and outer shell, frequency, R, and Y.

11. Repeat from step 6 using a different frequency until the calcu-

```
      $JOB  10133,448-40-3296,TIME=120,PAGES=30   JOE CRANE
      C
      C  TWO-SHELL DOUBLE PRECISION.  S(2) IS FUNCT(FREQ).  INPUT  4CARDS/SET
      C   S(4) VARIES OVER EXPERIMENTAL RANGE: E-4 TO E-1
      C
            DIMENSION DC(4),S(4)      ,FREQ(8),YSQ(8),SINF(4),SZERO(4),TS(3)
            DIMENSION  OTS1(4)
            DOUBLE PRECISION          A(8),DCA(4),SA(4),A1C,A2C,A3C,A123C,A23D21
            DOUBLE PRECISION    A3D32,R
            DOUBLE PRECISION  Y,DSQRT
            COMPLEX*16  G23,G34,G32,H41,H42,H43,H32,H21,N3F,C4CON,       G12
            COMPLEX*16    N1,N2,N3,N,D1,D2,D,W      ,C(4), DCONJG
            EQUIVALENCE(W,R)
            DCO = 8.854E-12
            K = 2
          1 READ(5,10) A1,A12,A23,CONST,(DC(I),I=1,4),(S(J),J=1,4)
           1 ,SINF(2),TS(2)  ,SINF(3),TS(3)
         10 FORMAT (4E8.1/8E8.1/2E8.1)
            WRITE(6,18)A1,A12,A23,CONST,(DC(I),I=1,4),(S(J),J=1,4)
           1 ,SINF(2),TS(2)  ,SINF(3),TS(3)
         18 FORMAT(/20X,'INPUT DATA',/4(4(5X,E14.7)/)///)
            A2 = A1 + A12
            A3 = A2 + A23
            DO 9 MM = 1,4
            DCA(MM) = DC(MM)
            SA(MM) = S(MM)
          9 CONTINUE
            SZERO(K) = S(K)
            WRITE (6,21)
         21 FORMAT(13X,'S(4)',16X,'S(3)',12X,'FREQUENCY',13X,'REAL(W)',21X,
           1 'Y'/)
            SA(1) = SA(4)
            SA(3) = SA(4) * CONST
            MZ = 1
         80 DO 4 I = 1,6
         40 FREQ(I) = 10.**(1+I)
            MZ = 2
            GO TO 33
         32 FREQ(I) = 3.*FREQ(I)
            MZ = 1
         33 OMEGRL = 6.2832 * FREQ(I) * DCO
            OMEGA = OMEGRL/DCO
            OTS1(K) = 1.+(OMEGA*TS(K))**2
            DCA(K)  = DC(K) -(SZERO(K)-SINF(K))*TS(K)/(DCO*OTS1(K))
            SA(K) = SINF(K) +(SZERO(K)-SINF(K))/OTS1(K)
            DO 5 L = 1,4
          5 C(L)=DCA(L)*(1.,0.)- SA(L)*(0.,1.)/OMEGRL
            G12 = C(1) + 2.*C(2)
            G23 = C(2) + 2.*C(3)
            G34 = C(3) + 2.*C(4)
            G32 = C(3) + 2.*C(2)
            H41 = C(4) - C(1)
            H42 = C(4) - C(2)
            H43 = C(4) - C(3)
            H32 = C(3) - C(2)
            H21 = C(2) - C(1)
            A1C = A1**3
            A2C = A2**3
            A3C = A3**3
            A123C = A1C*A2C*A3C
```

Figure 38. FORTRAN IV Program for Computing χ and $\chi^{\frac{1}{2}}$ for Dead Cells at Different Frequencies.

Figure 38 (Continued)

```
      A23D21 = A2C*A3C*(A2C-A1C)
      A3D32 = A3C*(A3C-A2C)
      N3F = G12*G23*A2C + 2.*H21*H32*A1C
      C4CON =DCONJG(C(4))
      N1 = 9.*C(2)*C(3)*H41*A123C
      N2 = 3.*C(3)*G12*H42*A23D21
      N3 = H43*A3D32*N3F
      D1 = A3C*G34*N3F
      D2 = 2.*A2C*H43*(G12*H32*A2C + G32*H21*A1C)
      N = -C4CON*(N1+N2+N3)
      D = D1 +D2
      W = N/D
      IF(R.GT.0.) GO TO 30
      Y = 0.
      GO TO 31
   30 Y = DSQRT(R)
   31 WRITE(6,110)  SA(4),SA(3),FREQ(I),R,Y
  110 FORMAT(2(10X,D9.2),10X,E9.2,10X,D14.7,10X,D14.7)
      IF(MZ.EQ.2) GO TO 32
    4 CONTINUE
      WRITE(6,22)
   22 FORMAT(10X)
   45 CONTINUE
      GO TO 1
      END
```

```
$ENTRY
```

INPUT DATA

0.2000000E 01	0.1000000E-01	0.4000001E-02	0.4900000E 04
0.6000000E 02	0.9000000E 01	0.4000000E 02	0.8000000E 02
0.1000000E-03	0.1000000E-05	0.4900000E 00	0.2800000E-03
0.9900004E-06	0.9999999E-03	0.1000000E 02	0.1000000E-04

S(4)	S(3)	FREQUENCY	REAL(W)	Y
0.28D-03	0.14D 01	0.10E 03	0.61637240 03	0.24826850 02
0.28D-03	0.14D 01	0.30E 03	0.61440210 03	0.24787140 02
0.28D-03	0.14D 01	0.10E 04	0.61483120 03	0.24795790 02
0.28D-03	0.14D 01	0.30E 04	0.62238220 03	0.24947590 02
0.28D-03	0.14D 01	0.10E 05	0.63752830 03	0.25249320 02
0.28D-03	0.14D 01	0.30E 05	0.63971610 03	0.25292610 02
0.28D-03	0.14D 01	0.10E 06	0.61714120 03	0.24842330 02
0.28D-03	0.14D 01	0.30E 06	0.46430640 03	0.21547770 02
0.28D-03	0.14D 01	0.10E 07	0.83442290 02	0.91346750 01
0.28D-03	0.14D 01	0.30E 07	-0.45759640 02	-0.00000000 00
0.28D-03	0.14D 01	0.10E 08	-0.64339820 02	-0.00000000 00
0.28D-03	0.14D 01	0.30E 08	-0.66022450 02	-0.00000000 00

INPUT DATA

0.2000000E 01	0.1000000E-01	0.4000001E-02	0.4900000E 04
0.6000000E 02	0.9000000E 01	0.4000000E 02	0.8000000E 02
0.1000000E-03	0.1000000E-05	0.4900000E 00	0.2100000E-02
0.9900004E-06	0.9999999E-03	0.1000000E 02	0.1000000E-04

lations have been made at all of the desired frequencies.

12. Read a new set of data and make the calculations for this set.

This particular program allows some flexibility in that SINF(3), the high frequency conductivity of the outer shell, can be used with its relaxation time. For the best results though, this is not needed and so is read in equal to SZERO(3). The parameter CONST gives further flexibility in that it can be used to relate two or more variables. It was used in this connection to relate SA(3) to SA(4), thus overriding the read in value for SA(3). Note that in statement 24, the conductivity inside the cell is assumed equal to that of the suspending medium. This assumption for dead cells is not applicable to other situations and so in that case should be deleted.

APPENDIX C

LIST OF SYMBOLS

A - Crossectional area

A_{in} - Legendre Coefficient

A_i - See Equation (VI-32).

a - particle radius, ellipsoid axis

a_1, a_2, a_3 - radii of spheres in two shell model

$\vec{B}$ - magnetic induction

b - ellipsoid axis

B_i - See Equation (VI-32)

B_{in} - Legendre Coefficient

C - Capicatance; particle concentration

$\vec{D}$ - Electric displacement

$\vec{D}$ - Total Displacement

D1, D2 - See Equations (VI-47-48)

d - sample thickness

$\vec{E}$ - Electric Field Strength

$\vec{F}$ - Force

f - frequency

f_σ - critical frequency for conduction relaxation

$\vec{H}$ - Magnetic Field

I - Current

$\vec{I}_f$ - Surface density of free current

$\vec{J}$ - Total current density

$\vec{J}_C$ - Conduction current density

$\vec{J}_D$ - Displacement current density

K - Complex conduction factor

k - Boltzmann's constant

L_1, L_2 - See Equations (VI-28-29)

ℓ - Sample thickness

$\vec{M}$ - Magnetization

$\vec{n}$ - Unit outward normal

N1, N2 - See Equations (VI-44-45)

$\vec{P}$ - Electric polarization

R - Resistance

r - Radius, polar coordinate

T - Kelvin temperature

t - Time

$\bar{U}$ - Time mean electric field energy

V - Voltage, volume

$\vec{v}$ - velocity

$\bar{w}$ - Time averaged energy of a body

X1, X2 - See Equations (VI-49-50)

Y - Admittance

y - Yield

Z - Impedance

ϵ - Permittivity

ε' - Real part of ε

ε'' - Imaginary part of ε

ε_e - Effective permittivity

ε_s - Permittivity at low frequencies (static)

ε_∞ - Permittivity at high frequencies

ε_o - Permittivity of free space

η - Viscosity

η_f - Surface density of free charge

θ - Polar coordinate, phase angle

μ - Micron (10^{-6} m)

ξ - Complex dielectric factor

ξ_r - Relative complex dielectric factor

ρ - Volume density of charge

ρ_f - Volume density of free charge

σ - Conductivity

σ' - Real part of σ

σ'' - Imaginary part of σ

σ_e - Effective conductivity

σ_s - Conductivity at low frequencies (static)

σ_∞ - Conductivity at high frequencies (static)

τ - Volume element, relaxation time

τ_ε - Relaxation time for permittivity

τ_σ - Relaxation time for conductivity

Φ - Potential function

ϕ - Polar coordinate

χ - Force parameter, See Equation (VII-6)

ψ - Potential function

ω - Angular frequency

∇ - Del Operator

$Re(\xi)$ - Real part of ξ.

APPENDIX D

ERROR ANALYSIS

The sources of error involved in the yield measurements have been pointed out in Chapter III. The effect of these errors on the yield will now be considered for those which can be given numerical estimates. Since a large number of measurements was not taken for each set of conditions, an empirical statistical analysis is necessary. The theoretical expression for the yield given by Equation (VII-17) will be assumed to apply and the propagation of error through this equation will be determined.

The deviation in the yield, assuming it to be a function of C, ϕ_1, σ, and f, is given by standard methods as (75, p. 273).

$$S_y = [(w_c S_c)^2 + (w_\phi S_\phi)^2 + (w_t S_t)^2 + (w_\sigma S_\sigma)^2 + (w_f S_f)^2 + (w_r S_r)^2]^{\frac{1}{2}} \quad \text{(D-1)}$$

where S_i is the deviation and w_i is the weighting factor for the parameter i, and r refers to the error in reading the scale. The probable error is obtained from this expression as (75, p. 255).

$$\text{P.E.} = 0.67\ S_y. \quad \text{(D-2)}$$

Using experience with the apparatus as a basis, the values of the products $w_i S_i$ are estimated to be:

$$w_c S_c = 0.05y$$

$$w_\phi S_\phi = 0.03\ (1 + \frac{\log f}{7})\ y$$

$$w_t S_t = 0.02y$$

$$w_\sigma S_\sigma = 0.05y$$

$$w_f S_f = 0.02y$$

$$w_r S_r = 0.25\ .$$

These values give the probable error as

$$\text{P.E.} = (0.67)\ [\{0.0058 + 0.0009\ (1 + \frac{\log f}{7})^2\}\ y^2 + 0.0625]^{\frac{1}{2}}. \qquad \text{(D-3)}$$

which has been evaluated for the yield and is shown in Figure 13.

These error limits express the confidence with which a particular curve can be drawn. Since the errors considered do not take into account such factors as cell age, cell size, cell makeup, and growth conditions, caution should be used when making quantative generalizations about behavior. Thus, when any of these quantities might be different, such as when a different culture of cells is used, the yield will generally not be reproducable within the error limits.

An example of just such a situation occurs when Figure 13 is compared to the curve of Figure 14 when $\sigma = 1.56 \cdot 10^{-2}$ mho/m. On a log scale, 10^{-2} mho/m lies about two thirds of the way between $2.12 \cdot 10^{-3}$ and $1.56 \cdot 10^{-2}$ mho/m so that one might expect the curve of Figure 13 to lie between the two middle curves of Figure 14. This is, in fact, the case for frequencies up to 10^5 Hz. However, above 10^5 Hz, the yield in Figure 13 exceeds all results shown in Figure 14. This would indicate some uncontrolled difference between the cells used in the two studies.

One further comment on errors concerns the comparison of experi-

mental results with theory. In the derivation of Equation (VII-17), the yield was related to the number of cells collected by assuming that the pearl chains were of equal length and cylindrical in form. As is obvious from the photographs of Figure 9, this is not the case. The question arises as to whether some other method might be used to estimate the number of cells collected.

Two methods which come immediately to mind are the direct count of all of the collected cells in place and the count of the cells after they have been removed to some suitable detection device. In the first case, the optics at the electrode are poor and a direct count at the surface would not only be tedious but also inaccurate. This would be particularly true for organisms smaller and more transparent than yeast.

The second method would be superior to the yield if it were possible to remove the collected cells without losing some or without gaining some which had not collected. In practice this is a difficult requirement to meet.

Thus, the two obvious alternatives to the yield as a measure of the number of cells collected, would require more involved experimental procedures and yet do not appear to be significantly more reliable. For routine work, then, the yield seems to be the best measure of the collection. Perhaps a useful compromise, in the form of a yield calibrated in terms of a direct count, would be the optimum approach.

VITA

Joe Stanley Crane

Candidate for the Degree of

Doctor of Philosophy

Thesis: THE DIELECTROPHORESIS OF CELLS

Major Field: Physics

Biographical:

Personal Data: Born in Tallant, Oklahoma, September 27, 1942, the son of Charles R. and Inez E. Wade Crane.

Education: Graduated from Barnsdall High School, Barnsdall, Oklahoma, in 1960; received the Bachelor of Science degree from Oklahoma State University in May, 1964, with a major in physics; awarded W. A. Jones Fellowship in September, 1964, and received the Master of Science degree from Oklahoma State University in July, 1966, with a major in physics; completed the requirements for the Doctor of Philosophy degree at Oklahoma State University in May, 1970.

Professional Experience: Held summer appointments with Argonne National Laboratory, Idaho Falls, Idaho, in 1963, with N.A.S.A., Houston, Texas, in 1964, and with Los Alamos Scientific Laboratory, Los Alamos, New Mexico, in 1967; became Instructor of Physics at Cameron State College, Lawton, Oklahoma, in September, 1969.

Other: Member of Sigma Pi Sigma, National Physics Honor Society; coauthor with H. A. Pohl of "The Study of Living and Dead Cells Using Dielectrophoresis", J. Electrochem. Soc., 115, 584 (1968).